SYSTEMATIC APPROACH TO INTEGRATED MINE BENCH OPTIMIZATION IN SOIL AND ROCK OF SRI LANKAN OPEN PIT MINES – A CASE STUDY

Widanalage Danushka Madushan De Mel

168953R

Degree of Master of Engineering

Department of Civil Engineering

University of Moratuwa
Sri Lanka

August 2020

SYSTEMATIC APPROACH TO INTEGRATED MINE BENCH OPTIMIZATION IN SOIL AND ROCK OF SRI LANKAN OPEN PIT MINES – A CASE STUDY

Widanalage Danushka Madushan De Mel

168953R

Thesis submitted in partial fulfillment of the requirements for the
Degree of Master of Engineering
in Foundation Engineering and Earth Retaining System

Department of Civil Engineering

University of Moratuwa
Sri Lanka

August 2020

DECLARATION

I declare that this is my own work and this thesis does not incorporate without acknowledgement any material previously submitted for a Degree or Diploma in any other University or institute of higher learning and to the best of my knowledge and belief it does not contain any material previously published or written by another person expect where the acknowledgment is made in text.

Also, I hereby grant to University of Moratuwa the non-exclusive right to reproduce and distribute my thesis, in whole or in part in print, electronic or other medium. I retain the right to use this content in whole or part in future works (such as articles or books).

....

Widanalage Danushka Madushan De Mel Date

The above candidate has carried out research for the Master's thesis under my supervision.

....

Professor U.G.A. Puswewala Date

SYSTEMATIC APPROACH TO INTEGRATED MINE BENCH OPTIMIZATION IN SOIL AND ROCK OF SRI LANKAN OPEN PIT MINES – A CASE STUDY

ABSTRACT

Instabilities and failures in rock slopes occur due to numerous factors such as unfavorable slope geometries, geological discontinuities, weak or weathered materials in the slopes, existing weather conditions and environmentally induced external factors such as heavy precipitation, seismic activities and groundwater. Bench optimization is carried out to maintain bench height and dip of the slope within an allowable factor of safety, thus avoiding rock slope failures and instabilities. Therefore, optimum determination of these geometrical features has become a most significant part of soil and rock slope stability analysis in Open Pit Mining where multiple benches of excavation are maintained.

Field work related to this research study primarily comprised of observation of structural geological features (dip and strike) and other measurements and observations (joint spacing, separation, condition of joint) required for analysis work, including Slope Mass Rating analysis, at the selected site of Halbarawa, Sri Lanka. Furthermore, soil and rock samples were collected from the selected site to perform laboratory tests. Proctor compaction test and direct shear test were carried out for selected samples to evaluate the overburden slope stability. Simultaneously, stability of soil and highly weathered rock slope was analyzed by SLOPE W software. In order to analyze rock slopes, initially possible rock failure modes were identified using Georient software. If it indicated some tendency to fail, a detailed analysis of wedge failure was carried out using GEO5 software. Further, Toppling and Planer modes of failure were analyzed via SMR analysis.

The study focused on optimizing the bench geometry of mine slopes necessarily consisting soil, highly weathered rock and fractured rock in order to explore ways for safe and economical bench designing. This was achieved by integrating kinematic, empirical and limit equilibrium approaches for slope stability investigation and guidelines were finally developed so that the same methodology can be universally applied for assessing the soil and rock slope stability in similar situations. This procedure was developed through the case study of Halbarawa Mine.

Results indicated that the stability is more sensitive to variation in cohesion than variation in friction angle of overburden profile. As far as the bench geometry is considered, multiple benches are seen as the most reliable mining methods for steeply dipping benches. According to RQD of each location, the rocks in the particular area varied from moderately hard rocks to hard rock. The Kinematic analysis disclosed that most of joint planes intersect with each other and produce various potential failure mechanisms. The dip and the dip direction of the slope faces determine the possibility of failure and the mode of failure with respect to the discontinuity plane.

For the Halbarawa site, as per the SMR analysis, face 1, 2 and 3 can be categorized into completely unstable (V), partially stable (III) and unstable (IV) rock stability classes respectively. It was also understood that surcharge load is a more critical factor than the static water pressure when a wedge failure is considered. The most successful, economical

and rapid remedial measures to enhance the stability of rock slope are reduction of bench height and reduction of bench angle.

KEYWORDS: Bench optimization, Open Pit Mines, SMR, surcharge load, stability classes, Kinematic analysis.

ACKNOWLEDGEMENT

First and foremost, I am deeply indebted to my research supervisor Professor. U.G.A Puswewala for his immense support throughout my study with his patience and knowledge. His challenging questions and critical suggestions were beneficial for me to remain on the correct path till towards the completion. Without his encouragement and motivation with continuous guidance, it would have not been possible to complete this study. It is a real privilege and honor for me to study under the supervision of an extraordinary teacher like you.

I also would like to express my sincere gratitude to Professor. S.A.S Kulathilaka, Professor. H.S.Thilakasiri, Dr. L.I.N. De Silva, Dr. U.P. Nawagamuwa, Dr. A.M.K.B. Abeysinghe, Dr. C. Jayawardana and Dr L.S.P. Rohitha for the support and guidance extended in terms of academic to pursue my goals. Their sincere and consistent encouragement is greatly appreciated.

Further, I am grateful to Eng. Chanaka Godawithana in China Harbour Pvt (Ltd) and the staff of Soil Mechanics Laboratory, Material Testing Laboratory and Mineral Engineering Laboratory University of Moratuwa for their support in different ways during this research period.

I also extend my sincere thanks to all my colleagues and friends, especially Nishadhi Nayanthara, Ashara Hettiarachchi, Tharindu Abeykoon, Thisuni Kodippili and Nimila Dushyantha for their support in numerous ways whenever I needed it. The assistance extended in difficult times is highly appreciated.

Last but not least, I would like to share my heartfelt thanks to my parents, wife, sister and brother for their unconditional support, encouragement and love throughout this study. It would have not been possible to come this far without them.

Table of Contents

LIST OF FIGURES

LIST OF TABLES

ABBREVIATIONS

D/D – Dip Direction

GSI – Geological Strength Index

HWR – Highly Weathered Rock

Jn – Number of joint sets

Jv – Volumetric Joint Count

M-B – Multiple bench orientation with slip circle exit through HWR

M-T – Multiple bench orientation with slip circle exit through top soil

P – Planer failure

RMi – Rock Mass Index

RMR – Rock Mass Rating

RQD – Rock Quality Designation

S – Joint Spacing

S-B – Single bench orientation with slip circle exit through HWR

SMR – Slope Mass Rating

S-T – Single bench orientation with slip circle exit through top soil

T – Toppling failure

UCS – Unconfined Compressive Strength

W – Wedge failure

σ_{cm} – Unconfined Compressive Strength of rock mass

1 INTRODUCTION

The stability of rock slopes is deliberated critical in ensuring community safety along highways passing through road cuts, especially in mountainous areas as well as safety of personnel and machinery in open pit mines. The instabilities and failures in rock slopes arise due to numerous factors such as unfavorable slope geometries, geological discontinuities, weak or weathered slope materials and the existing climate conditions (Basahel and Mitri, 2017). Further, environmentally induced external factors such as heavy precipitation, seismic activities and water in slope can also play a substantial role in slope failure (Pantelidis, 2009).

The significant detrimental consequences related with rock slope instabilities in open pit mines make it necessary to systematically evaluate and manage the stability of slopes. Open pit mines are one of the leading geotechnical structures in the world from where ores/aggregates are mined economically. Excavation generally takes place in a series of benches of different sizes depending on the site conditions. Since excavation and disposal of materials are major cost drivers in open pit Mining, it is mandatory to minimize the volume of material that needs to be excavated as much as possible, which is possible by steepening the slopes (Karam et al, 2015). However, steeper the slopes, greater the chance to failure. Therefore, the geometry of the slopes should be maintained at optimum conditions considering a safe as well as an economic operation of the mine.

When the bench geometry is considered, height, width and the angle of bench slope are the most important geometrical parameters of the bench. These features can directly affect the slope stability. The geometrical features of the mine bench are shown in Figure 1-1. Slopes can be broadly classified as natural slopes and man-made slopes. Man-made slopes can be sub divided into cut slopes and fill slopes. In the open pit mines, generally cut slopes are produced for the excavation purpose. As aforementioned, the stability of cut slope is critical for safe and economical Mining operation. The stability of a slope will decrease with increasing bench height and slope.

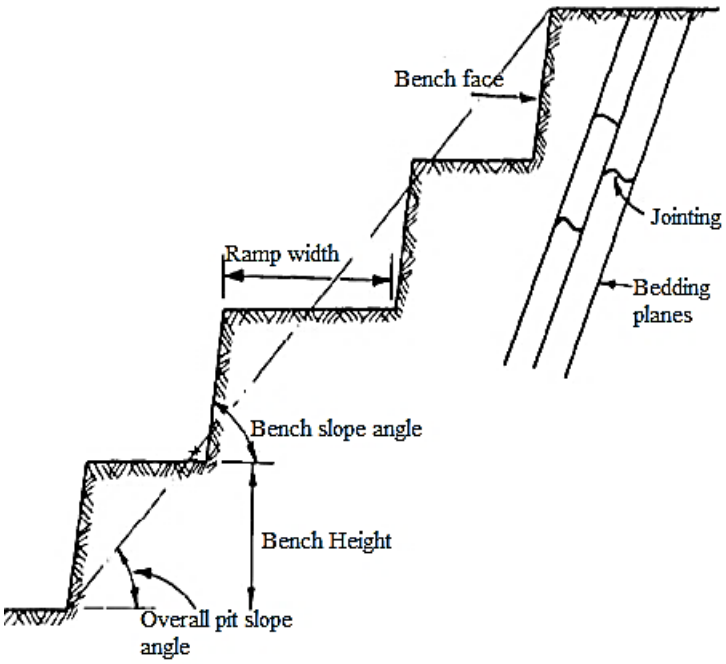

Figure 1-1: The geometrical features of the multiple mine bench

The bench optimization is to maintain bench height and dip of the slope with allowable factor of safety. Optimum determination of these geometrical features are the most important parts of soil and rock slope stability analysis in open pit mines, as it maintains multiple benches of excavation.

Basically, slope stability can be explained by a description of the balance of forces which exist in undisturbed cut slopes and how these forces behave with load combination. As mentioned earlier, the stability and behavior of both natural and engineered rock slopes are crucially dependent on the geological structures such as folds, faults, and discontinuities (Stead and Wolter, 2015). Therefore, design and Mining in such rock masses requires structural geology considerations from micro-scale to regional tectonic scales. The major concern of this research is to build relationships between structural features of rocks and geotechnical considerations to analyze their effects on rock slope instability.

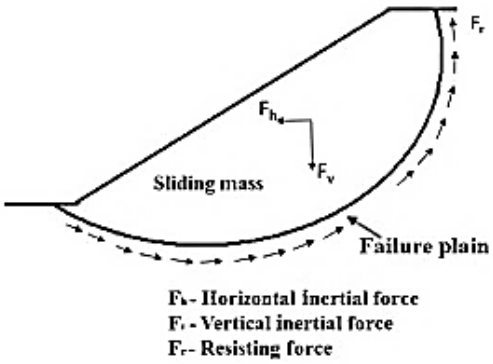

Figure 1-2: Basic forces applied on a mobilized soil slope.

Open pit limestone mine at Aruwakkalu and phosphate mine at Eppawala are the leading open pit mines in Sri Lankan Mining context. Apart from that, aggregates for construction purposes are provided by open pit rock quarry mines located in different parts of the country. This research is associated with rock quarry slope stabilization via geotechnical analytical method. Majority of quarry aggregates in Sri Lanka are metamorphic rocks which contain geological discontinuities.

1.1 Problem statement

About 90% of Sri Lankan rocks are metamorphic rocks. Majority of metamorphic rock Quarries in Sri Lankan mining context do not contain proper procedure for rock benching. Due to this reason several types of instabilities and failures can delay the production chain as well as menace human life and machinery. Through this research, it is intended to propose a scientific investigation method for soil integrated with metamorphic rocks in order to determine optimum bench height and bench angle for overburden and safe dip direction and dip angle for rock terrain, which can keep the excavation safe during all seasons of the year.

1.2 Objectives

This study has the following objectives.

(a) Optimization of bench of the mine slopes consisting of soil, highly weathered rock and fractured rock by considering and integration of kinematic, Empirical and Limit equilibrium method for slope stabilization and exploring the ways to design safe and economical mine benches for rock quarries.

The specific objectives are,

(b) To understand the structural geological features that could cause different types of failures.

(c) To classify the rock mass by Rock Mass Rating and Rock Quality Designation.

(d) Determining the stability classes of rocks on one Sri Lankan rock quarry.

(e) Validating GEO5 software via real case study.

(f) Determining the most suitable rock slope stability improvement techniques.

1.3 Study area

The selected study area is a Halbarawa Quarry site operated by China Harbor Pvt. Ltd. This is located close to Padukka and is 35km away from Colombo. The extent of the site is about 9 acres consisting of highly fractured metamorphic rocks with overburden. Operation has been suspended due to rock flight during blasting. Hydrological, geological and geotechnical aspects of the entire area are considered in this study. The relevant data obtained from quarry that had slid site at Thalathu Oya, is used for validation purposes of GEO5 software.

1.4 Limitations of the research study

(a) This is mostly applicable for jointed metamorphic rock terrain with overburden.

(b) When boulders encountered were treated as soil.

(c) At the design stage, outcrops should be visible to measure structural geological features.

2 LITERATURE REVIEW

2.1 Structural geological features

2.1.1 Foliation

Planer arrangements of structural or textural features in rocks are known as foliation which can occur in any type of rock. They are mostly visualized in metamorphic and sedimentary type formation. Foliation often occurs parallel to original bedding. Sometimes rock slope failure occurs along foliation planes.

2.1.2 Joints

Joints are planes of separation in which significant shear displacement has not taken place. Joints could result from regional tectonics, faulting, folding and internal stress relief during uplift or cooling. Joints are formed as a set and associated properties are similar in a particular joint set.

2.2 Structural geological measurement

2.2.1 Strike

Strike is the intersection of a horizontal plane with any planer geological structure such as foliation, joints, fault plane etc.

2.2.2 Dip

Dip angle is the steepest angle formed between horizontal plane and the inclined geological planar structures.

2.2.3 Dip direction

Slope direction of the plane structure is simply known as dip direction. Dip direction is always perpendicular to the Strike and it can be obtained by deducting or adding 90 degrees to the strike.

2.2.4 Trend

The trend is the azimuth of a linear geological feature. It is known as compass bearing. The trend implies the orientation of linear feature.

2.2.5 Plunge

The plunge is the angle between a line and a horizontal datum plane. This indicates the angle of linear features. The plunge is measured in the trending direction in a vertical plane with respect to horizontal line.

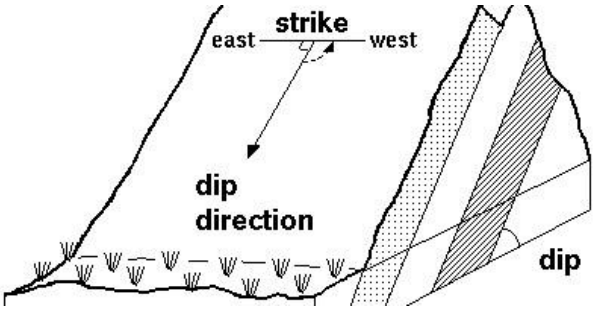

Figure 2-1: Structural geological measurements.

2.3 Types of slope failures

Mainly there are four types of cut slope failures.

Plane failure
Wedge failure
Toppling failure
Circular failure

2.3.1 Plane failure

Plane failure is a comparatively rare case in rock cut slopes. To realize it, all the geometrical conditions should be fulfilled in the actual slope. For sliding to occur on a single plane, the following geometrical condition must be satisfied. (Maerz, 2000)

- The strike of the plane on which sliding occurs must be parallel or nearly parallel to the slope face.
- The failure plane must daylight in the slope face. That implies the dip of discontinuity to be smaller than the dip of the slope.
- The dip of the failure plane must be greater than the angle of friction of this plane.
- The upper end of the sliding surface either intersects the upper slope, or terminates in a tension crack.

- Release surfaces that provide negligible resistance to sliding must be present in the rock mass to define the lateral boundaries of the slide. Alternatively, failure can occur on a sliding plane passing through the convex "nose" of a slope.

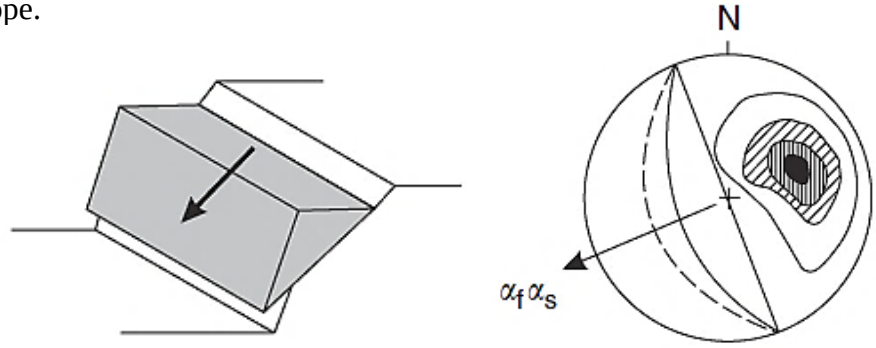

Figure 2-2: Stereo plots of structural condition for plane failure

2.3.2 Wedge failure

When two or more discontinuity planes in the slope intersect each other and form a wedge, the slope may fail as wedge failure. The basic requirements for wedge type of slope failure to happen are as follows (Hoek and Bray, 1981).

- Two planes will always intersect along a line.
- Plunge of the line of intersection must be flatter than the dip of the face and steeper than the average friction angle of the two slide planes.
- The line of intersection must be dip in a direction out of the face for sliding to be feasible.

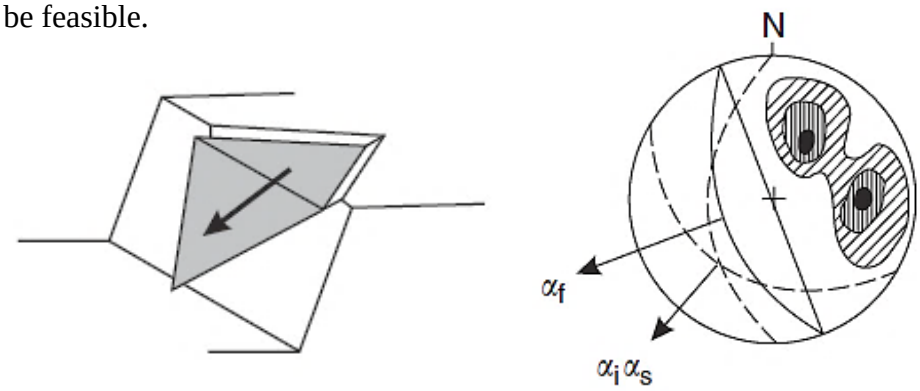

Figure 2-3: Stereo plots of structural condition for Wedge failure

2.3.3 Toppling failure

Toppling failure is a general method of instability in blocky type rock slopes where rock blocks rotate about their toes and overturn. There are different types of toppling failure modes. Among those, one of the most vital types of toppling failure is slide-toe-toppling mode. In this scenario, rock blocks at the toe of the slope are overturned by the pressure of sliding mass from the upper part of the slope.

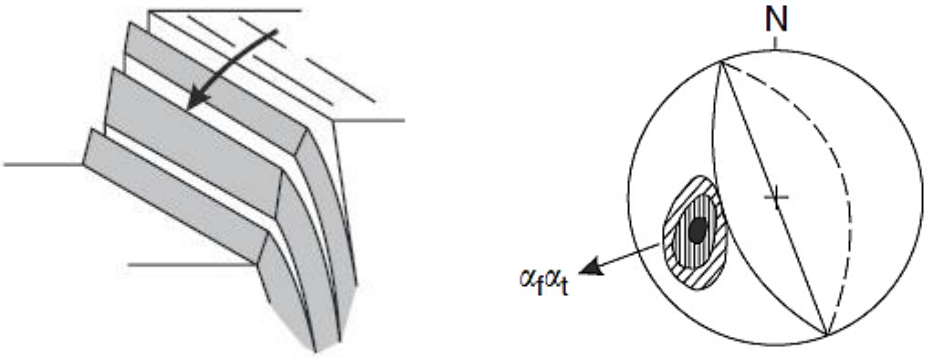

Figure 2-4: Stereo plots of structural condition for toppling failure

2.3.4 Circular failure

The circular type slope failure in rocks is basically controlled by the weak planes. When there are lots of fractures exist with closely spaced, the slope automatically finds the smallest resistance route to failure. The failure surface in such highly fractured situation is mostly circular.

The following basic requirements should be satisfied for occurrence of the circular type of slope failures.

- This happens when the individual elements in rock mass are very small related with the size of the slope.
- Broken rock in a fill will tend to behave as “soil” and fail in a circular mode when the slope dimensions are considerably greater than the dimensions of the rock fragments.
- Highly weathered rocks and rocks with closely spaced and randomly oriented discontinuities will also tend to fail in this mode.

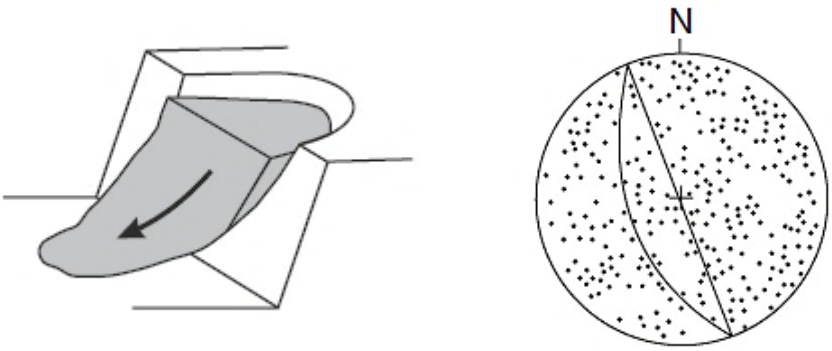

Figure 2-5: Circular type failure

Vásárhelyi and Kovács (2017) presented and reviewed empirical methods of calculating the mechanical parameters of the rock mass associated engineering properties include Uniaxial Compressive Strength (UCS), deformation modulus of rock mass, Poisson ratio, tensile strength .In this study, they have presented several correlations for determination of cohesion, friction angle with Rock Mass Rating (RMR), Rock Quality Designation (RQD) and UCS.

2.4 Correlations to calculate friction angle of rock mass

Various correlations for friction angle of intact rock found in literature are;

$\emptyset_m = 25(1 + 0.01RMR)$ (Sen and Sadagah) Equation (1)

$\emptyset_m = 20{\sigma_{cm}}^{0.25}$ (Aydan) Equation (2)

$\emptyset_m = 20 + 0.5RMR$ (Aydan and Kawamoto) Equation (3)

$\emptyset_m = 0.5RMR + 15.5$ (Trunck and Honisch) Equation (4)

2.5 Correlations to calculate cohesion of rock mass

$C_m = \frac{\sigma_{cm}(1-\sin\emptyset_m)}{2\cos\emptyset_m}$ Equation (5)

$C_m = 3.625RMR$ Equation (6)

2.6 Estimation of Rock Quality Designation

Palmstrom (2005) has carried out research on measurements of and correlations between block size and Rock Quality Designation (RQD). Different parameters

(block volume, volumetric joint count and total joint frequency) related to rock joints address the measurement of RQD. Three-dimensional block volume and volumetric joint count (Jv) may provide a better characterization of the block size. At least three joint sets intersect each other to produce a block. Block size is normally expressed in terms of density of joints, degree of jointing, block volume and joint spacing. The term joint relates to joints, fissures, fractures, cracks and breaks penetrating rock mass. A Joint set forms when a series of joints are oriented parallel with roughly equal spacing. Block size is vitally important parameter for rock mass engineering classification systems to obtain following parameters.

- Joint spacing and RQD in the Rock Mass Rating system.
- The ratio between factor for the number of joint sets and RQD in the Q system.
- Block volume in the Rock Mass Index and the number of joint sets once RMI is applied in rock support assessment.

The volumetric joint count (Jv) (Palstrom, 1982) is defined as the number of joints intersecting a volume of one meter cube. Volumetric joint count can be defined as,

$$Jv = \frac{1}{S_1} + \frac{1}{S_2} + \frac{1}{S_3} + \cdots + \frac{1}{S_n} \qquad \text{Equation (7)}$$

Where $S_1, S_2\ and\ S_3$ are the average spacing for joint sets.

Rock Quality Designation (RQD) provides a quantitative evaluation of rock quality with the aid of core logs. RQD is a percentage of core pieces which are longer than 100 mm to the total length of the core. The classification of rock quality based on RQD is presented in Table 2-5 (Deere, 1988). RQD provides an indication of degree of jointing along the actual section. Joints intersecting a rock mass separates rock into blocks. Block size is a vitally important parameter in rock mass behavior. Initially, a relationship between the block size (Jv) and RQD was proposed by Palstrom (1974). The subsequently amended relationship gives more appropriate average correlation than previous one.

RQD = 110-3.3Jv Equation (8)

Bieniawski, in 1979 offered Rock Mass Rating (RMR) system to classify rock classes. The basic RMR is computed by adding rating value for five parameters as strength of intact rock, rock quality designation, spacing of joints, condition of joints and ground water condition. Romana (1985) and Romana et al, (2003) suggested the Slope Mass Rating system (SMR). This is derived using basic RMR with four adjustment factors. Adjustment factor 1 (F_1) depends on parallelism between joints and slope face strike. F_2 is referred to joint dip angle in the planer mode of failure. F_3 is dependent on the relationship between slope and joint dip. F_4 reflects an adjustment factor for the method of excavation.

2.7 Geological Strength Index

The Geological Strength Index (GSI) system facilitates a path to enumerate the strength and the deformation parameters of a rock mass based on visual observation of the rock surfaces and structural geological characteristics of a rock mass. Hoek (1994) and Hoek et al, (1995) presented the Geological Strength Index as a tool for collecting field observations for facilitate strength parameters of rock mass. This system enables to estimate the rock mass quality under different geological conditions by field observations and the Figure 2-6 illustrates the modified Geological Strength Index classification system which was suggested by Sonmez and Ulusay (1999).

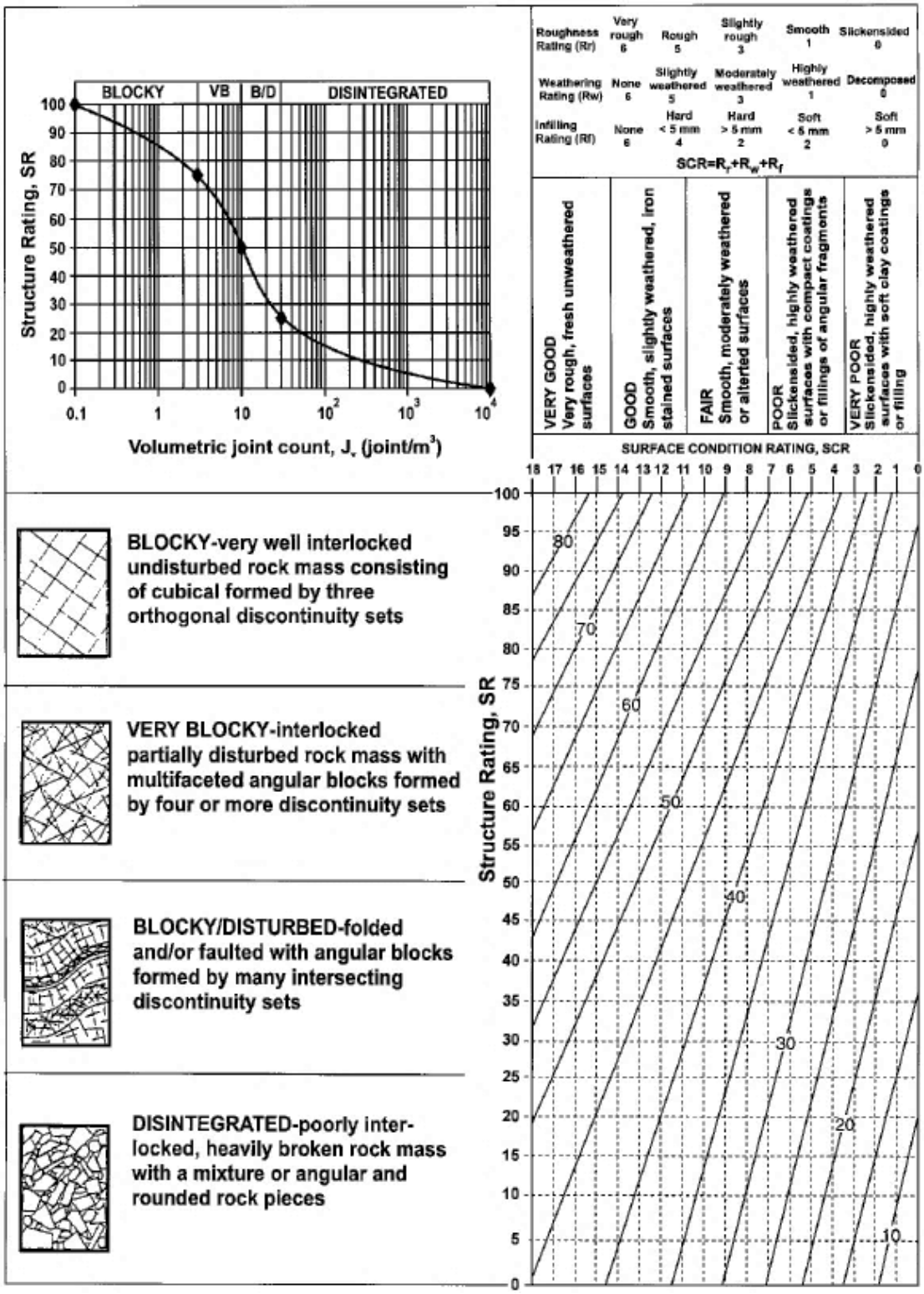

Figure 2-6: The modified GSI classification

Table 2-1: Rock Mass Rating system

RMR_B = BASIC RMR = $\sum RATINGS$ (BIENIAWSKI,1979)							
Parameter	**Intervals**						
UCS (MPa) Unconfined Compressive Strength of intact rock material	>250	250 – 100	100 – 50	50 – 25	<25		
					25 -5	5 -1	< 1
	15	12	7	4	2	1	0
RQD (%) Rock Quality Designation	100 – 90	90 – 75	75 – 50	50 – 25	< 25		
	20	17	13	8	3		
Spacing (mm) between discontinuities	>2000	2000 - 600	600 – 200	200 – 60	< 60		
	20	15	10	8	5		
Condition of discontinuities Roughness ,Persistence, Separation, Weathering of walls and gouge	Very rough surfaces, No separation, unweathered wall rock, not continuous	Slightly rough, separation < 1mm slightly weathered, not continuous	Slightly rough separation < 1 mm Highly weathered wall	Slicken sided walls or gouge < 5 mm or separation 1 – 5mm	Soft gouge >5 mm or separation>5mm Continuous		
	30	25	20	10	0		
Ground water in joint (pore pressure ratio)	Completely dry (0)	Damp (0-0.1)	Wet (0.1 – 0.2)	Dripping (0.2 – 0.5)	Flowing (0.5)		
	15	10	7	4	0		

Table 2-2: Slope Mass Rating adjustment factors

SMR = $RMR_B + (F1 \times F2 \times F3) + F4$ (ROMANA,1985)						
ADJUSTING FACTORS FOR JOINTS (F_1,F_2,F_3)		**αj = DIP DIRECTION OF JOINT** **αs = DIP DIRECTION OF SLOPE**		**βj = DIP OF JOINT** **βs = DIP OF SLOPE**		
		Very favorable	favorable	Fair	Unfavorable	Very Unfavorable
Plane failure $\propto j - \alpha s$ Toppling $\lvert \propto j - \alpha s - 180^0 \rvert$ F1 Value Relationship		$>30^0$	30^0 -20^0	20^0- 10^0	10^0- 5^0	$< 5^0$
		0.15	0.40	0.70	0.85	1.00
		$F_1 = (1 - SIN \lvert \propto j - \alpha s \rvert)^2$				
βj		$<20^0$	20^0-30^0	30^0 - 35^0	35^0-45^0	$>45^0$
F_2 Value	Plane failure	0.15	0.40	0.70	0.85	1.00
	Toppling	1.00				
	Relationship	**$F_2 = tg^2 \beta j$**				
Plane failure $\beta j - \beta s$ Toppling $\beta j + \beta s$		$>10^0$ $<110^0$	10^0- 0^0 110^0 - 120^0	0^0 $>120^0$	0^0- (-10^0) -	$< (-10^0)$ -
		0	-6	-25	-50	-60
F_3 Value		**F_3 (BIENIAWSKI ADJUSTMENT RATINGS FOR JOINTS ORIENTATION,1976)**				
Adjusting factors for Excavation method		**F_4 = EMPIRICAL VALUES FOR METHOD OF EXCAVATION**				
		Natural Slope	Pre-splitting	Smooth Blasting	Blasting or Mechanical	Deficient Blasting
F_4 Value		+5	+10	+8	0	-8

ROMANA (1993) illustrated rock stability class classification based on Slope Mass Rating values. In that classification, he proposed five classes from Class I to Class V. The stability of the slope depreciates with increasing class number. He also proposed type of possible slope failure as well as precaution to be adopted to stabilize the existing slope.

Table 2-3: Classification of rock slope according to SMR

SMR	Class	Description	Stability	Failure	Support
81-100	**I**	Very good	Completely stable	None	None
61-80	**II**	Good	Stable	Some blocks	Occasional
41-60	**III**	Fair	Partially stable	Some joints or many wedges	Systematic
21-40	**IV**	Bad	Unstable	Planar or big wedges	Important/ corrective
0-20	**V**	Very bad	Completely unstable	Big planar or soil-like	Re-excavation

Slope Mass Rating facilitates an impartial determination of the rating adjustment values based on the discontinuity and slope orientation, respective dip angles and slope excavation approaches. A more sustainable approach to rock slope stability analysis combines the Slope Mass Rating with determination of peak friction angle of the discontinuity surface (Rafek et al, 2016). According to his approach four stability classes can be determined as bellows:

SMR rating predicts failure and the geological discontinuity dip angle (β_ι) $>$ peak friction angle (α_p), the slope has very high failure potential.

SMR rating predicts failure and the geological discontinuity dip angle (β_ι) $<$ peak friction angle (α_p), the slope has intermediate failure potential.

SMR rating predicts stability and the geological discontinuity dip angle (β_ι) $>$ peak friction angle (α_p), the slope has low failure potential.

SMR rating predicts stability and the geological discontinuity dip angle (β_ι) $<$ peak friction angle (α_p), the slope is stable.

Table 2-4: Shear strength parameters for Rock Mass Rating values

RMR	Class No	Description	Cohesion of Rock mass(kPa)	Friction angle of rock mass
100-81	**I**	Very good rock	>300	$> 45^0$
80-61	**II**	Good rock	200-300	$40^0 - 45^0$
60-41	**III**	Fair rock	150-200	$35^0 - 40^0$
40-21	**IV**	Poor rock	100-150	$30^0 - 35^0$
20-0	**V**	Very poor rock	<100	$< 30^0$

Table 2-5: Classification of rock quality based on RQD

RQD	Rock Quality
0-25	Very poor
25-50	Poor
50-75	Fair
75-90	Good
90-100	Very good

2.8 Case studies

Siddique et al, (2015) carried out research on Slope Mass Rating and Kinematic analysis of slopes along the national highway -58 near jonk, Rishikesh, India. The research was carried out to observe safe zone and their vulnerability to sliding and present condition in Himalaya active convergent plate. The observed RQD values range from 82% to 95% and average UCS of intact rock is about 43 MPa. That indicates rock is moderately strong. For the study area SMR value varies from 66 to 70 showing that the rock mass is in stable class. There are certain parameters governing slope stability, that were not accounted in the SMR. SMR & kinematic analysis show slope is stable; however, slope stability method should be adopted only after observing site condition.

Samarawickrama et al, (2014) carried out a study on criteria to asses Rock Quarry slope stability and design in landslide vulnerable areas of Sri Lanka: a case study at Thalathu Oya Rock Quarry. That particular quarry is a site with slope failure. In his study, he was able to determine shear strength parameters of rocks using empirical equations and subsequent back analysis and stabilizing the vulnerable area. The given site conditions are modeled with the GEO5 software and factor of safety against sliding check with the actual condition of the site. Hence, the suitability of the software can be proved for this particular analysis. The aforementioned research has been carried out on metamorphic rock terrain. However, bench optimization and soil rock integrated stability analysis have not been carried out in that investigation.

3 METHODOLOGY

3.1 Selection of the study area

The current research mainly focused on slope stability analysis integrating soil and rock. The selection of a suitable study area for the investigations proved difficult due to lack of subsurface information. To mitigate those difficulties, it was decided to select a suitable open pit rock quarry so that soil rock profile can be properly observed. If the rock is fresh and competent, it has less probability to fail. Therefore, The Halbarawa quarry site was selected as a representative location for this research. It satisfied major requirements to carry on this research.

Figure 3-1: Arial photograph of the site

3.2 Summary of Methodology

At the preliminary survey stage, structural geological features and rock types in the selected area were identified using area geological maps. Rainfall data was collected from the Irrigation Department, Sri Lanka to analyze annual hydrological behavior in the particular area. Then, the mean groundwater table of the study area was roughly demarcated with aid of collected rainfall data and observations made from the existing wells.

Field work comprised of collection of soil and rock samples to perform laboratory tests. Furthermore, structural geological features (Dip and strike) and several other measurements (joint spacing, separation, condition of joint) dealing with rock which facilitate Slope Mass Rating analysis were gathered from the site.

Most of the collected samples were disturbed samples. Thus, it is necessary to provide actual site conditions prior to performing laboratory tests. Proctor compaction tests were performed on samples collected from top soil layer to get the maximum dry density and optimum moisture content and remolded the soil to 95% dry density to conduct direct shear test. Same tests were performed on samples obtained from highly weathered rock layer to determine cohesion and friction angle. Specific gravity test and UCS test were performed to selected rock samples.

Soil and highly weathered rock slope stability was analyzed by SLOPE W software. In order to analyze a rock slope, initially possible type of rock failure modes were identified using Georient software. If it showed some tendency to fail as plainer or toppling, Slope Mass Rating analysis was carried out to determine slope stability class. Further, a detailed analysis of wedge failure was carried out using GEO5 software.

3.3 Algorithm of Methodology

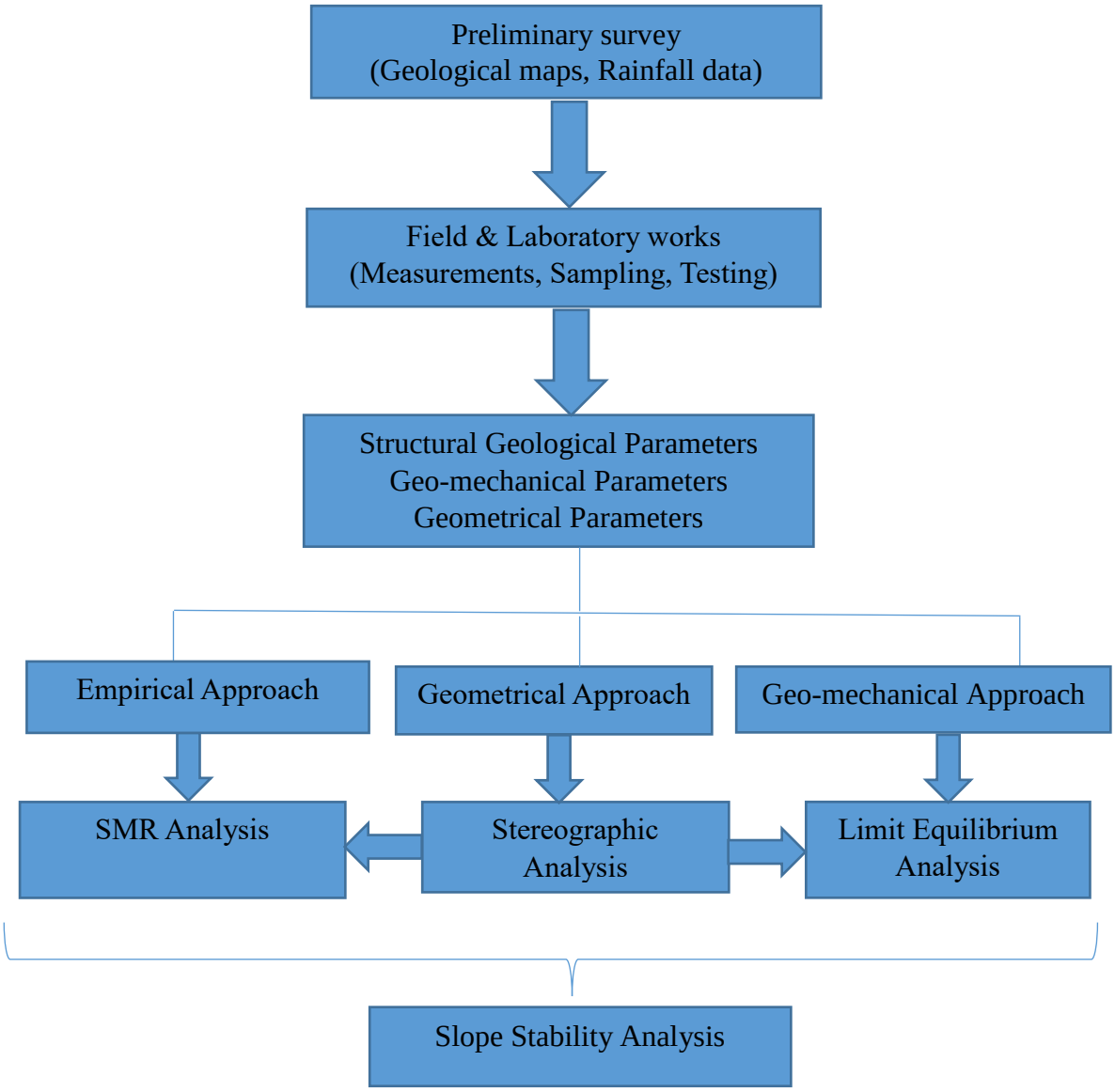

Figure 3-2: Flow chart of Methodology

3.4 Preliminary survey

3.4.1 Geology of area

The site area falls within the sheet 16: Colombo-Ratnapura (1:100,000) geological map (Figure 3-3). Regional geology of the area comprises high-grade lithologically and isotopically distinct Proterozoic Metamorphic rocks. Rocks of the area comprise

mainly Paragneissic lithologies of the Highland Complex of Sri Lanka. Here a series of Paragneisses garnet biotite gneisses, calc gneisses, hornblende biotite gneisses, cordierite gneisses, rare marbles, Quartzites and Quartz–Schists, Biotite bearing Quartzofeldspathic rocks, Garnet–Biotite–Sillimanite–Graphite Gneisses (Khondalites), Charnockitic Biotite Geisses is interlayered with each other and with more massive Charnockitic Geisses probably of both Para and Otho geneissic origin. Fault and fracture or major joint zones are extended in the direction of NE-SW across the study area. A major shear zone which extends in the direction of NW-SE has been identified few km away from the selected quarry site to the southwest and northeast of the quarry.

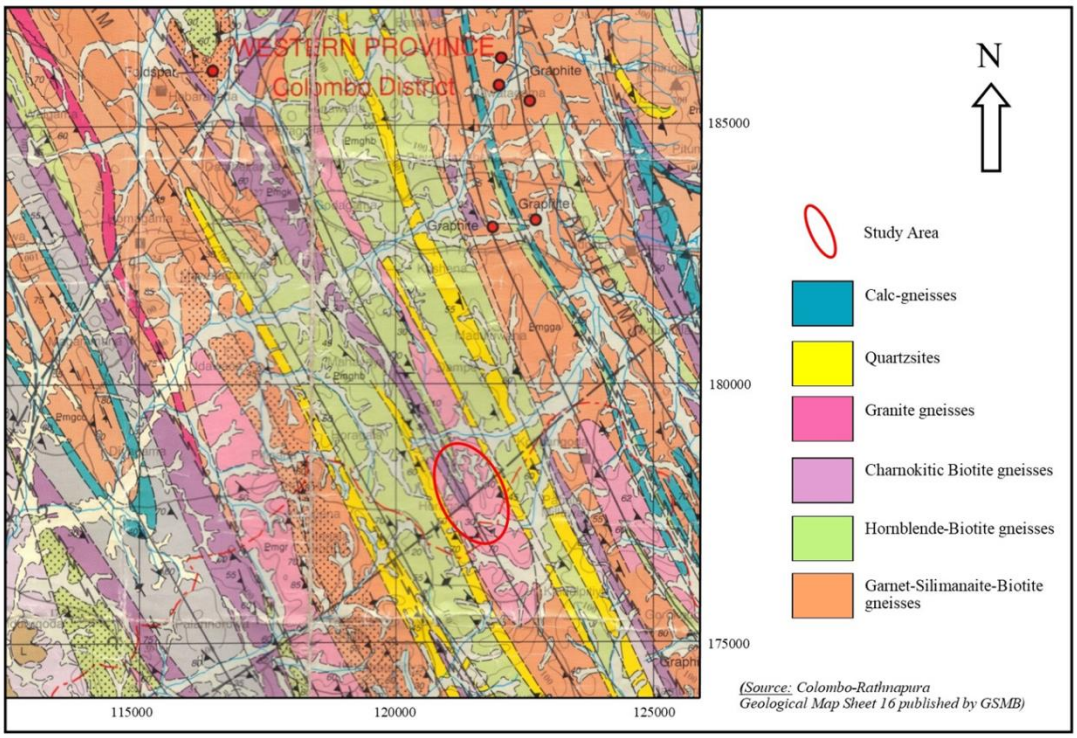

Figure 3-3: Area geological map

3.4.2 Prediction of periotic surface using annual precipitation data

Groundwater flow and rainfall infiltration play a vital role in slope stability. The amount of infiltration basically depends on land covering and land usage types. A considerable amount of rainfall is infiltrated into the ground and end up as groundwater. Therefore, determination of the condition of ground water for RMR

calculations, as well as prediction of the water table for limit equilibrium analysis are important in this research. Thus, rainfall data were gathered to analyze annual hydrological behavior of the particular area. Then, groundwater level from existing wells was determined and with the aid of rainfall data, ultimately, mean groundwater table of that particular area was roughly estimated. The analysis of hydrological data is shown in Section 4.

3.5 Rock, soil sample collection

The rock profile was visually observed and demarcated into zones in terms of top soil, highly weathered rock and fractured rock. Samples of disturbed soil and highly weathered rock layers were collected from the site to determine strength parameters of the profile. Two sampling locations as shown in Figure 3-1 were selected for the soil sample collection. In the case of top soil, surface was initially striped and disturbed samples were obtained. Further, disturbed rock samples were selected in six locations to facilitate SMR analysis.

3.6 Sample preparation for the laboratory test

Disturbed soil samples generally do not represent the actual site conditions. But, direct shear test can be carried out for a known density to simulate the natural site conditions. The maximum dry density and the optimum moisture content of the soil in concern can be obtained by conducting the Proctor compaction test. However, soil on the site may not be compacted to a maximum dry density although there is a possibility for compaction up to a certain level due to heavy vehicle movement. Considering this fact and preserving the conservativeness, 95% of maximum dry density was taken as the site compaction level and soil samples were subsequently compacted to achieve 95% of maximum dry density indicated by Proctor compaction test. Compacted soil samples were then collected into the core cutters and were dipped in water for 48 hours to achieve a fully saturated condition before carrying out the direct shear test.

Figure 3-4: Sample preparation for direct shear test

60×60×25mm cubic specimens were cut from highly weathered rock samples employing a micro cutter machine. Similar to the procedure for soil samples, highly weathered rock samples were also saturated before performing the direct shear test. Further, rock core samples of diameter 5 cm and height 10 cm were obtained using a mobile rock core cutter to perform UCS test.

Figure 3-5: Preparation of core sample

3.7 Tests on Overburden

3.7.1 Proctor compaction test procedure

Standard Proctor compaction test was carried out following the ASTM D 698.

About 6 kg of representative portion from the soil sample was separated. Sample was air dried at room temperature for 48 hours. The air dried sample was sieved using 19 mm sieve. The mass of the empty mold without the base plate was measured. Sufficient amount of water was added to the soil and mixed thoroughly to dampen it with an approximate water content of 4-6%. The soil was then placed in the mold in 3 layers and compacted using 25 well distributed blows per each layer with the 2.5 kg rammer falling through. Then the collar was removed, top of the compacted soil was trimmed using a straight edge. Afterwards, base was dismantled and the mass of the mold with the soil was measured. Soil was removed from the mold and small samples were taken to determine the moisture content. Subsequently, similar amount of water was again added to the soil and mixed properly to increase the moisture content by one or two percentage points and same procedure was repeated for each increment of water added. This series was continued until the mass of the mold and the soil reached a highest level and decreased.

3.7.2 Direct shear test procedure

The direct shear test was carried out following the ASTM D 5321.

The empty weight and dimensions of the core cutter were initially measured. Then the weight of core cutter with soil sample was measured. Saturated soil sample with shear box was assembled into the apparatus. All the dial gages were positioned and readings were set to zero. The loading plates were placed on top of the upper porous plate. The alignment screws which hold two halves of the shear box together were removed and a normal load of 50kN was applied. Then, the motor was started to achieve the anticipated constant rate of shearing. The readings of shear load from the proving ring, shear displacement, vertical displacement at every 10-division increment in horizontal dial gauge were recorded. Ultimately, the test was terminated once the shear loads started to reduce. Soil sample was removed and the procedure was repeated to 100kN and 150kN normal load combinations in a similar manner.

3.8 Slope stability analysis using Slope W software

3.8.1 Stepwise approach for slope stability analysis

The steps in analysis using Slope W software are illustrated by Figure 3-6 to 3-12.

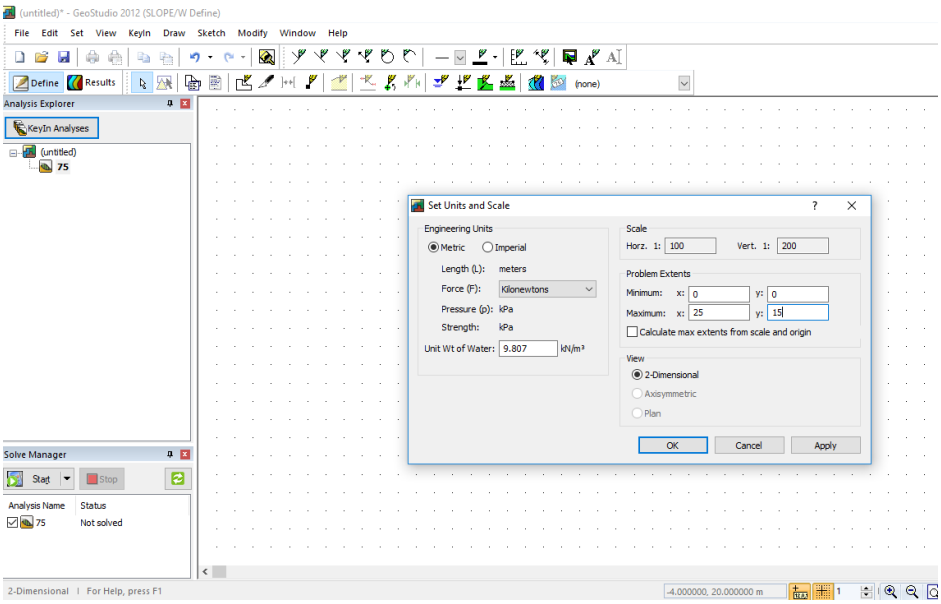

Figure 3-6: Opening a new project

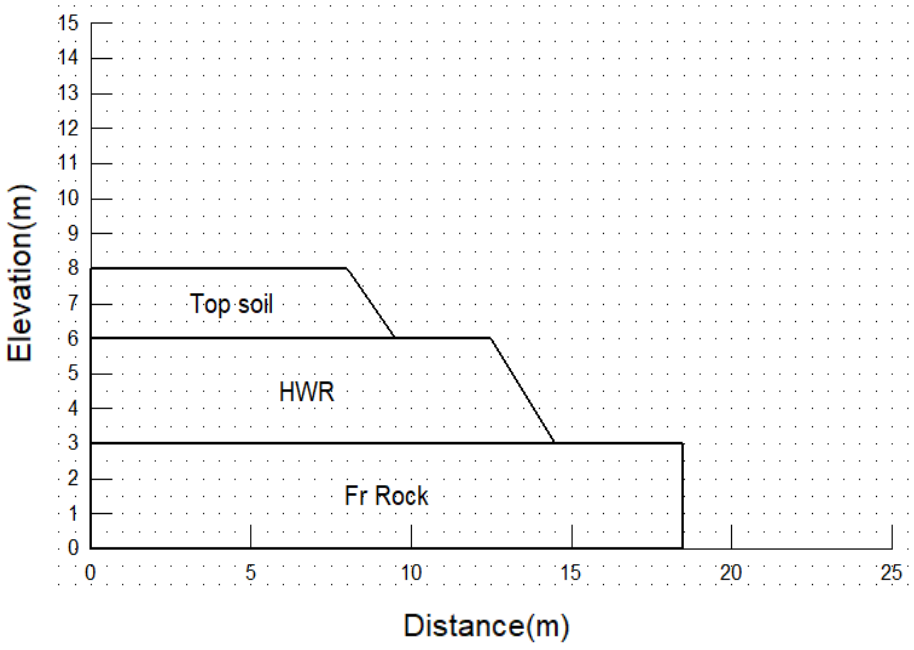

Figure 3-7: Draw the profile regions

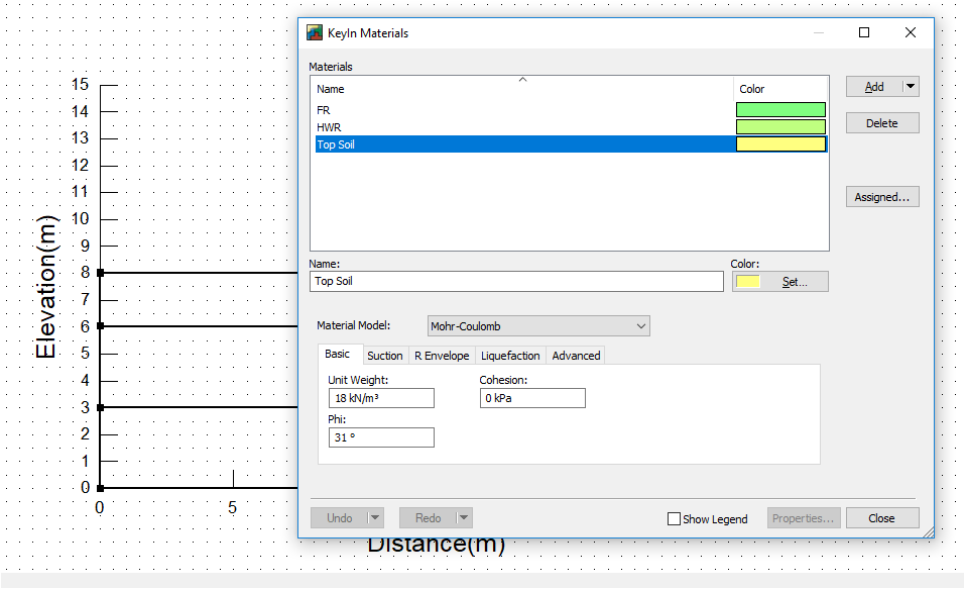

Figure 3-8: Introduce the material properties

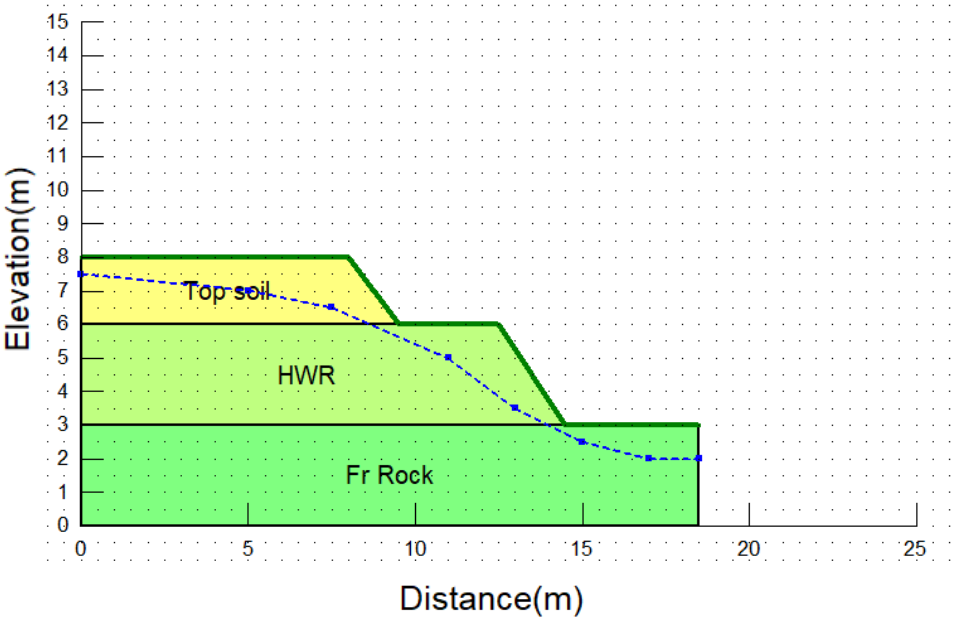

Figure 3-9: Define the phreatic line

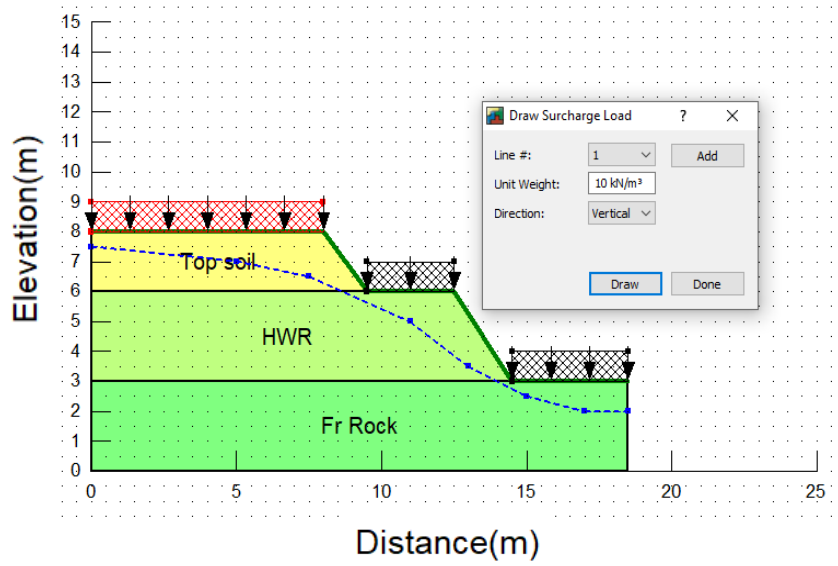

Figure 3-10: Introducing surcharge loads

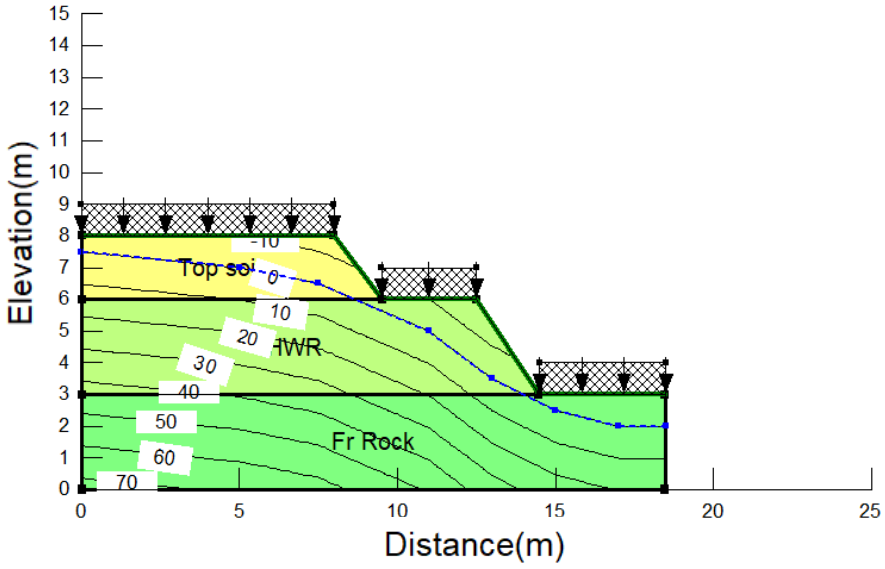

Figure 3-11: Generation of pore water pressure contours.

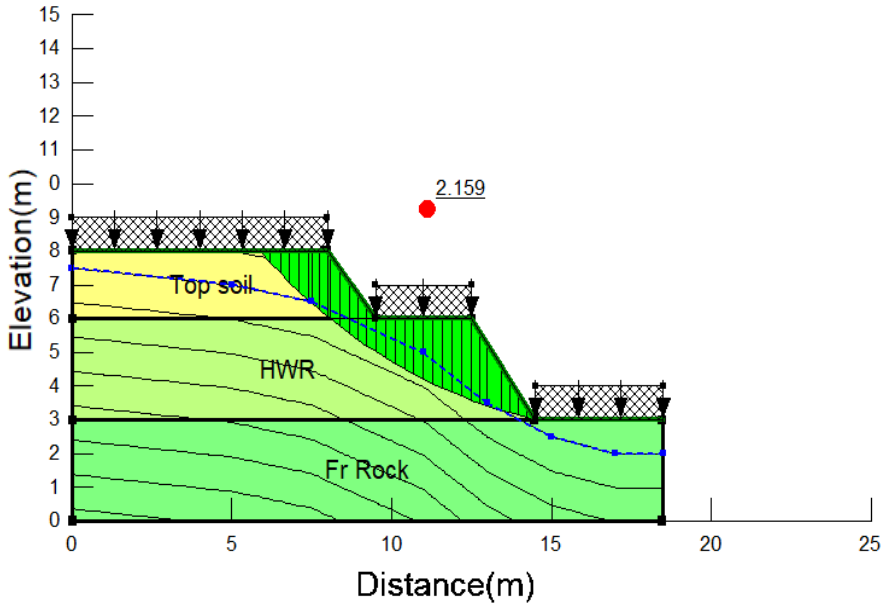

Figure 3-12: Obtaining slip surface with lowest FOS

3.9 Rock Mass Rating analysis

3.9.1 GPS coordinates of the positions

A GPS location tracker was used to obtain the coordinates where data were collected. To get the most accurate reading at least four satellites should be connected to the instrument. The Northing and Easting coordinates were recorded while taking the other supplementary readings (Figure 3-13).

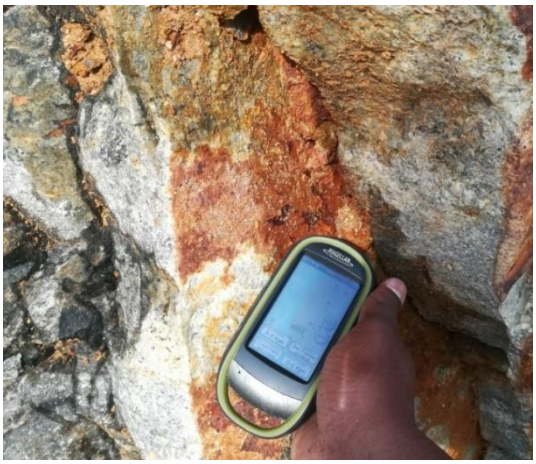

Figure 3-13: Obtaining of GPS coordinates of the locations

3.9.2 Measurement of parameters of major rock joint sets

The major rock joint sets were initially visually identified. The properties of joints such as spacing of the joint, discontinuity length, joint separation, roughness of joint, infilling, weathering condition and groundwater condition were measured to obtain Rock Mass Rating values.

3.9.3 Measuring of joint spacing

Spacing within a joint set is approximately same, but when there are several joint sets with the same dip, measuring of joint spacing was much more difficult. In such cases, the joint spacing was drawn to scale and the joint sets were differentiated.

Figure 3-14: Measuring of joint sets spacing

3.9.4 Measuring of joint separation

In certain cases, joint separation was negligible. In such cases accurate measuring of separation was very difficult. To mitigate such difficulties, a crack meter which has higher accuracy than a ruler was used. The minimum reading of the crack meter was 0.1mm. Apart from those aforementioned parameters, others were determined by visual observations.

Six locations were selected to collect rock joint properties so that whole study area will be covered. The field observation sheet of rock joint properties is attached in the ANNEX- A.

Figure 3-15: Measuring of joint separation

3.9.5 Attaining of RQD using joint spacing

Joints spacing were used to determine Rock Quality Designation. Average spacing of each joint set was obtained and RQD was calculated with aid of Equation (8) proposed by Palmstrom (1974). The outcomes will be discussed in Section 5.

3.9.6 Uniaxial Compressive Strength test

Uniaxial Compressive Strength plays a vital role in calculation of RQD. Three rock samples were collected from each and every location mentioned in Section 3.5 to perform the Uniaxial Compressive Strength test. When collecting the samples, it was ensured that rock specimen represents a particular area of the location. Core samples of 50 mm diameter and 100 mm height were obtained using the mobile core drilling machine for the test. The lab observation sheets are attached in the ANNEX- B.

3.9.7 Friction angle of rock mass

Among different correlations mentioned in the literature review section the relationship proposed by Aydan and Kawamoto (2001) Equation (3) was the most suitable model to calculate the friction angle of rock mass for this particular case.

3.10 Stereographic Projection

3.10.1 Measurement of dip, strike and dip direction using Brunton compass

In the current study, the dip and strike of foliation and joints were measured using a Brunton pocket transit. Measuring was commenced by taking the strike of the discontinuity plane. In order to measure the strike, the edge of the compass was placed against the plane of the discontinuity. Then the compass was tilted by keeping lower side edge of the compass fixed, until the circular level bubble was centered. With the circular bubble centered, the number of the compass needle was recorded as the strike/direction of joint plane (Figure 3-16).

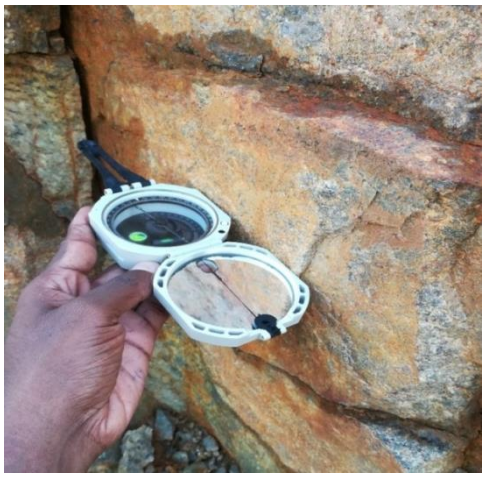

Figure 3-16: Measuring of strike of the joint and foliation

Figure 3-17: Measuring of dip angle of discontinuity

To measure the dip of the discontinuity plane, compass was put with its side against the rock (Figure 3-17). It was done easily by rotating the compass by 90 degrees angle. Then clinometer was rotated until tube bubble was centered. After centering, clinometer value was recorded as the dip of the discontinuity.

To obtain dip direction, compass front was directed to the dipping direction of the discontinuity (Figure 3-18). Then needle direction was measured as SW, NW, NE, SE etc. The field observation sheets of discontinuities are attached in the ANNEX - C.

Figure 3-18: Obtaining of dip direction

3.10.2 Stereo plot study using Georient software

Three cut faces were mainly identified in this particular quarry site. Coordinates of discontinuity, strike of discontinuities and cut slope, dip angle and dip direction were tabulated for each cut face.

3.10.2.1 Stepwise approach for Georient analysis

The steps in using Georient software are illustrated by Figure 3-19 to 3-21.

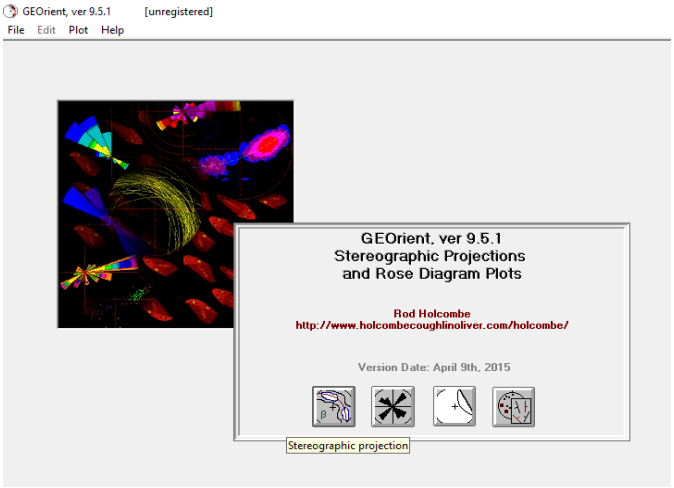

Figure 3-19: Selection of analysis

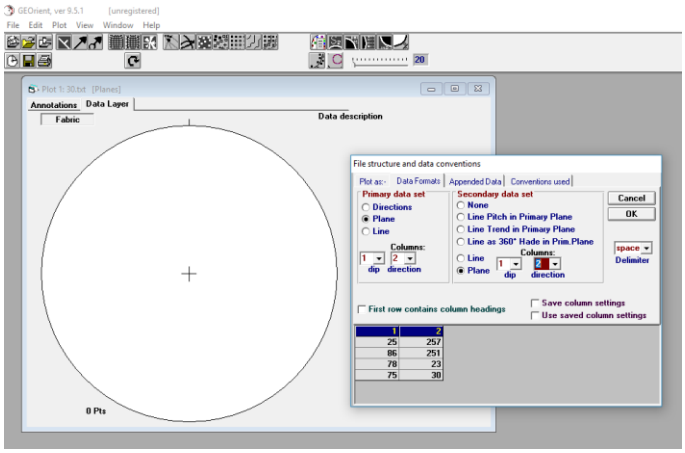

Figure 3-20: Selection of data format

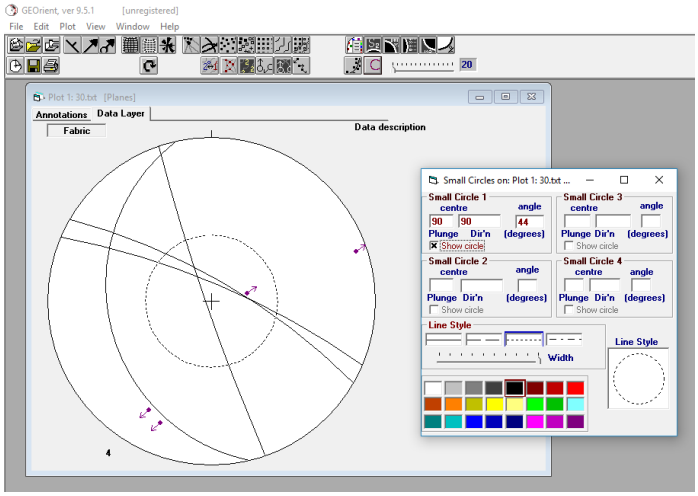

Figure 3-21: Introducing of friction angle

3.10.2.2 The methodology involved in obtaining dip and dip direction of joint sets

The raw data structural geological features were converted into dip / dip direction format and saved as a text file format since it is the convenient format in which data can be fed into the Georient software.

Three data sets (three faces) were separately introduced into the software and the pole concentrated contour maps were obtained using number of main joint sets identified on each and every face. Calculations of dip and strike of major joint sets are shown in Section 4.

3.11 Slope Mass Rating system

Among six locations, 1st and 2nd locations were in the first face, 3rd and 4th locations were selected on the second face and 5th and 6th locations lied on the third face. Two RMR values were calculated for each face. Therefore, two Slope Mass Ratings were separately calculated with respect to each RMR value. The way of analysis according to Slope Mass Rating system is explained in Section 4.

3.12 Rock stability analysis using GEO5 software

3.12.1 Validation of GEO5 software

The Thalathu Oya Quarry site is a case where rock slope failure had occurred in an open pit mine in Sri Lankan context. In this particular research GEO5 software was used to analyze the rock slope stability. But software should be validated via a real example, before use. Geological and geotechnical data of Thalathu Oya site had been obtained to validation purpose from the research (Criteria to Assess Rock Quarry Slope Stability and Design in Landslide Vulnerable Areas of Sri Lanka) done by Samarawickrama (2014). The detail of the validation process is explained in Section 4.

3.12.2 Steps involved in slope stability analysis using GEO5 software

Set the analysis method and analysis type to standard safety factor and plane slip surface respectively (Figure 3-22). This is because this slope has been failed as a plain failure case.

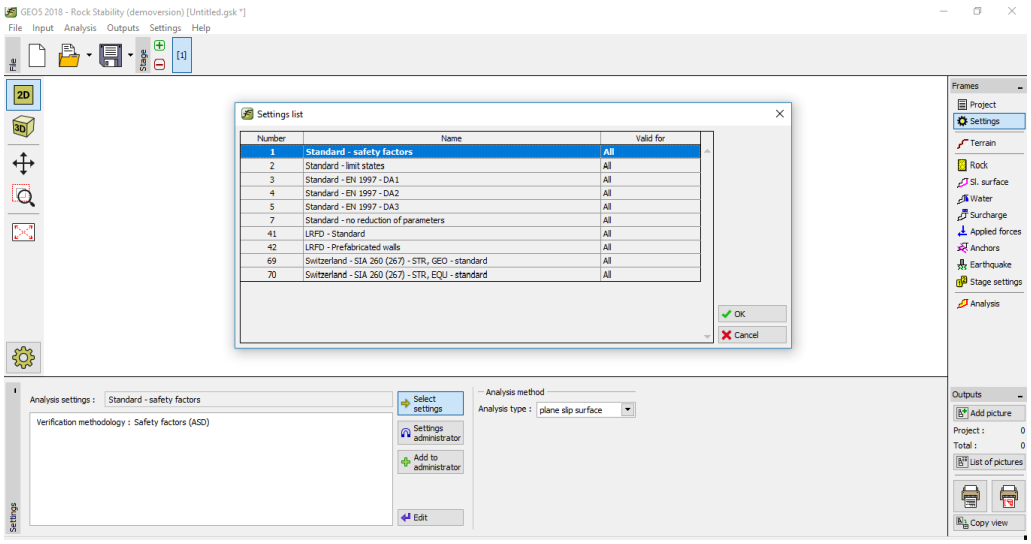

Figure 3-22: Selection of analysis method

Inclination and length input type used to define the site geometry of the cross section (Figure 3-23).

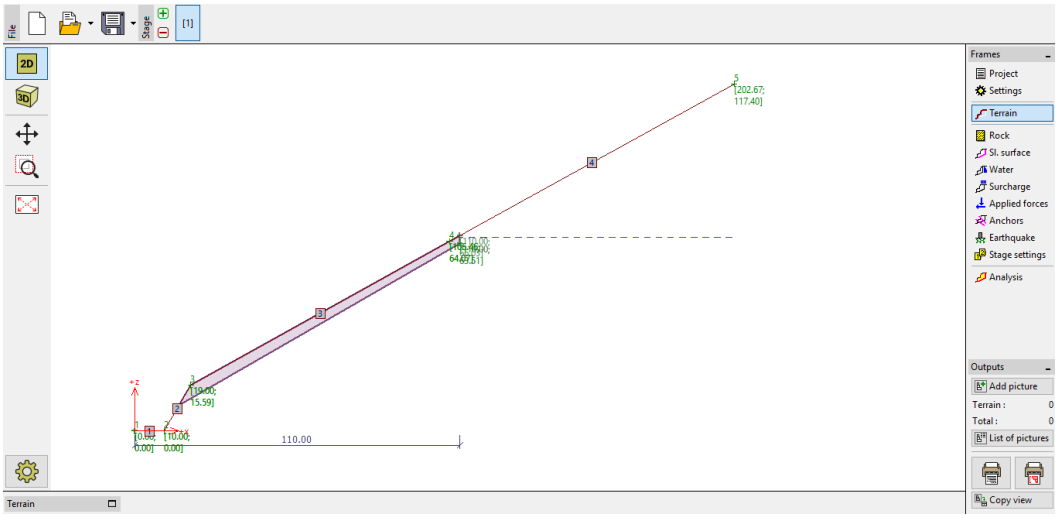

Figure 3-23: Defining of geometry

Cohesion, friction angle and unit weight of rock are inserted at this stage. Furthermore a Mohr coulomb criteria is selected as analysis method (Figure 3-24).

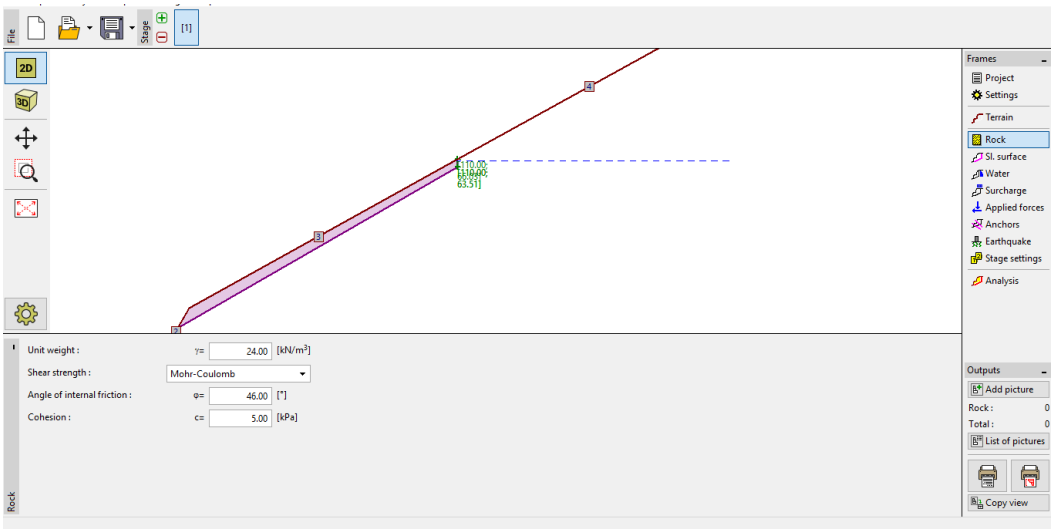

Figure 3-24: Introducing design parameters

Isometric view of slope geometry can be seen (Figure 3-25). Thereafter properties of slip surface and tension crack would be input (Figure 3-26) and ground water condition should be defined (Figure 3-27). There after rock slope analysis is carried out by the software (Figure 3-28).

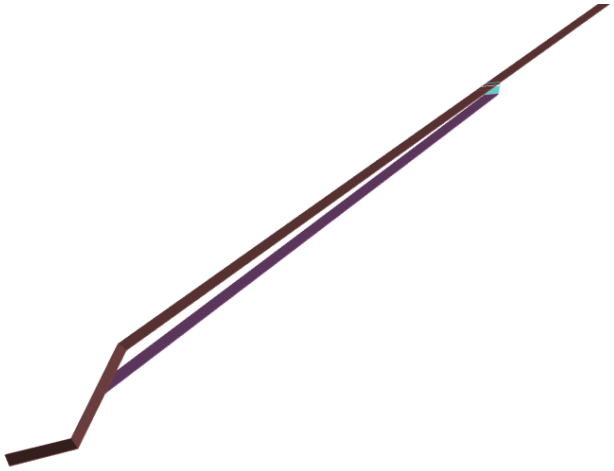

Figure 3-25: Isometric view of slope geometry.

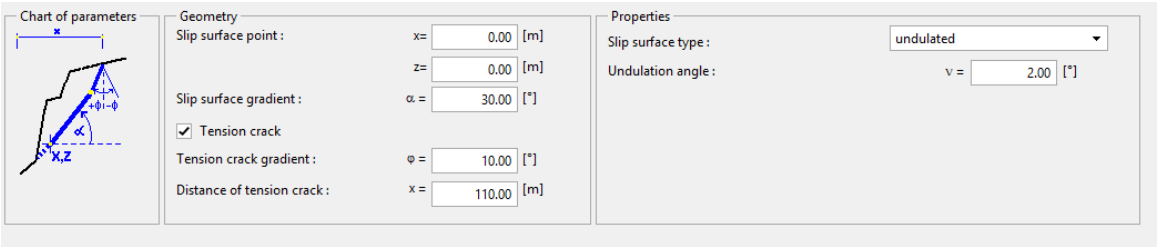

Figure 3-26: Properties of slip surface and tension crack

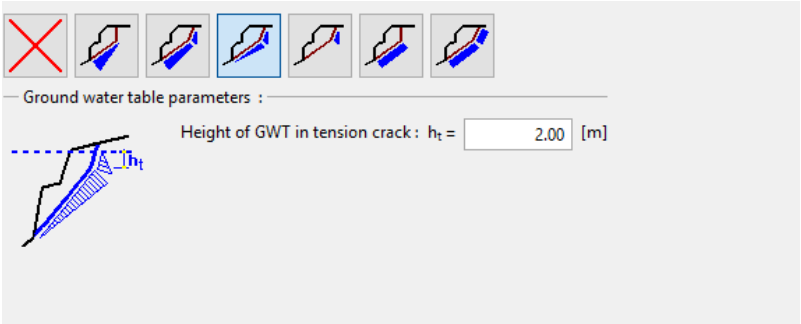

Figure 3-27: Defining of ground water condition

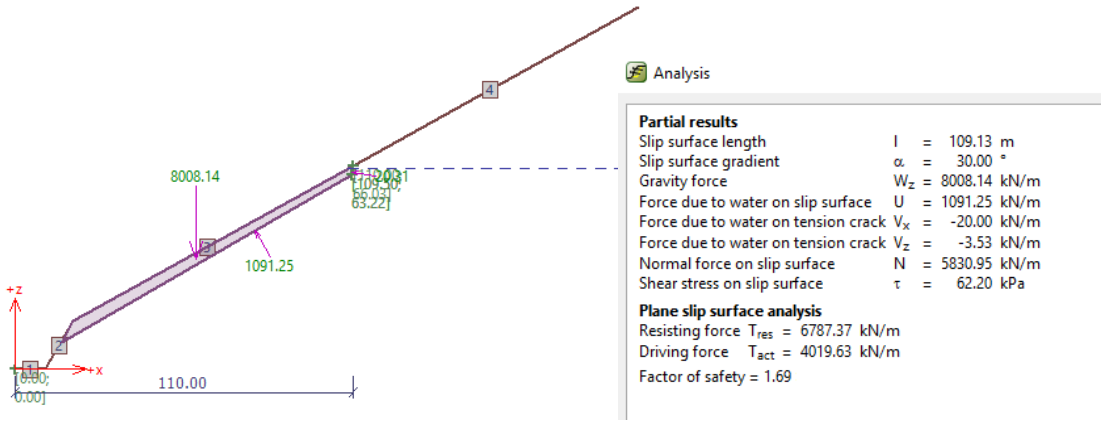

Figure 3-28: Analysis of rock slope stability

3.12.3 Wedge failure identification

Since the rock mass cannot be modeled using finite element software (due to complexity of the geometry and material parameters involved) fractured rock slope stability analysis was performed by GEO5 software. Potential wedge failure cases can be identified with aid of Stereographic analysis. As shown in Table 5-8 possible wedge geometry and properties introduced to the GEO5 software and factor of safety against failure was determined. The analysis of wedge failure is discussed in Section 4.

3.12.4 Specific gravity test procedure for rock

A small piece of rock samples were selected from each six locations. Samples were saturated about five days to absorb water into the void space and each sample was weighted in the air. Then those were submerged into the water with aid of holder and the weight was measured. The lab observation sheet for specific gravity test is attached in the ANNEX- D. Example calculations for the specific gravity test and determination of surcharge load are shown in Section 4.

4 ANALYSIS OF DATA

4.1 Analysis of annual precipitation data

Figure 4-1 to 4-5 show monthly rainfall variation from 2014 to 2018 in the vicinity of the selected area. Figure 4-6 shows the cumulative annual precipitation of same location. According to Figure 4-6, it shows relatively higher rainfall in 2017 and average annual rainfall is just above 3000 mm. With aid of these data and surrounding domestic well water condition, the prediction of average ground water table will be discussed in Section 5.

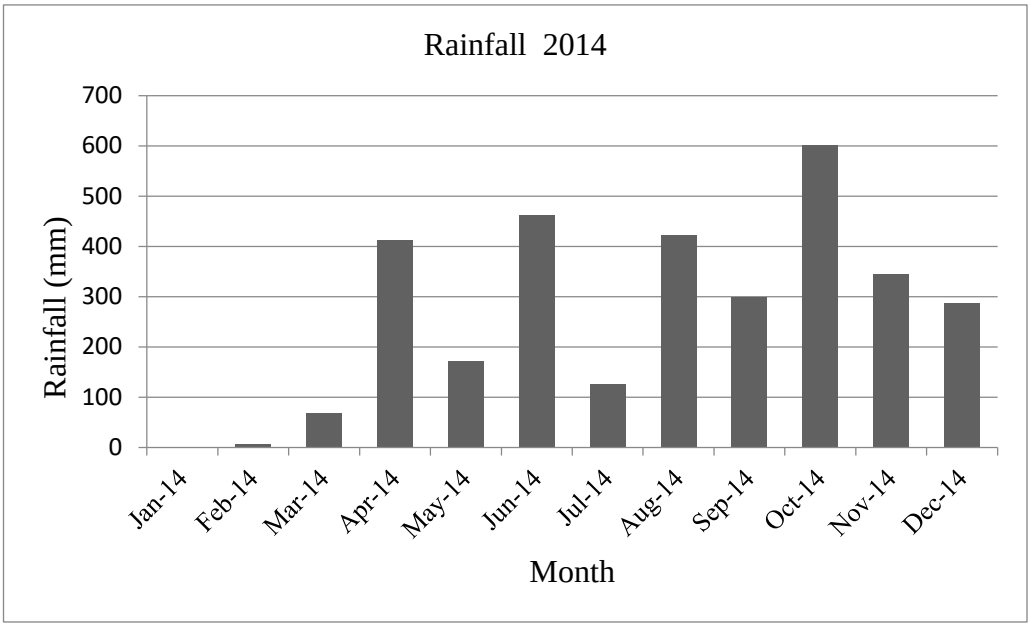

Figure 4-1: Monthly rainfall variation in 2014

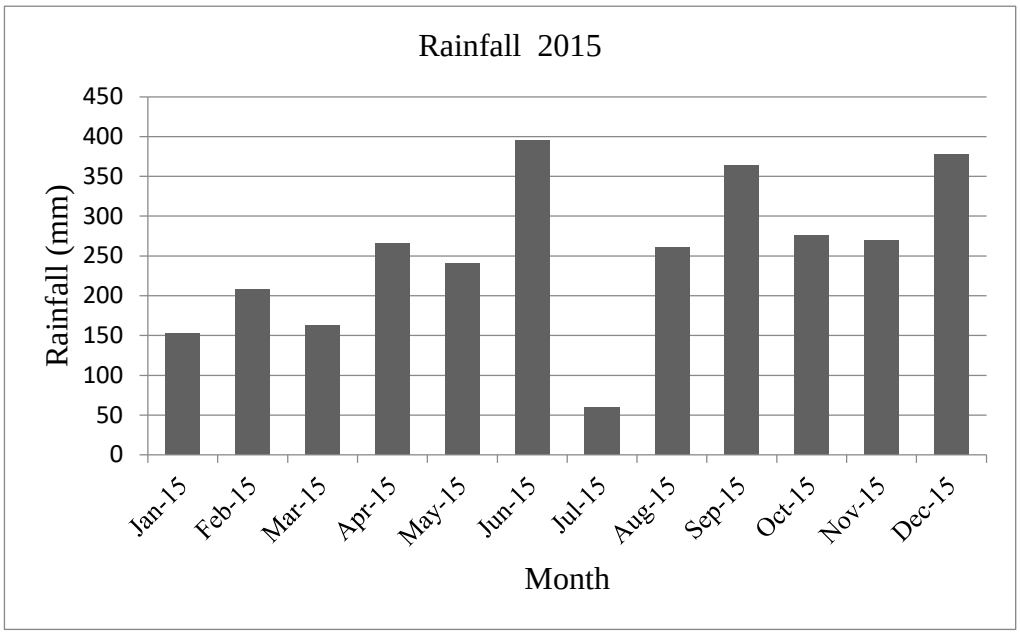

Figure 4-2: Monthly rainfall variation in 2015

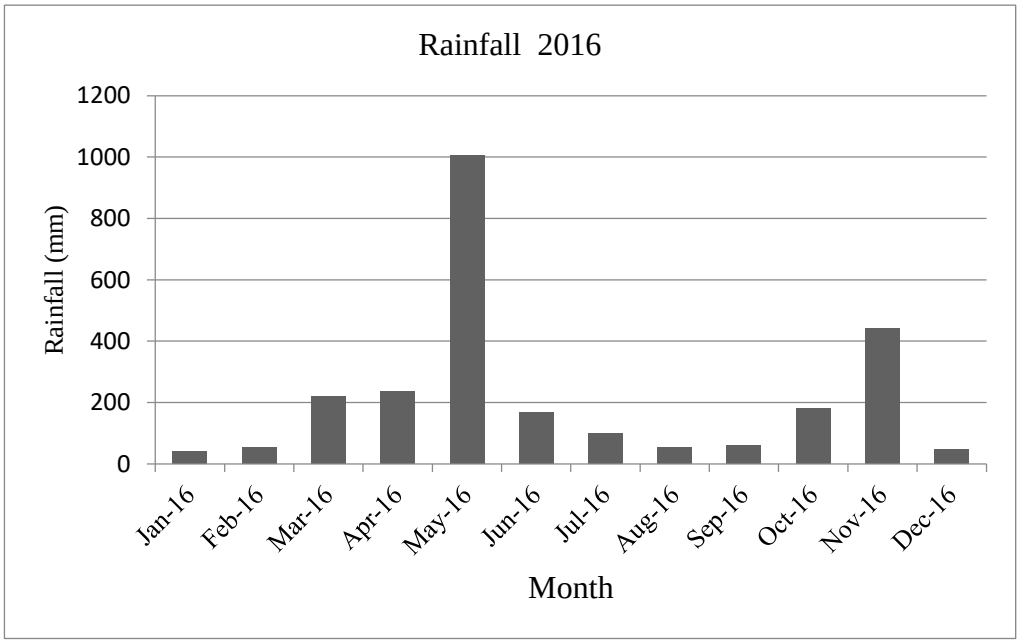

Figure 4-3: Monthly rainfall variation in 2016

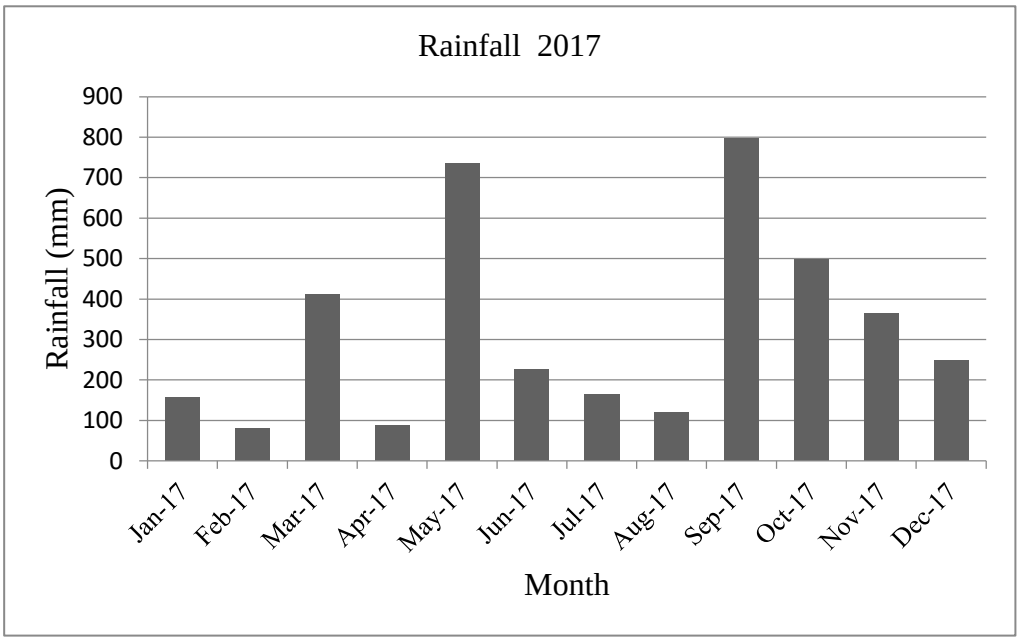

Figure 4-4: Monthly rainfall variation in 2017

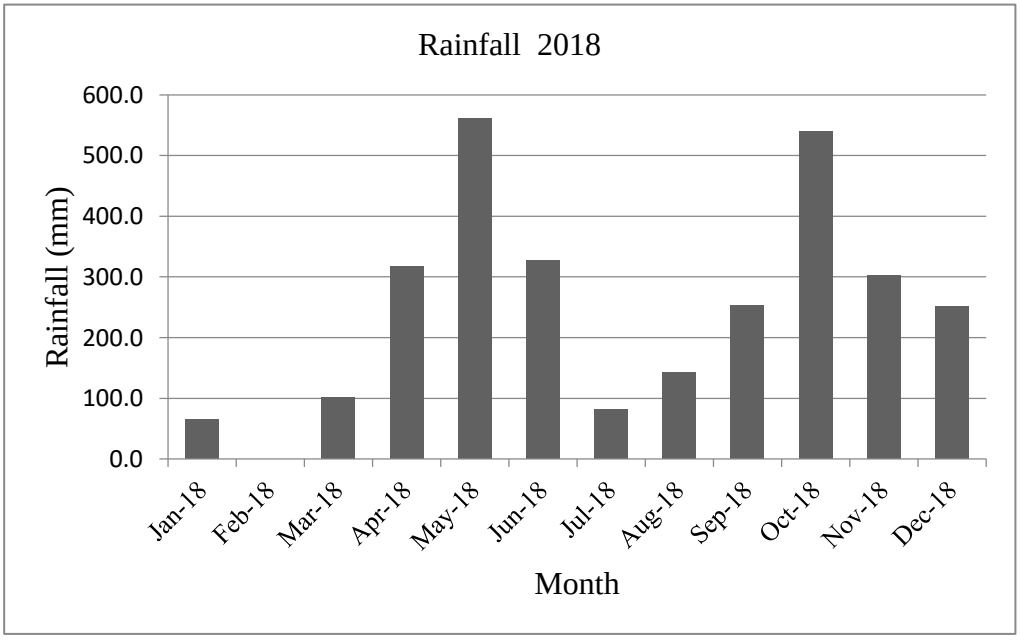

Figure 4-5: Monthly rainfall variation in 2018

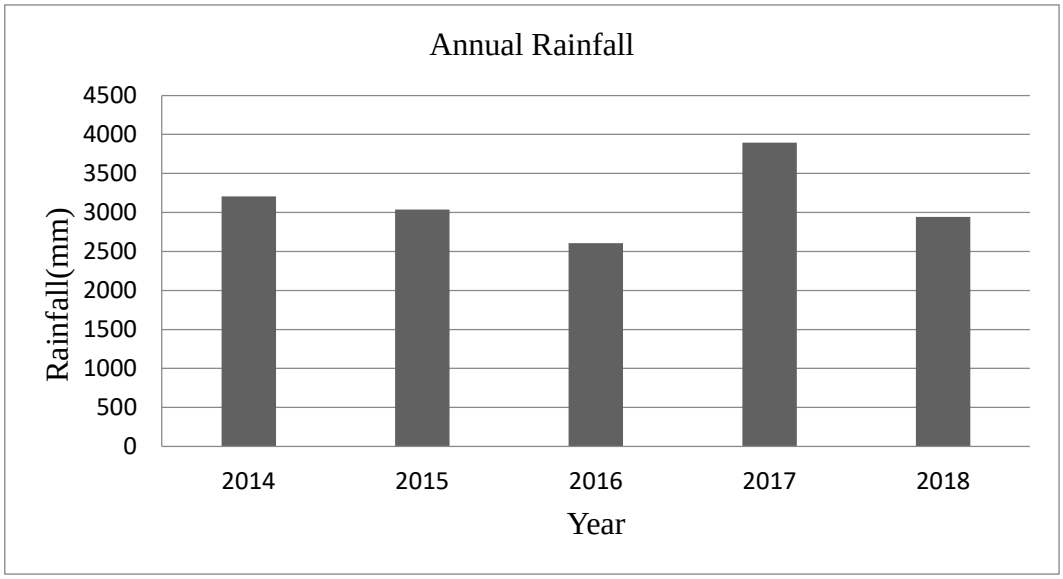

Figure 4-6: Annual rainfall variation

4.2 Overburden slope stability analysis

A sample calculation for determining the dry density of the sample 1 of top (overburden) soil is shown below. The lab observation sheets are attached in the ANNEX- E.

Table 4-1: Calculation of dry density of soil

Description	Amount
Weight of sample +mold	5780.00 g
Weight of mold	3995.30 g
Volume of mold	965 cm^3
Bulk density of soil	1.849 g/cm^3
Weight of Container	14.80 g
Weight of wet Sample + Container	39.70 g
Weight of dry Sample + Container	38.07 g
Weight of water	1.63 g
Weight of dry sample	23.27 g
Moisture Contents	6.68%
Dry density of soil	1.733 g/cm^3

The proctor compaction curves are shown in Figure 4-7, 4-8

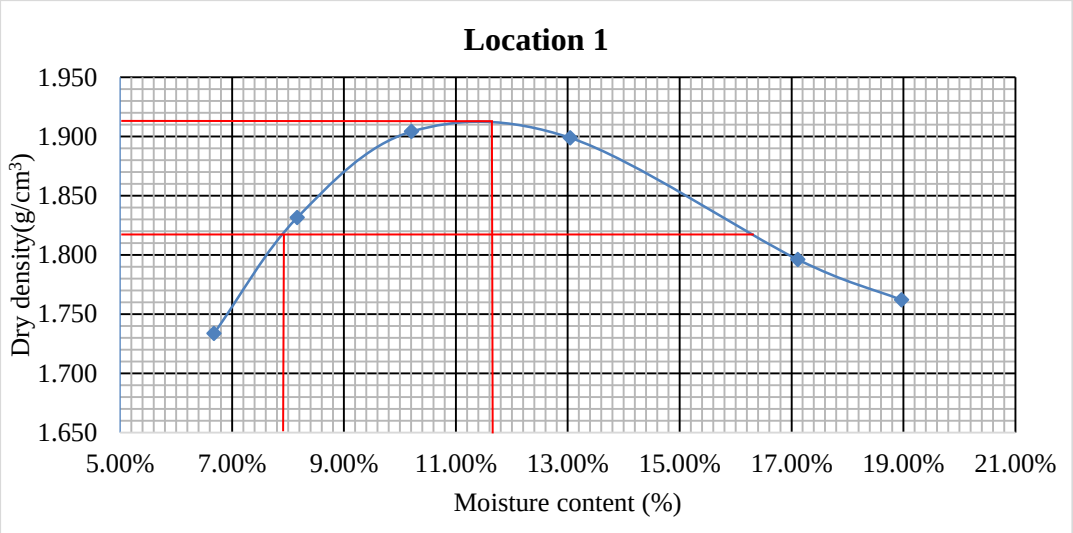

Figure 4-7: Variation of dry density of soil against moisture content for Location 1

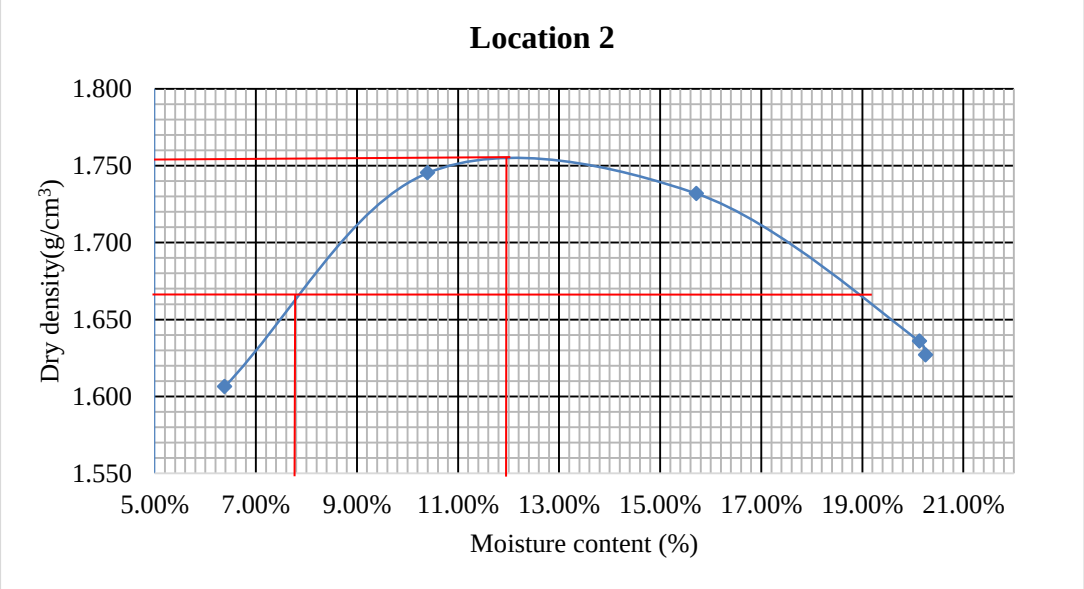

Figure 4-8: Variation of dry density of soil against moisture content for Location 2

Direct shear test was performed to samples collected from top soil layer as well as highly weathered rock layer in order to find shear strength parameters, cohesion and

friction angle. Three specimens were subjected to the direct shear test under 50kN, 100kN, 150kN normal loads per location. Laboratory observation sheets are attached in the ANNEX- F.

Calculations related to direct shear test readings for sample no 1 is shown below Table 4-2. Similarly, the same calculation procedure was carried out for each test.

Table 4-2: Calculation of shear stress of overburden soil

Description	Value
1 division of horizontal dial gauge reading	0.01mm
1 division of proving ring reading	1.707N/div
For shear displacement 10 div	0.1mm
Shearing area	3594mm^2
Corresponding proving ring reading	42.675
Shear stress	11.87 kN/m^2

The results of the direct shear tests are shown in Figure 4-9 to 4-12 for overburden soil at Location 1.

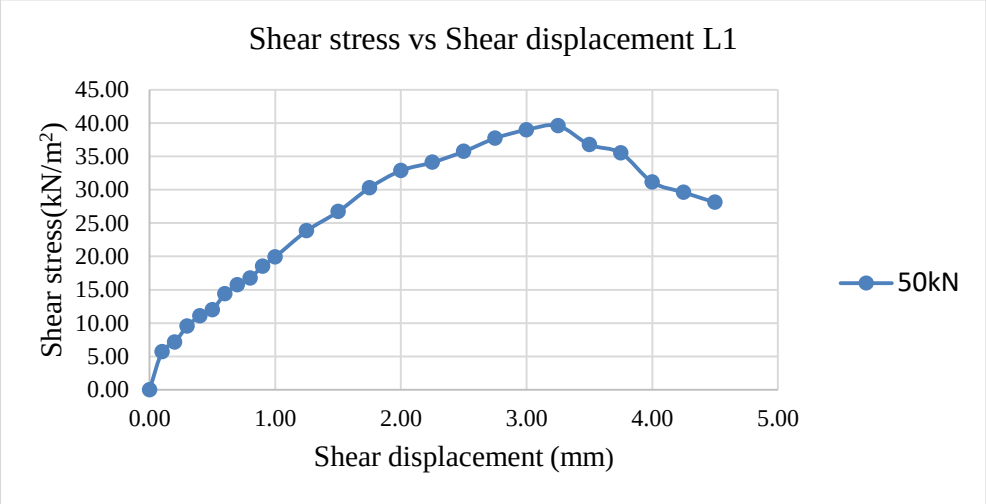

Figure 4-9: Shear stress against shear displacement curve for overburden soil under 50KN normal load at Location 1

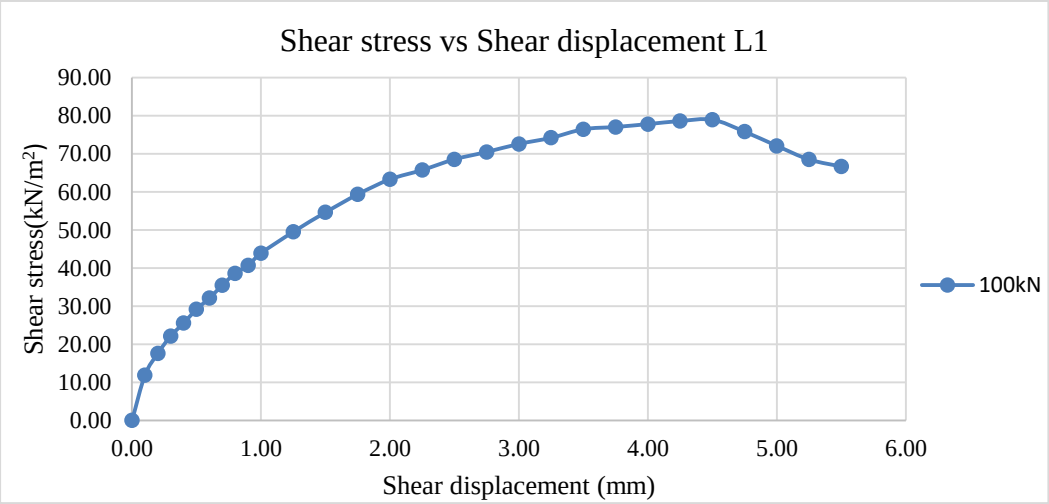

Figure 4-10: Shear stress against shear displacement curve for overburden soil under 100KN normal load at Location 1

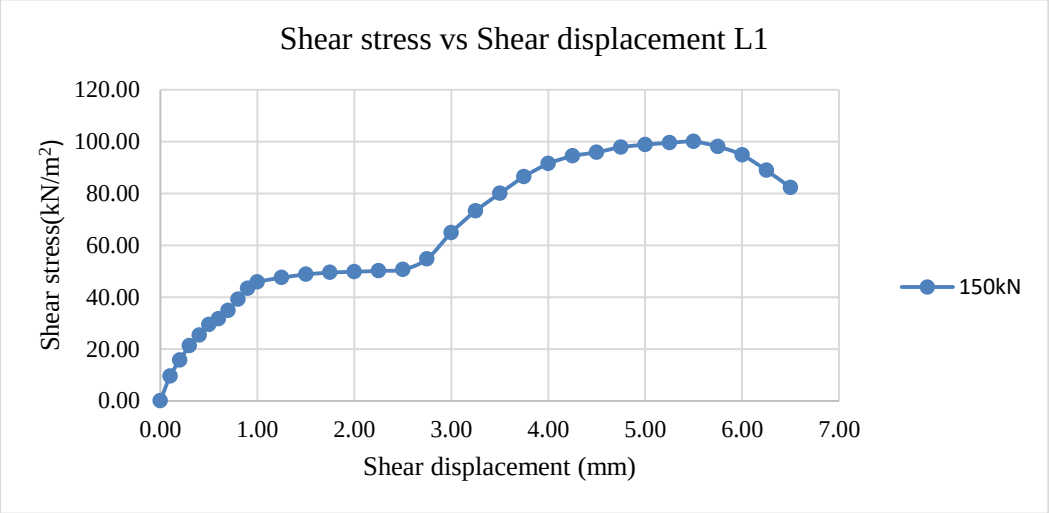

Figure 4-11: Shear stress against shear displacement curve for overburden soil under 150KN normal load at Location 1

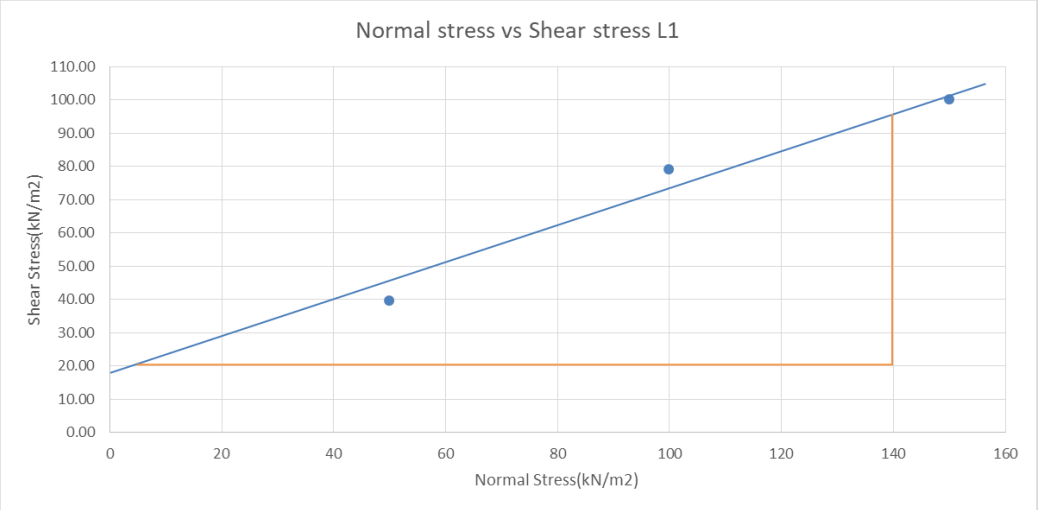

Figure 4-12: Shear stress against normal stress curve for overburden soil at Location 1

The maximum shear stress was obtained from Figure 4-9 to 4-11 showing shear stress against shear displacement. Cohesion and friction angle were calculated with the aid of Y intercept and gradient from Figure 4-12 plotted for maximum shear stress vs normal stress.

The results of the direct shear test are shown in Figure 4-13 to 4-16 for overburden soil at location 2.

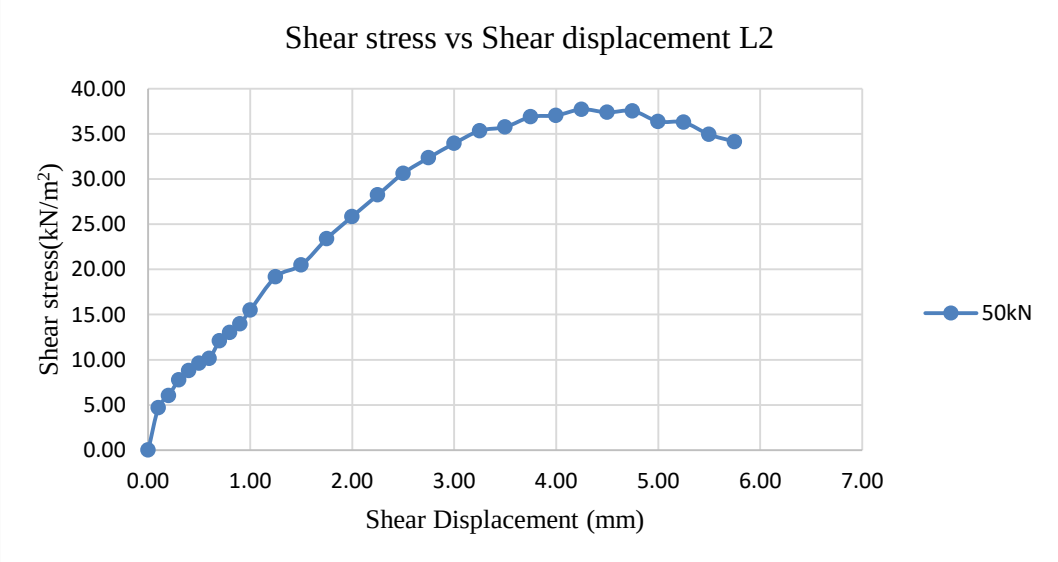

Figure 4-13: Shear stress against shear displacement curve for overburden soil under 50KN normal load at Location 2

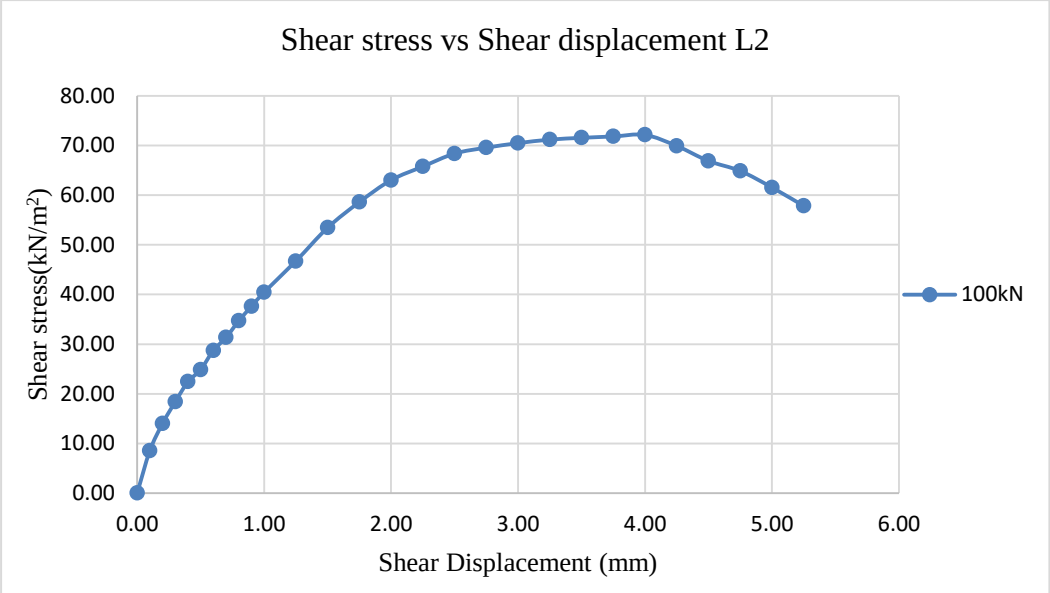

Figure 4-14: Shear stress against shear displacement curve for overburden soil under 100KN normal load at Location 2

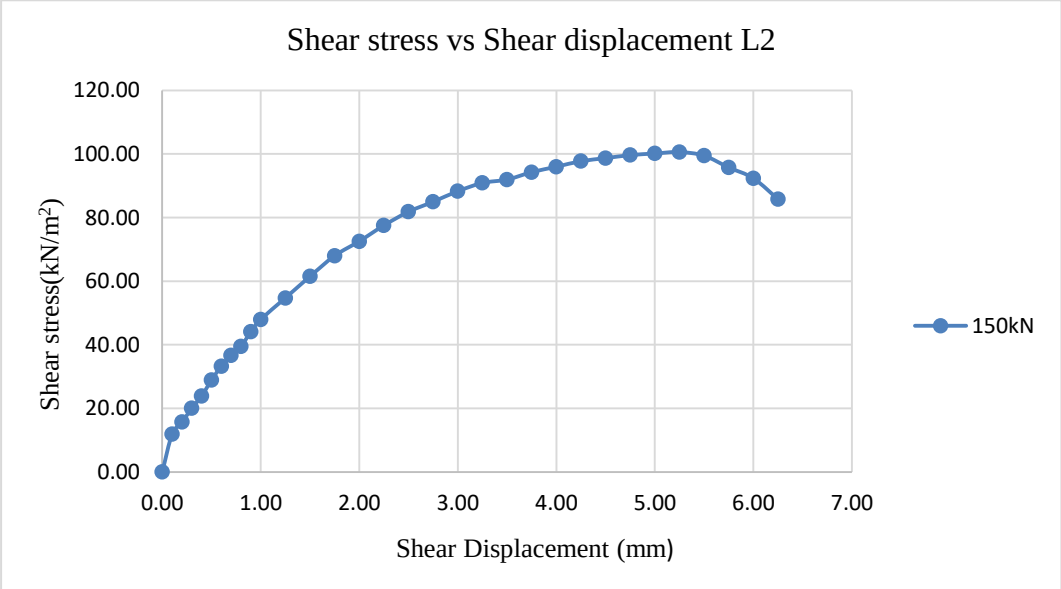

Figure 4-15: Shear stress against shear displacement curve for overburden soil under 150KN normal load at Location 2

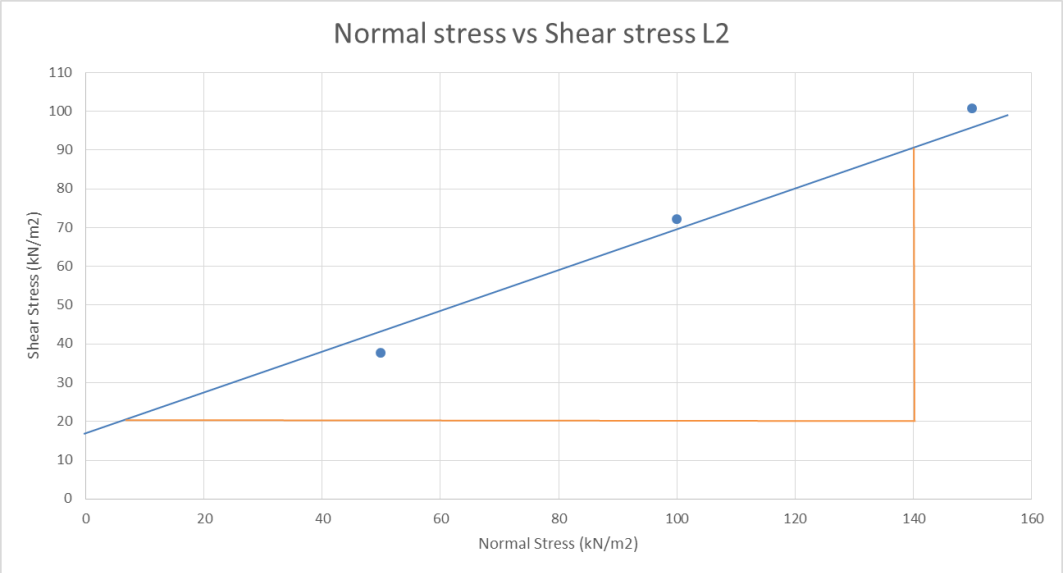

Figure 4-16: Shear stress against normal stress curve for overburden soil at Location 2

The results of direct shear tests for highly weathered rock at location 1 are shown on Figures 4-17 to 4-20.

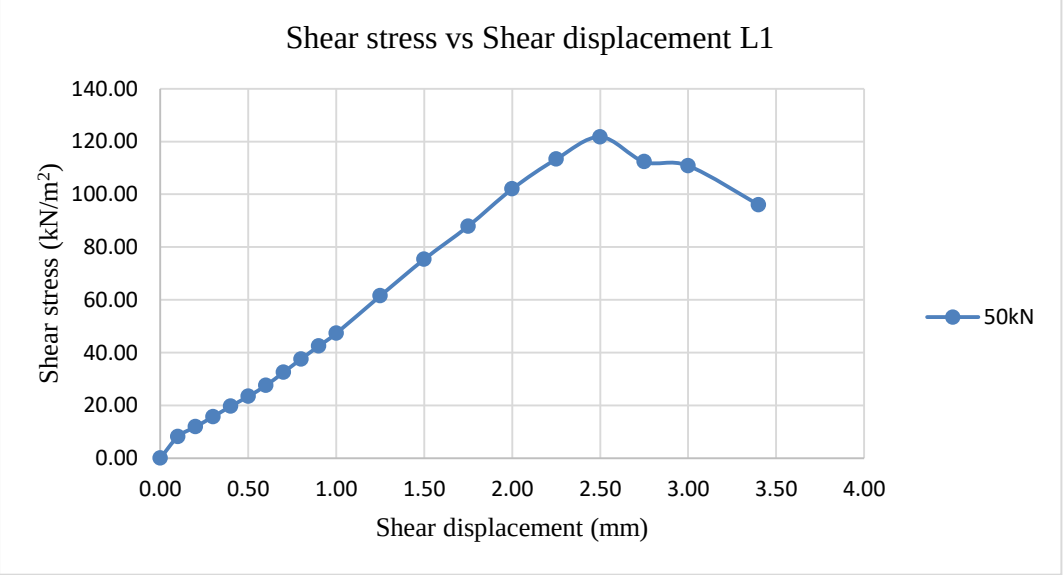

Figure 4-17: Shear stress against shear displacement curve for highly weathered rock under 50KN normal load at Location 1

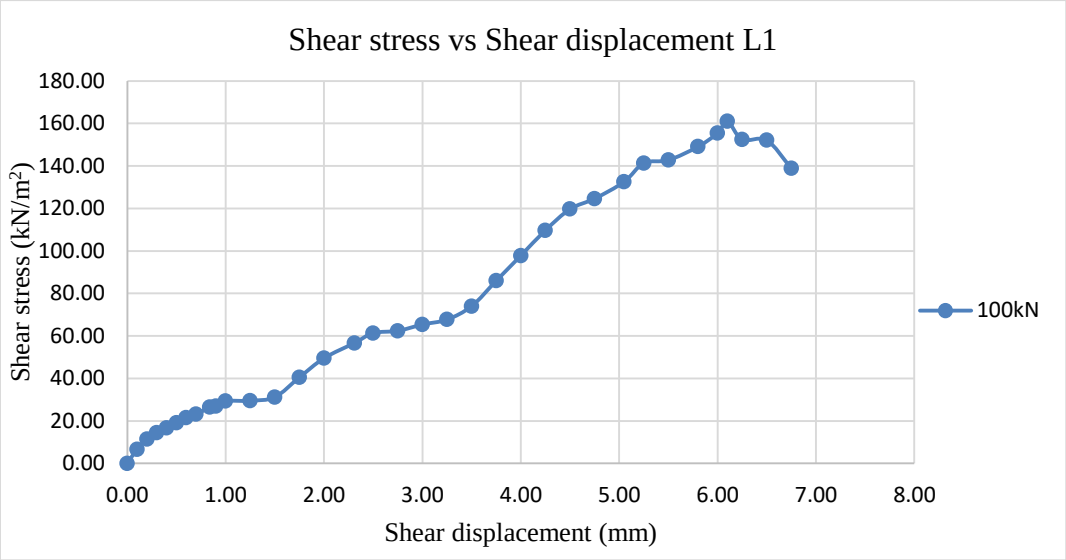

Figure 4-18: Shear stress against shear displacement curve for highly weathered rock under 100KN normal load to Location 1

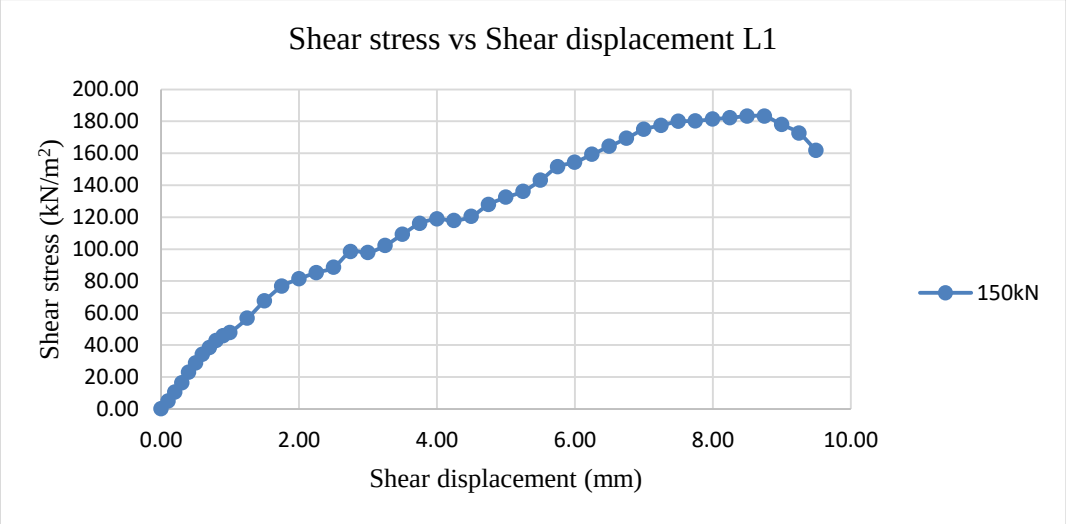

Figure 4-19: Shear stress against shear displacement curve for highly weathered rock under 150KN normal load to Location 1

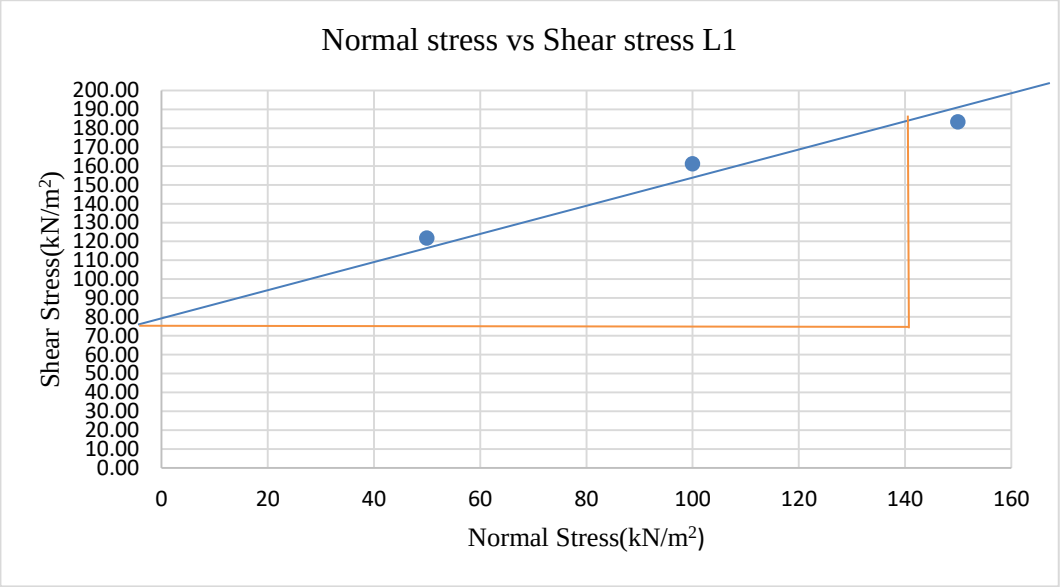

Figure 4-20: Shear stress against normal stress curve for highly weathered rock for Location 1

The results of direct shear tests for highly weathered rock at location 2 are shown in figures 4-21 to 4-24.

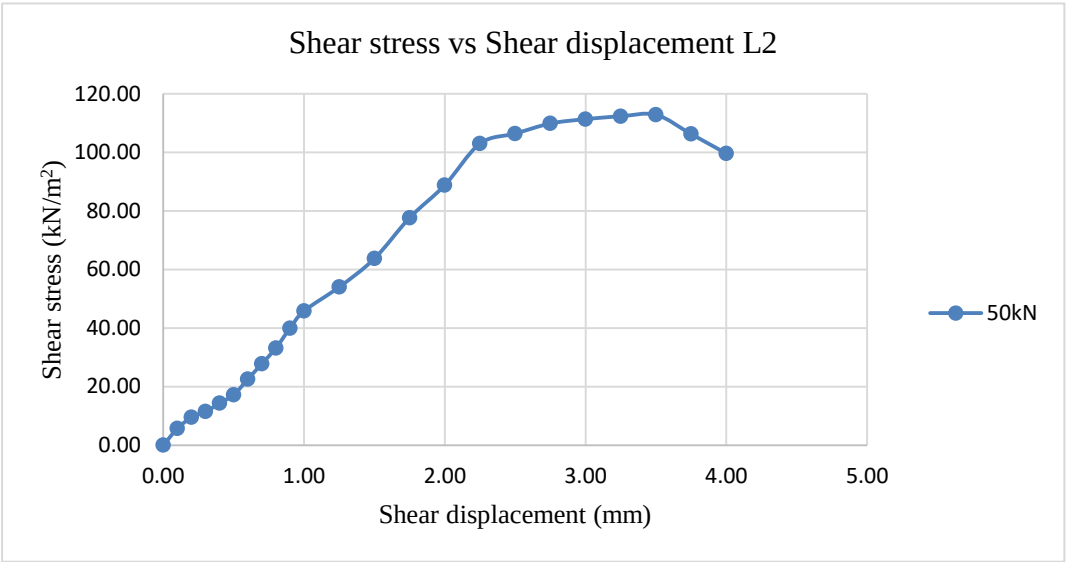

Figure 4-21: Shear stress against shear displacement curve for highly weathered rock under 50 KN normal load to Location 2

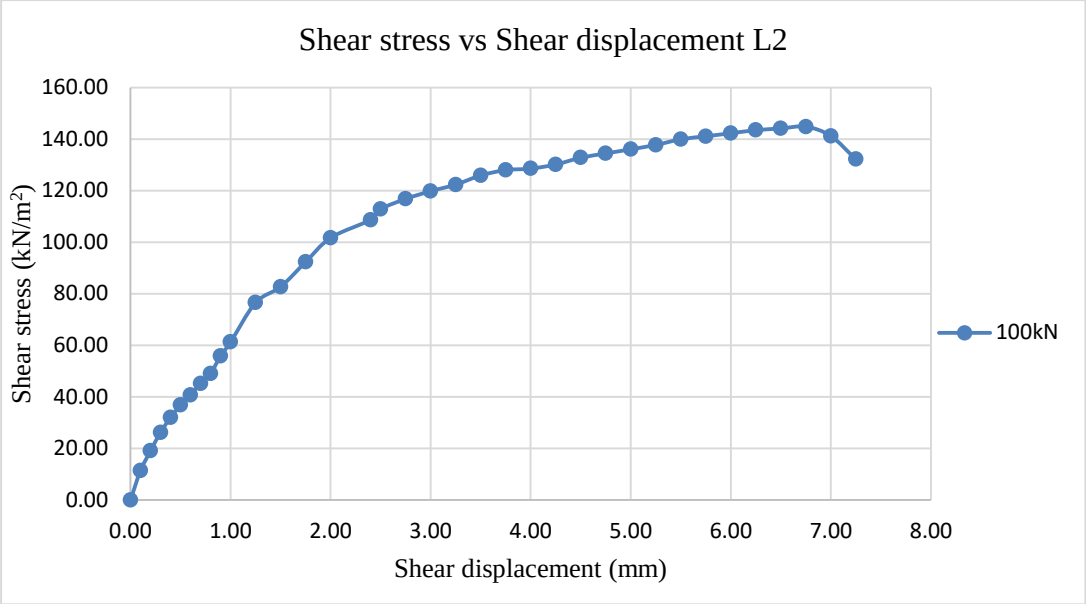

Figure 4-22: Shear stress against shear displacement curve for highly weathered rock under 100 KN normal load to Location 2

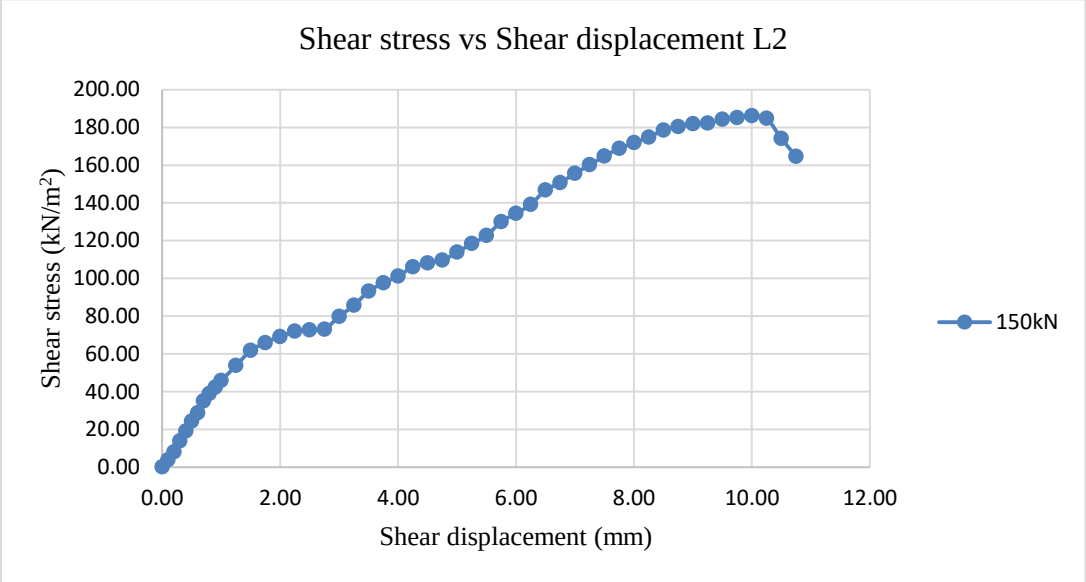

Figure 4-23: Shear stress against shear displacement curve for highly weathered rock under 150 KN normal load to Location 2

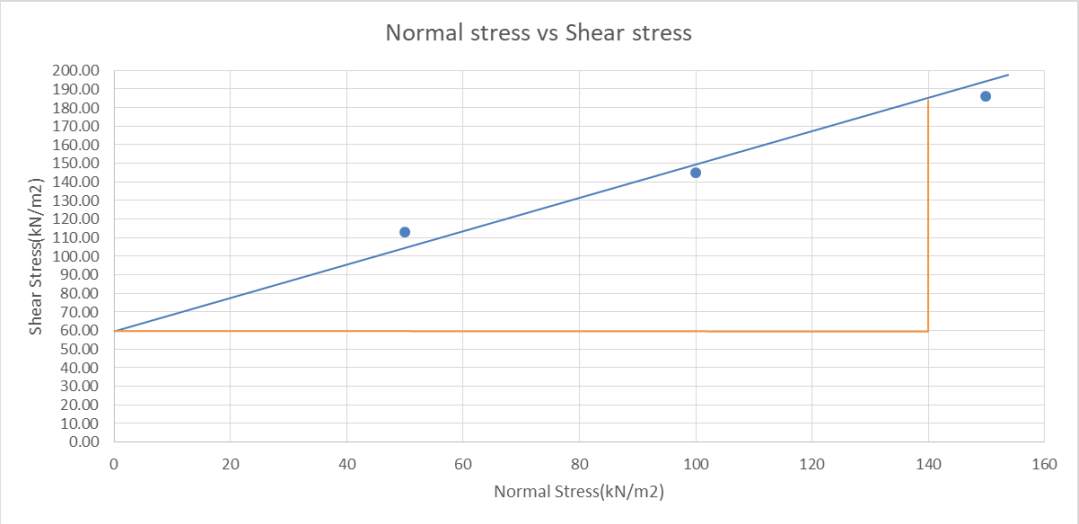

Figure 4-24: Shear stress against normal stress curve for highly weathered rock for Location 2

Calculated cohesion friction angle and unit weights of overburden soil profile is tabulated in Table 5-1 and discussed in Section 5. The shear strength parameters obtained from the above step, minimum friction angle and half of minimum cohesion of soil and HWR among two locations were used for Slope W analysis as conservative way.

4.2.1 Slope stability analysis via Geo Studio software

Slope stability analysis was executed for single bench as well as multiple bench operations. Each bench was analyzed for its stability by varying the slope angle from 45 to 75 degrees using Slope W software. Limit equilibrium method with effective stress analysis was carried out to achieve optimum bench geometry. Table 5-1 indicates that cohesion is negligible in the top soil whereas the values are significant for the highly weathered rock. There are two soil layers in the target profile. The stability analysis was performed for each geometry by assuming slope failure may occur either through top soil or highly weathered rock. The scenarios with lowest factor of safety are shown in Figures 4-25 to 4-28. The rest of the analytical scenarios attached in the ANNEX- G. Further, analysis was extended to determine

the stability behavior of overburden slope with Percentage variation from shear strength parameter values measured in laboratory.

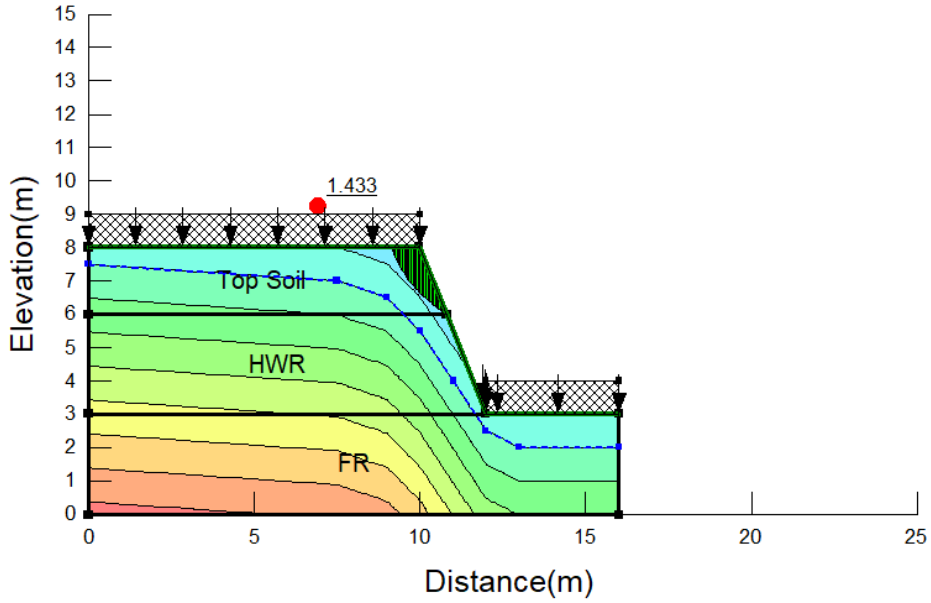

Figure 4-25: Minimum FOS as failure exit occurs in top soil when slope maintains a single bench.

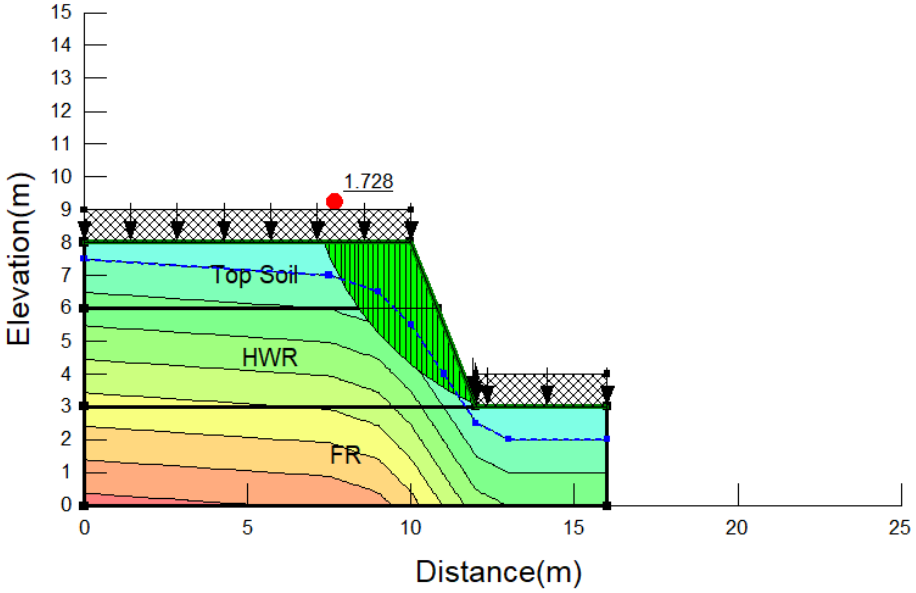

Figure 4-26: Minimum FOS as failure exit occurs in highly weathered rock when slope maintains a single bench.

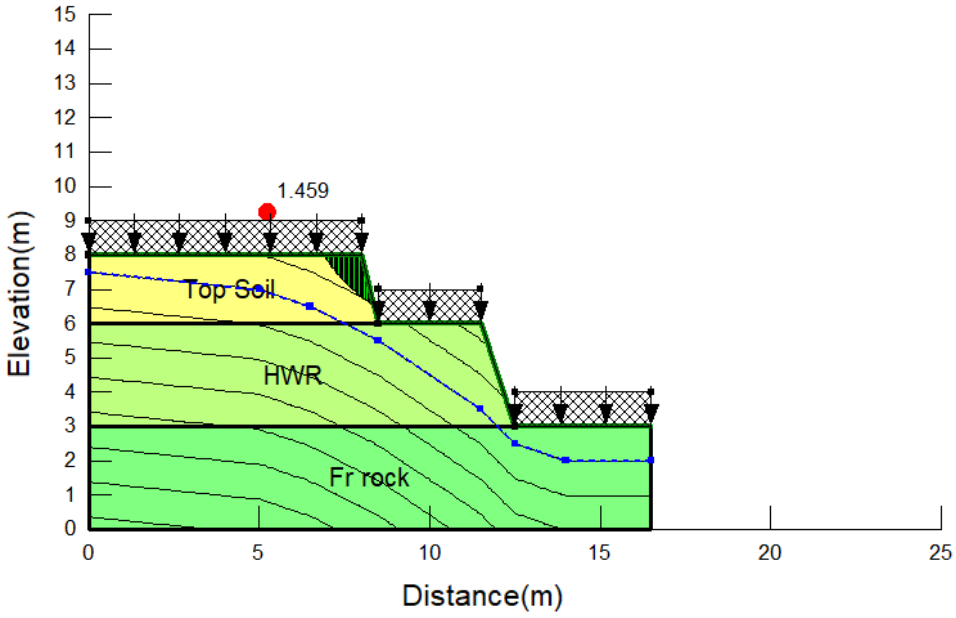

Figure 4-27: Minimum FOS as failure exit occurs in top soil when slope maintains multiple benches.

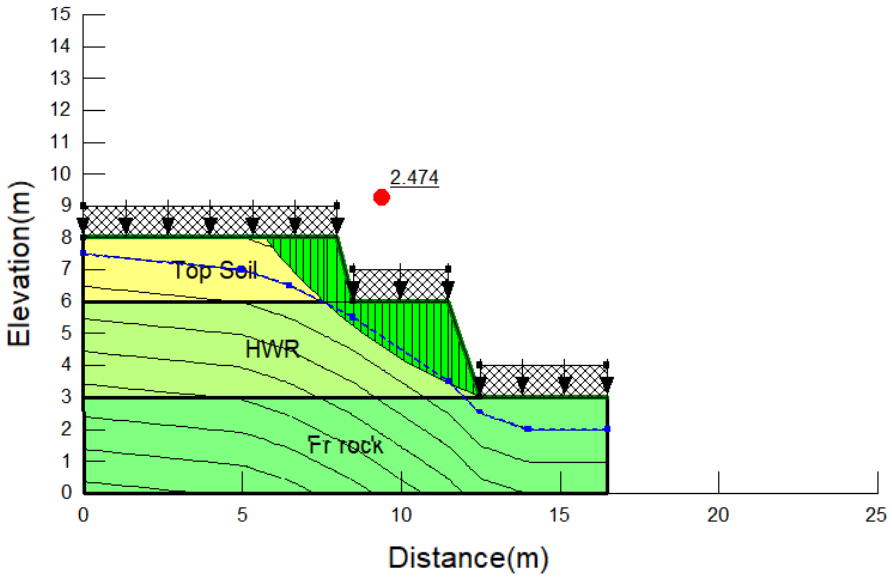

Figure 4-28: Minimum FOS as failure exit occurs in highly weathered rock when slope maintains multiple benches.

4.3 Rock Mass Rating analysis

4.3.1 Calculation of RQD using joint spacing

Calculations for a single joint set at location 1 are shown below.

Average spacing of joint set 1 - 0.170m

Average spacing of joint set 2 - 0.305m

Average spacing of joint set 3 - 0.413m

$$Jv = \frac{1}{S_1} + \frac{1}{S_2} + \frac{1}{S_3} + \cdots + \frac{1}{S_n}$$

$$Jv = \frac{1}{0.17} + \frac{1}{0.305} + \frac{1}{0.413}$$

$$Jv = 11.58$$

$$RQD = 110 - 3.3Jv$$

$$RQD = 110 - 3.3 \times 11.58$$

$$RQD = 76.785$$

For, each location calculated volumetric joint count and particular RQD tabulated in Section 5.

4.3.2 Obtaining of Uniaxial Compressive Strength of rock

Due to presence of joints, some specimens were little bit shorter than the standard size according to the ASTM D 2938. In such cases, UCS values were standardized by the Equation 9.

$$\sigma_{cz} = \frac{\sigma_c}{(0.88 + \frac{0.24d}{h})} \qquad \text{Equation (9)}$$

Where, σ_{cz}- Standardized compressive strength

σ_c - Measured compressive strength

The UCS calculation for the illustration specimen is demonstrated as shown in Table 4-3.

Table 4-3: Calculation of Unconfined Compressive Strength of rock

Description	Values
Average diameter of core sample	55mm
Height of core sample	75.516mm
Failure load	65KN
Unconfined Compressive Strength	27.35MPa
Corrected Unconfined Compressive Strength	25.87MPa

This calculation was performed for all samples and average UCS values for each location were obtained separately to execute RMR analysis. For each location, calculated Unconfined Compressive Strength values are tabulated and discussed in Section 5.

4.3.3 Rock Mass Rating system adaptation

Combination of above calculations and field measurements were utilized to estimate RMR values with the aid of a Bienwaski RMR rating system for each of the locations.

Table 4-4: Rock Mass Rating for Location 1

parameter	Results	Rating
UCS (MPa)	24.61	2
RQD (%)	69	13
Minimum spacing of joint(m)	0.108	8
Discontinuity length	4.3	2
Maximum separation(mm)	1.42	1
Roughness	Slightly rough	3
Infilling	No filling	6
Weathering	Weathered rock face	3
Ground water	Present	7
Total rating		45

Table 4-5: Rock Mass Rating for Location 2

parameter	Results	Rating
UCS (MPa)	22.01	2
RQD (%)	58	13
Minimum spacing of joint(m)	0.148	8
Discontinuity length	3.1	2
Maximum separation(mm)	5.12	0
Roughness	Slightly rough	3
Infilling	No filling	6
Weathering	Weathered rock face	1
Ground water	Water flow out through joint	0
Total rating		35

Table 4-6: Rock Mass Rating for Location 3

parameter	Results	Rating
UCS (MPa)	72.90	7
RQD (%)	86	17
Minimum spacing of joint(m)	0.29	10
Discontinuity length	3	2
Maximum separation(mm)	11	0
Roughness	Rough	5
Infilling	Infilling in cracks	2
Weathering	Weathered rock	5
Ground water	Not Present	10
Total rating		58

Table 4-7: Rock Mass Rating for Location 4

parameter	Results	Rating
UCS (MPa)	32.02	4
RQD (%)	72	13
Minimum spacing of joint(m)	0.16	8
Discontinuity length	5.7	2
Maximum separation(mm)	4.5	1
Roughness	Smooth	1
Infilling	Some cracks are filled with clay	2
Weathering	Highly weathered rock	3
Ground water	Present	7
Total rating		41

Table 4-8: Rock Mass Rating for Location 5

Parameter	Results	Rating
UCS (MPa)	34.84	4
RQD (%)	80	17
Minimum spacing of joint(m)	0.258	10
Discontinuity length	6.1	2
Maximum separation(mm)	2.38	1
Roughness	Smooth	1
Infilling	No filling	6
Weathering	Weathered rock face	3
Ground water	Present	7
Total rating		51

Table 4-9: Rock Mass Rating for Location 6

parameter	Results	Rating
UCS (MPa)	39.65	4
RQD (%)	76	17
Minimum spacing of joint(m)	0.170	8
Discontinuity length	5.4	2
Maximum separation(mm)	3.76	1
Roughness	Rough	5
Infilling	Infilling in cracks	4
Weathering	Weathered rock	5
Ground water	Not Present	10
Total rating		56

4.3.4 Determination of friction angle of rock mass

Friction angle of rock mass was calculated for each and every location considering RQD tables and the average friction angle obtained from the correlation proposed by Aydan & Kawmoto was selected as the representative friction angle of the rocks in the area for the generation of friction angle in Kinematic analysis. Cohesion on the discontinuity plane was considered negligible when rock joints produced rock mass with small block (Singh and Narendrula, 2007). To be conservative, it was taken as a $5kN/m^2$ in this analysis. Those obtained values were then directly used in GEO5 software for rock slope stability analysis. Table 4-10 shows the Friction angle with UCS and RMR obtained by different correlations for each of the locations

Table 4-10: Friction angle with RMR & UCS for Locations 1 to 6

Location	UCS	RMR	Friction Angle			
			Trunck & Honisch	Aydan	Sen & Sadagah	Aydan & Kawmoto
1	24.61	45	38.0	44.0	36.2	42.5
2	22.01	35	33.0	43.3	33.7	37.5
3	72.90	58	44.5	58.4	39.5	49.0
4	32.02	41	36.0	47.5	35.2	40.5
5	34.84	51	41.0	48.6	37.7	45.5
6	39.65	56	43.5	49.9	39.0	48.0

4.4 Stereo plot analysis using Georient software

4.4.1 Identification of major joint sets

After identifying the joint sets by means of contoured pole plot the mid point of the relevant pole concentration was marked as the representative pole of each major joint set. The diameter, which passes through the marked pole was drawn. Then the bearing of the opposite ends of the diameter gives the dip directions of joint sets. The radius of the circle as well as distance from center to marked poles were measured to calculate the dip angle. Contoured pole plots for faces 1 to 3 are shown on Figures 4-29 to 4-31, respectively.

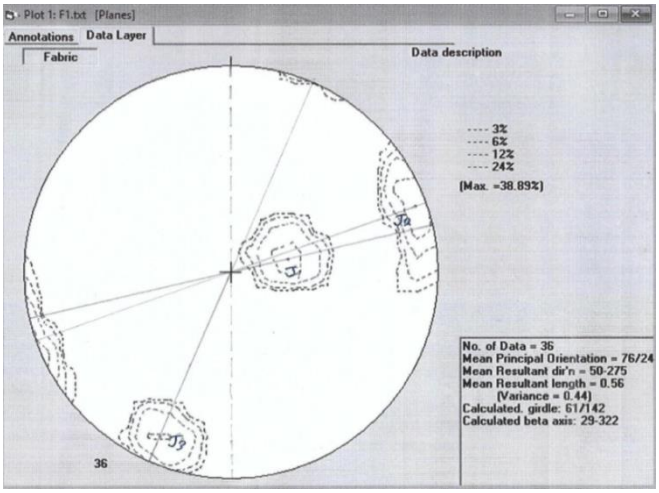

Figure 4-29: Contoured pole plot of Face 1

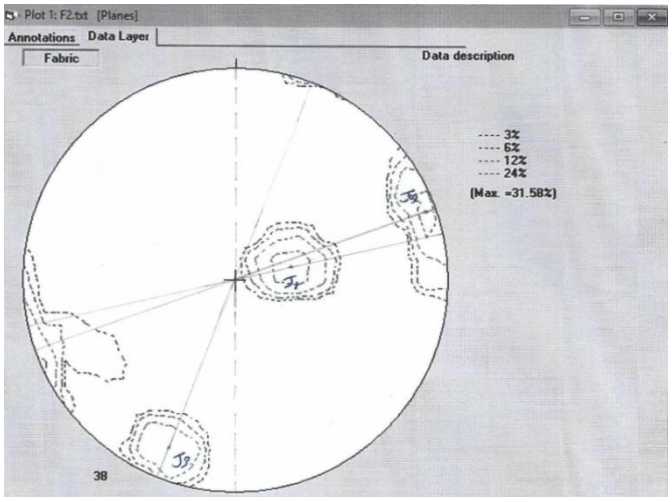

Figure 4-30: Contoured pole plot of Face 2

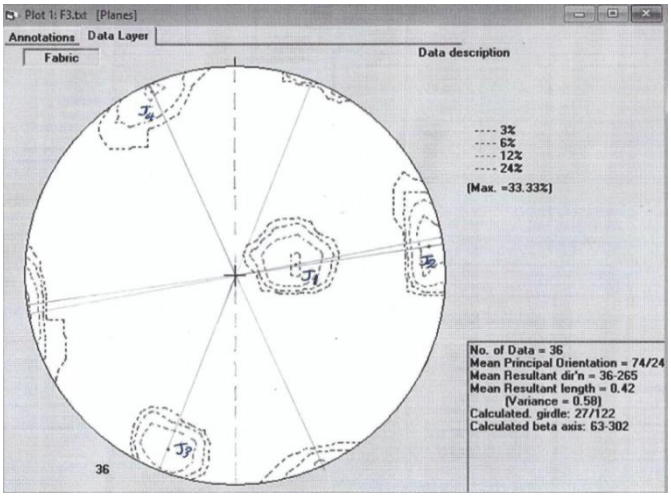

Figure 4-31: Contoured pole plot of Face 3

4.4.2 Determination of dip and dip direction of joint sets

As an example, joint dip was calculated for Joint 1 in Face 3 as shown below. This is done as a linear interpolation.

Radius of circle – 5.2cm

Distance from center to pole – 1.5cm

Dip of Joint 1 = $\frac{90}{5.2} \times 1.5 = 25.96^0$

Similarly, dip angles were calculated for other joint sets. Calculated dip angles and dip direction of major joint sets are tabulated in Section 5.

4.4.3 Kinematic analysis of joint sets

Overall, three joint sets were identified in first and second faces and four joint sets were identified in the other face. Each face was kinematically analyzed by changing dip direction of slope by twenty degrees with dip of slope varying seventy to ninety degrees. An average friction angle of rock mass which was obtained during the RMR analysis was used to generate the friction circle.

Possible modes of failures were recognized by carefully observing stereographic plots shown as in Figure 4-32. The rest of the stereographic plots are attached in the ANNEX- H. The results of stereographic analysis are tabulated in Section 5 under the face number, dip and strike of slope, joint set number and mode of failure.

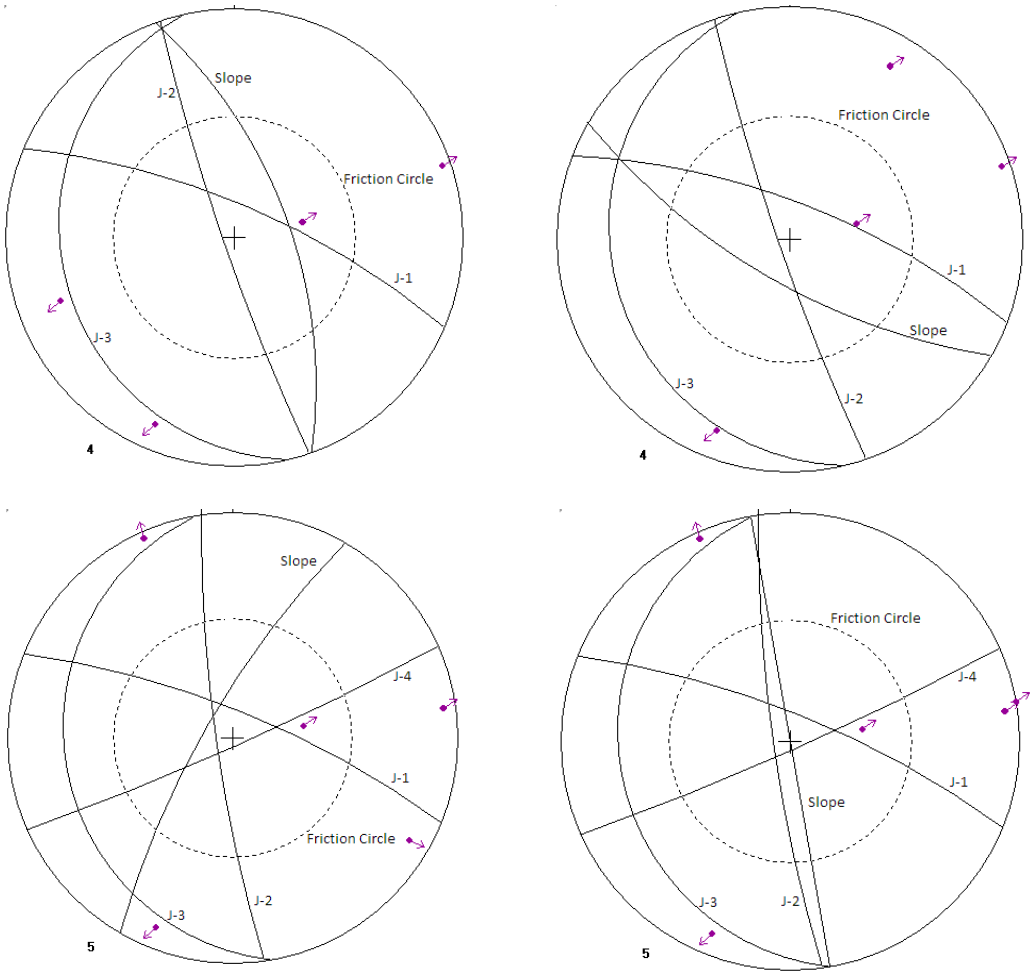

Figure 4-32: Stereographic projection of discontinuities

4.5 Slope Mass Rating analysis

For this task, stereographic analysis results were utilized by combining with calculated RMR values. Sample calculations for Slope Mass Rating (SMR) for the toppling and planer failure are illustrated as follows.

4.5.1 The SMR calculation for Toppling failure (First face, Joint number 3)

Slope dip angle (β_s) - 70

Joint set dip angle (β_j) -25

Slope dip direction (α_s) -50

Joint set dip direction (α_j) -257

For F_1

For F_3

A =$|\propto j - \alpha s - 180|$

$C = \beta_j + \beta_s$

$=|257-50-180|$ $= 70+25$

$= 27$ $= 95$

$F_1 = 0.4$ (A lies 20-30 range) $F_3 = 0$ (C less than 110)

F_2 = 1 (for toppling failure) $F_4 = 0$ (Blasting or Mechanical)

SMR = $RMR_B + (F1 \times F2 \times F3) + F4$

SMR = 45 +$0.4 \times 1 \times 0 + 0$

SMR = 45

4.5.2 The SMR calculation for Planer failure (Third face, Joint number 3)

Slope dip angle(β_s) - 70 Joint set dip angle(β_j) -26

Slope dip direction(α_s) -260 Joint set dip direction(α_j) -260

For F_1 For F_3

A =$|\propto j - \alpha s|$ $C = \beta_j - \beta_s$

$=|260-260|$ $= 26-70$

$= 0$ $= -44$

$F_1 = 1$ (A< 5) $F_3 = -60$ (C< -10)

F_2 = 0.4 (β_j, between $20-30$) $F_4 = 0$ (Blasting or Mechanical)

SMR = $RMR_B + (F1 \times F2 \times F3) + F4$

SMR = 51 +$1 \times 0.4 \times (-60) + 0$

SMR = 27

Similar calculations were carried out considering other probable discontinuity planes which were identified in the stereographic projection analysis and Slope Mass Rating values obtained through the SMR analysis are tabulated as shown in Table 4-11.

Table 4-11: Slope Mass Rating values.

Face	Slope Dip	Slope D/D	Plane dip	Plane D/D	Joint No	F/T	F1	F2	F3	F4	Av. RMR	Av. SMR
1	70	70	86	251	J2	T	1	1	-25	0	40	15
1	75	70	86	251	J2	T	1	1	-25	0	40	15
1	80	30	78	23	J1	P	0.85	1	-50	0	40	-2.5
1	80	70	86	251	J2	T	1	1	-25	0	40	15
1	85	30	78	23	J1	P	0.85	1	-50	0	40	-2.5
1	85	70	86	251	J2	T	1	1	-25	0	40	15
1	90	30	78	23	J1	P	0.85	1	-60	0	40	-11
1	90	70	86	251	J2	T	1	1	-25	0	40	15
2	70	190	77	21	J1	T	0.15	1	-25	0	49.5	45.75
2	70	210	77	21	J1	T	0.15	1	-25	0	49.5	45.75
2	75	190	77	21	J1	T	0.15	1	-25	0	49.5	45.75
2	75	210	77	21	J1	T	0.15	1	-25	0	49.5	45.75
2	80	190	77	21	J1	T	0.15	1	-25	0	49.5	45.75
2	80	210	77	21	J1	T	0.15	1	-25	0	49.5	45.75
2	85	190	77	21	J1	T	0.15	1	-25	0	49.5	45.75
2	85	210	77	21	J1	T	0.15	1	-25	0	49.5	45.75
2	90	190	77	21	J1	T	0.15	1	-25	0	49.5	45.75
2	90	210	77	21	J1	T	0.15	1	-25	0	49.5	45.75
3	70	220	80	22	J1	T	0.15	1	-25	0	53.5	49.75
3	75	220	80	22	J1	T	0.15	1	-25	0	53.5	49.75
3	80	220	80	22	J1	T	0.15	1	-25	0	53.5	49.75
3	85	260	84	262	J2	P	1	1	-50	0	53.5	3.5
3	90	260	84	262	J2	P	1	1	-50	0	53.5	3.5

The determination of slope stability classes based on the Slope Mass Rating values for each discontinuity and ultimately variation of average stability class for each slope is discussed in Section 5.

4.6 Rock slope analysis using GEO5 software

4.6.1 Validation of GEO5 software with aid of Thalathu Oya quarry

Thalathu Oya quarry is a location where sliding of rock slope has occurred. Therefore it is used for validation of GEO5 software.

Table 4-12: Rock Mass Rating results of Thalathu Oya rock quarry

Parameter	Results	Rating (%)
Average intact rock strength	43.50 MPa	04
RQD (%)	42%	08
Joint spacing	Minimum spacing=0.3mm	10
Joint condition	Irregular, planer joint surface, continuous, joint separation<1mm soft joint wall	20
Ground water condition		10
Total rating		52

4.6.1.1 Identification of possible failure modes

The structural geological details on the joint sets, slip plane and the slope face are tabulated as follows. Thalathu Oya inspection revealed that the slope failed as a plane failure. Furthermore, it is obviously detected according to the stereonet shown as Figure 4-33.

Table 4-13: Rock joints and slope geological properties

Discontinuities	Dip	Dip direction
Slip plane	30	60
Joint No 1	90	73
Joint No 2	90	180
Joint No 3	40	30
Joint No 4	50	84
Joint No 5	60	70
Slope face	60	60

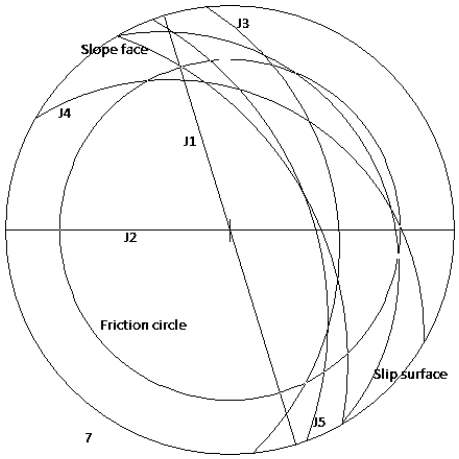

Figure 4-33: Stereonet analysis used to identify different types of failure modes.

The failure surface has been extended around 108m to the uphill direction with having 30 degree dip. Post investigation reviled that failure occurred due to presence of tension crack in the crest as shown in Figure 4-34.

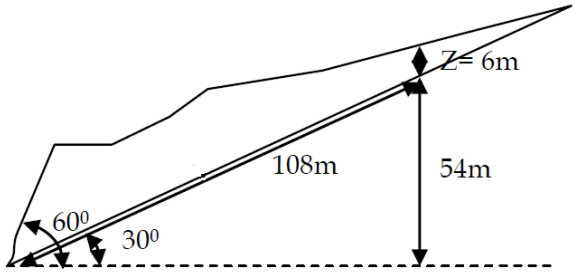

Figure 4-34: Approximate geometry of failed slope

The validation procedure was carried out by considering two cases. Case A was carried out by without considering surcharge load and ground vibration due to blasting operations while case B model was done by considering minimum ground acceleration (0.1.g) since there are lacks of vibration details regarding rock blasting. The validation result of Thalathu Oya slided quarry will be discussed in Section 5.

4.6.2 Wedge failure analysis using GEO5 software

Wedge failure analysis was carried out with aid of GEO5 software. Initially possible geometries were recognized using stereographic projections. Then, secondary check for failure was performed by comparing the dip of the slope, the friction angle and the plunge of the line. Joint sets that would consist possible wedge failure are indicated in Table 5-9 in Section 5.

Dip of the slope (ψ_f) = 85

Plunge of the line (ψ_i) = 69

Friction angle (ϕ) = 44

$\psi_f > \psi_i > \phi$, Implies that sliding might occur

4.6.2.1 Determination of the unit weight of rock

The average friction angle was obtained as a rock mass friction angle. The cohesion of the rock mass was negligible on the discontinuity plane. Specific gravity of rocks was obtained to determine unit weight of the rock as shown below.

Table 4-14: Calculation of unit weight of rock

Description	Amount
Dry weight of the specimen in air	8.7 g
Weight of the specimen while suspended in water	4.8 g
Specific gravity of the rock sample	2.23
Unit weight of the rock specimen	24 KN/m^3

4.6.2.2 Determination of Surcharge load

The surcharge load was determined by considering overburden and live loads. The same soil profile that was used in the Slope W analysis was used to the surcharge load calculation also.

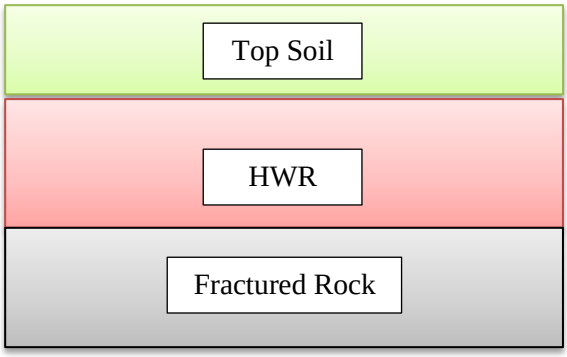

Figure 4-35: Soil profile of the area

Table 4-15: Properties of the Soil layers

Type of Layer	Height (m)	Unit Weight (kN/m^3)
Top soil	2	18
HWR	3	22

Surcharge load due to overburden soil is 112 KN/m^2

By considering 1m length, surcharge load is 112 KN/m.

4.6.2.3 Detail analysis of Wedge failure

Initial rock bench height was taken as 5m to define geometry of the Bench. Dip and dip direction of discontinuity as well as slope were defined according to the Table 5-9. Analysis was carried out with different site conditions. For some critical analytical cases, water level was assumed to be 5m elevation. Certain analysis were carried out by considering either the water table or surcharge load effects. Other analysis was performed by considering both ground water table and surcharge load. Further analysis were conducted by considering neither ground water table nor surcharge

load. One of analysis case is shown in Figure 4-36 to 4-39 as an example and rest of analysises are attached in the ANNEX- I.

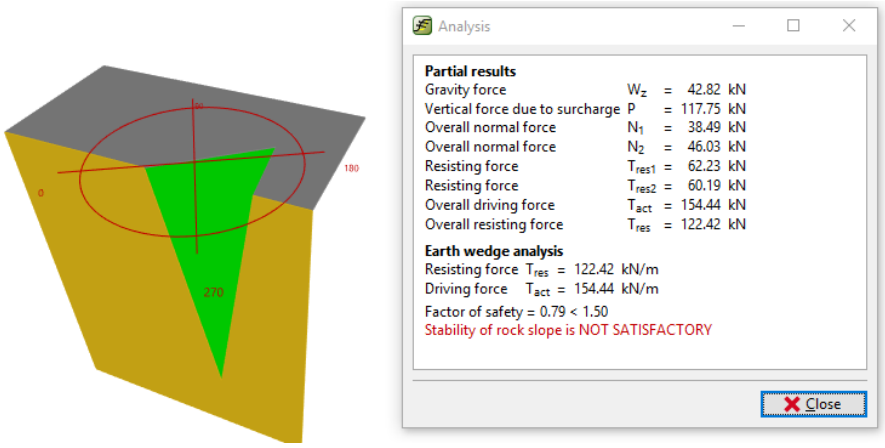

Figure 4-36: Wedge failure analysis by considering surcharge load only

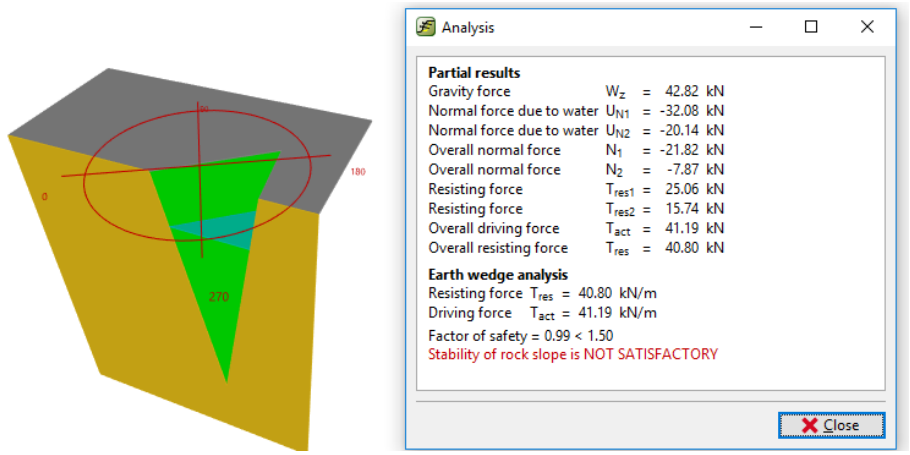

Figure 4-37: Wedge failure analysis by considering water table only

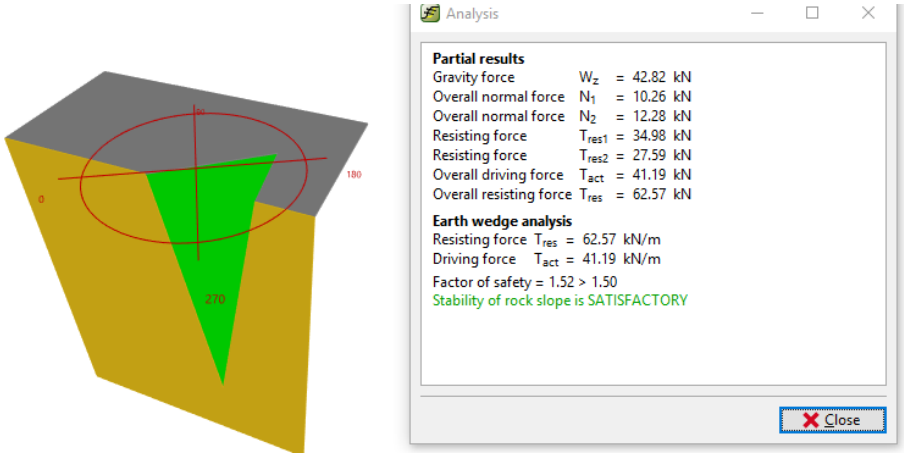

Figure 4-38: Wedge failure analysis without considering water table and surcharge load

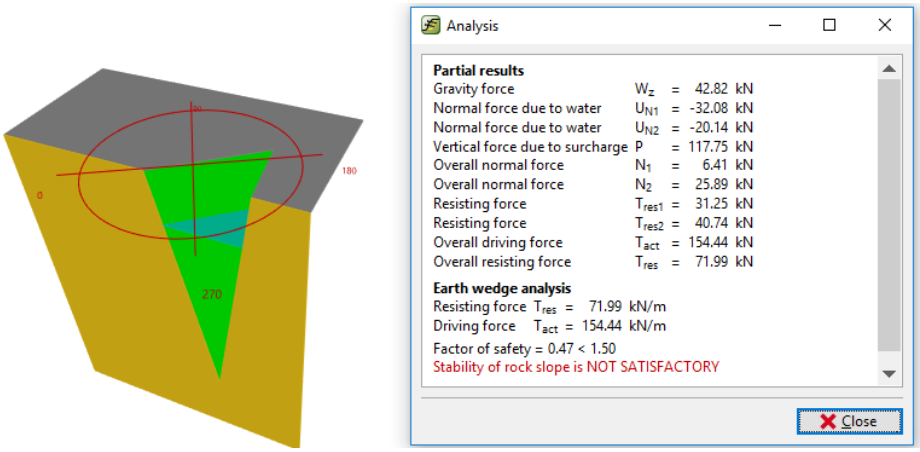

Figure 4-39: Wedge failure analysis with considering water table and surcharge load

Furthermore, analysis was extended to compare different types of improvement techniques such as reduction of slope angle, reduction of slope height, drainage improvement, increasing of shearing resistant, reduction of surcharge load and varying of unfavorable conditions like increasing of ground vibration to find out how it will affect to the stability of the slope. The amount of improvement percentage or variation of different techniques and unfavorable conditions are listed in Table 4-16. The results of the analysis are discussed in Section 5.

Table 4-16: Variation of favorable and unfavorable conditions of rock slope

Variation of conditions	Bench height (m)	Bench angle (^{0})	Surcharge load (KPa)	Ground water table (m)	Anchor force (KN)	Seismic action
00%	10	90	120	0	0	0.4
25%	8	80	90	2	50	0.3
50%	6	70	60	3	100	0.2
75%	4	60	30	4	150	0.1
100%	2	50	0	5	200	0

5 RESULTS AND DISCUSSION

5.1 Estimation of ground water table

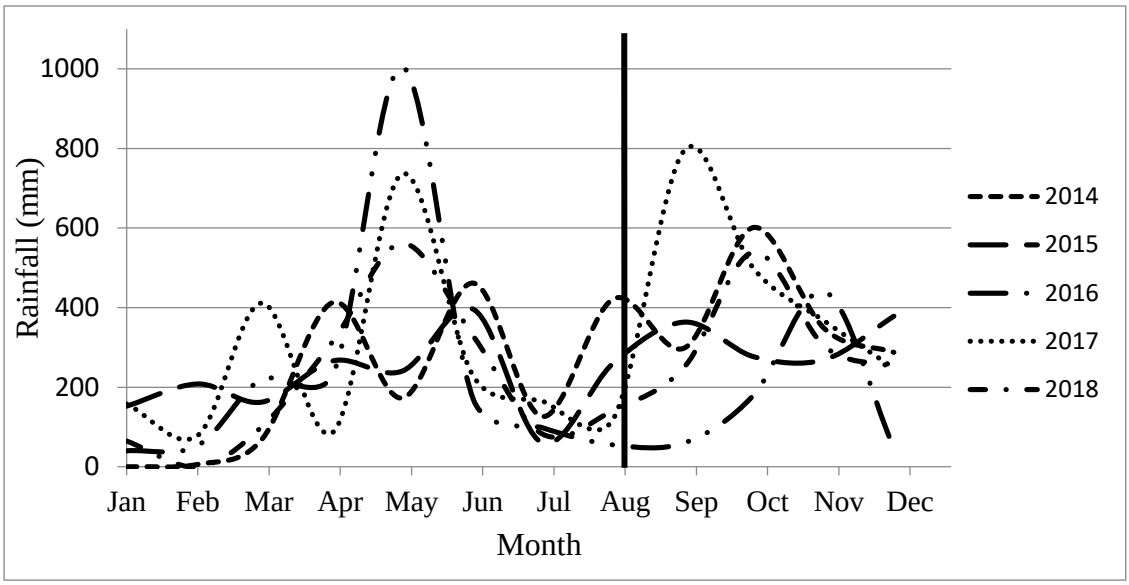

Figure 5-1: Annual rainfall intensity

As is evident in Figure 5-1, maximum rainfall is obtained during the periods May to June and September to October. A preliminary site visit was done in the month of August. It is marked with a black colour vertical line in the Figure 5-1. According to the Figure 5-1, it can be seen that a relatively medium precipitation is obtained in that particular time than in other periods. The ground water level of the domestic wells (about 100m away from the site) of the surrounding area was at a depth of about 5m depth from the surface at that time period. Therefore, during the maximum rainy season, ground water table level would be heigher. To be conservative, shallower depth of water table is considered in the slope stability analysis. Averagely, the study area receives 3185mm rainfall per year during 2014 -2018. Rainfall is a dominant factor which motivates chemical weathering. It controls the supply of moisture content for the chemical reactions and the deletion of soluble elements of the minerals in the selected area. The average overburden thickness is 4-6m. Therefore, rainwater infiltrates in to the subsurface and raises the pore water pressure which increases the probability of failure along the discontinuity planes.

Rain causes the unit weight of the overburden soil mass to increase and then to decrease stability of the soil mass. Ground water also increases the pore water pressure within the soil causing instability.

5.2 Overburden slope stability analysis

5.2.1 Variation of mechanical strength parameters

Table 5-1: Mechanical properties of soil layers

Location	Cohesion (kN/m^2)	Friction angle (^{0})	Unit weight (kN/m^3)
L1 (top soil)	16	32	18
L2 (top soil)	17	31	16
L1 (W/R)	80	39	22
L2 (W/R)	59	41	22

Table 5-1 shows relevant mechanical properties of soil and highly weathered rock layers. Effective stress analysis was conducted to obtain the soil shear strength parameters. The top soil in both locations shows approximately similar values of cohesion and friction angle. Therefore, it can be assumed that the same soil layer with almost same density extends throughout the site. However, in highly weathered rock, cohesion shows some variation, although the friction angle remains approximately same. This might have occurred as selected HWR samples might have been of different weathering classes.

5.2.2 Optimization of overburden bench angle with different bench geometries

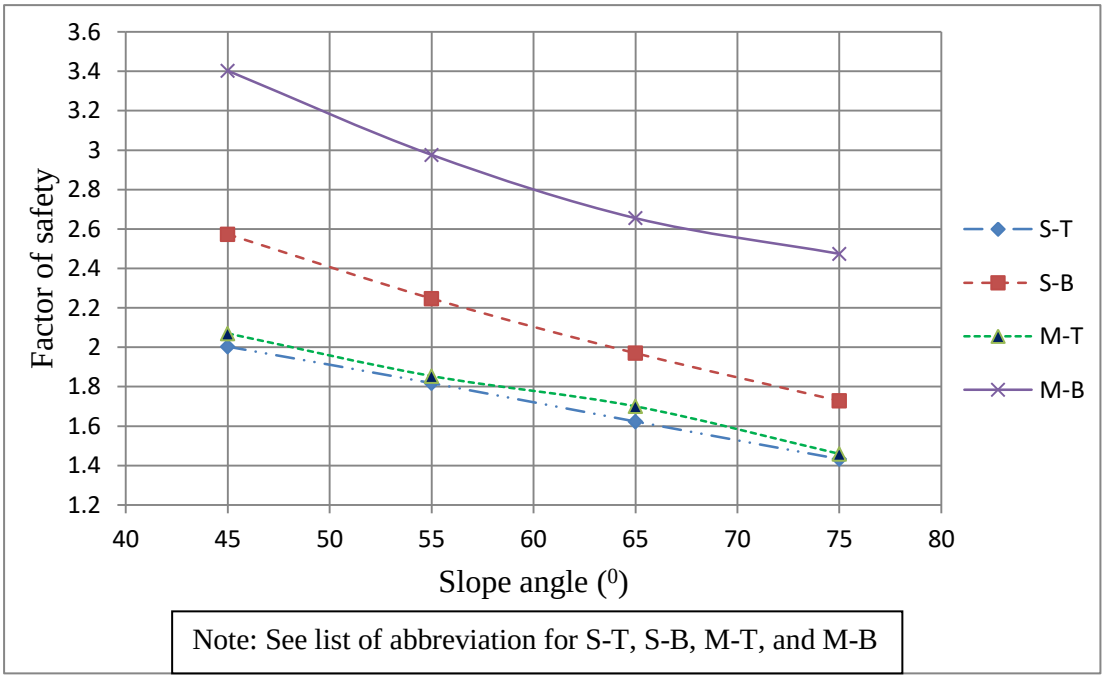

Figure 5-2: Variation of factor of safety with bench angle

Figure 5-2 shows the variation of factor of safety with the bench angle in different geometrical orientations of the slope. According to the Figure 5-2, a greater factor of safety will be achieved when failure surface exits through the highly weathered rock (M-B & S-B). Further, comparing the two cases of failure exiting through the top soil, higher factor of safety is obtained in the multiple bench orientation. Also, similar result can be obtained between the two cases of failure exists through highly weathered rock. The factor of safety reduces non-linearly as the slope angle is increased. The factor of safety is minimum when slip circle exits through top soil. Therefore, top soil layer is critical in designing of safe bench slope. According to the Figure 5-2, different safe bench angles can be introduced separately to the top soil and highly weathered rock for the purpose of Mining.

5.2.3 Effect of the variation of shear strength parameters of overburden soil

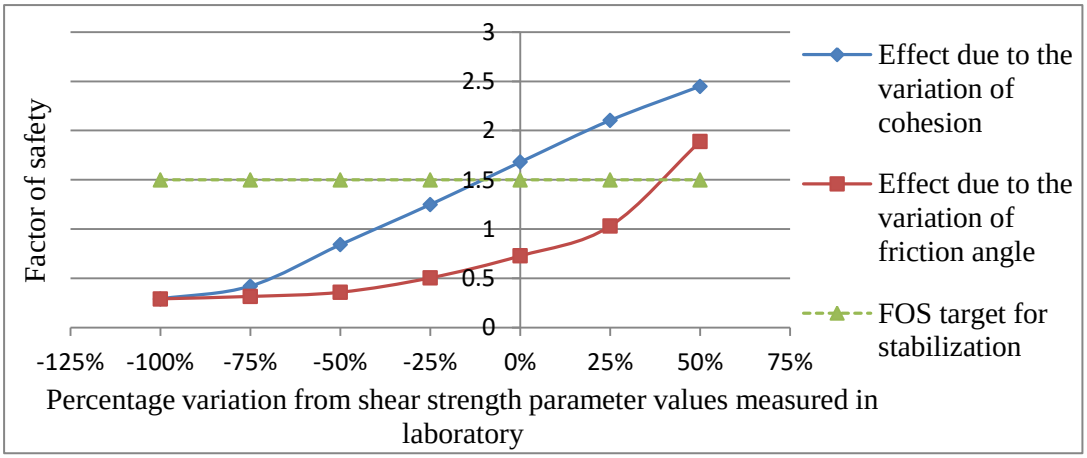

Figure 5-3: Variation of factor of safety with variation of shear strength parameter values measured in laboratory

Figure 5-3 shows the variation of factor of safety with percentage variation of shear strength parameters of overburden soil profile. The factor of safety was calculated by assuming the worst conditions of shear strength parameters. The values of the mechanical properties of soil obtained from the laboratory test were considered as 0% of the shear strength parameters in Figure 5-3. It is evident in Figure 5-3 that the variation of cohesion is more significant than the improvement of friction angle. For some failure surfaces where failure exists through top soil, nearly parallel to the slope, the depth of failure surface is small compared to length of the slope. Therefore, such failures can be identified as translational slides. Similarly, as increase in the depth of failure surface tends to show a rotational slide rather than a translational slide. It implies that top soil compromises with fissured over consolidated clayey soil. According to the Figure 5-3 the targeted factor of safety can be achieved by improving the cohesion of soil rather than friction angle. But improvement of friction angle of soil is a practical method than improvements of cohesion for open pit mines. Alternatively, compaction of loose overburden soil can also increase the friction angle of top soil thereby enhancing the factor of safety. Further, movements of ground water apply extra lubricating action along the weak zone and can reduce the shear strength of soil. Therefore, adoption of proper drainage system will also lead to an enhancement in the stability of slope.

5.3 Rock classification according to Rock Quality Designation

Table 5-2: RQD according to Volumetric Joint Count

Location	Average spacing of joint sets (m)			Maximum Average joint Separation (mm)	Volumetric joint count (JV)	RQD (%)
	S1	S2	S3			
1	0.108	0.390	0.540	01.42	13.7	69
2	0.150	0.148	0.265	05.12	17.2	58
3	0.302	0.287	0.530	11.00	8.7	86
4	0.286	0.162	0.320	04.50	12.8	72
5	0.354	0.258	0.276	02.38	10.3	80
6	0.170	0.305	0.413	03.76	11.6	76

Due to the unavailability of core loggings, the correlation proposed by Palmstorm (1974) was used to acquire rock quality designation with the aid of the volumetric joint count. At least, there should be three joint sets to apply this method but, in location 1, only two joint sets were observed. Therefore, five times of the largest spacing value is taken as the third spacing (Palmstorm, 2005). Spacing between two fractures in same joint set should be approximately same. If it is not satisfied, there can be another joint set embedded with same dip and dip direction. Volumetric joint count is an indication for degree of jointing. At location 3, rock consists of a moderate degree of jointing while all other places can be categorized as high degree of jointing (Plamstorm, 2005). This method cannot be used to calculate RQD when joints are irregularly oriented. Rocks at location 1, 2 and 4 are classified as of fair rock category according to the RQD classification index. Alternatively, these can be classified into moderately hard rock class. Rocks at location 3, 5 and 6 are classified into good or hard rock category. Overall by considering Table 5-2, rocks in the particular area varies from moderately hard rock to hard rock in view of RQD classification.

5.4 Application of Geological Strength Index for rock mass classification

Table 5-3: Variation of Geological Strength Index over the site

Location	Volumetric Joint Count	Structure Rating (SR)	Surface Condition Rating (SCR)	GSI
1	13.7	44	12	46
2	17.2	35	10	39
3	8.7	54	12	49
4	12.8	46	6	33
5	10.3	50	10	43
6	11.6	48	14	52

The Table 5-3 depicts the outputs of the Geological Strength Index (GSI) to classify the rock mass. Geological Strength Index utilizes two fundamental parameters through geological classification process, namely; blockiness of the rock mass and the condition of discontinuities. In this process, the GSI was obtained by the structural and surface condition rating values as shown in the Table 5-3. Hence, the quality of the rock mass was determined. As stated by Table 5-3, condition of rock mass according to the Geological Strength Index varies from blocky to very blocky for Face 2 and blocky for Face 1 and Face 3. According to the surface condition of the discontinuities, rock mass in Face 1 and Face 3 vary from fair to good and for Face 2, it varies from poor to good. Further, GSI facilitates to estimate shear strength parameters and deformational parameters of the rock mass.

5.5 Grading of rock mass according to Unconfined Compressive Strength

Table 5-4: Average UCS of rocks at different locations

Location	Average UCS (MPa)
1	24.61
2	22.01
3	72.90
4	32.02
5	34.84
6	39.65

Laboratory test results of the Uniaxial Compressive Strength test are as given in Table 5-4. The Uniaxial Compressive Strength of rock is one of a most widely used rock property in Geotechnical and Mining Engineering practices. The UCS is desired to estimate the Rock Mass Rating system (Bieniawski, 1973) and Rock Mass Index (Palmstrom, 1995). It was observed that, most of the rock samples failed along the well developed inclined foliation plane or discontinuity plane. But, tested samples in location 3 failed axially, almost perpendicular to the foliation plane. Therefore, the orientation of the discontinuity with respect to the direction of application of load will influence the failure load in UCS test. Additionally, intact rock strength can be classified based on UCS value. According to Brown (1981), samples from location 1 and 2 can be classified as grade R-2 with weak rock category. The rocks with grade R-2 can be peeled with a pocket knife. Rocks in location 4, 5 and 6 can be classified as grade R-3 with medium strong rock. But, rocks in this grade cannot be scraped with a pocket knife. Location 3 some what differs from the other locations. It shows a much higher value of UCS which belongs to grade R-4 with strong rock. It needs more than one blow of a geological hammer to fracture. Overall, the majority of rocks in this area can be categorized as moderately weak rock mass in view of Uniaxial Compressive Strength. UCS is a critical rock property once considering a

variety of issues encountered during the design and drilling, blasting and construction of open pit slopes. The strength and geological features of a rock mass cannot be changed. But, awareness of those properties assist the sensible selection of blast design factors such as Explosive Charge Factor, Spacing Factor and Burden Factor. Therefore, according to the strength and specific gravity of rock, an Explosive Charge Factor of 80, Spacing Factor of 14 and Burden Factor of 1.2 are suggested to quarries with this type of rocks (Singh and Narendrula, 2007).

5.6 Stereographic Projection analysis

Table 5-5: Dip and dip directions of major joint sets

Face	Joint set	Dip (^{0})	Dip direction (^{0})
Face 1	J1	25	257
	J2	86	251
	J3	78	23
Face 2	J1	24	257
	J2	86	251
	J3	77	21
Face 3	J1	26	260
	J2	84	262
	J3	80	22
	J4	87	156

Table 5-5 illustrates the average dip and dip direction of joint sets in each face. These were obtained using pole concentration maps of bench faces. Face 1 and 2 are involved with three joint sets while Face 3 is involved with four joint sets. Table 5-5 provides the evidence that same three joint sets extend throughout the site area since, approximately same dip and dip direction are illustrated in first, second and third joint sets in each face. Those three joint sets may produce cubic shaped blocks as they intersect with each other. In the third face, an extra joint set (J4) with steeper dip with a different dip direction is observed. That is not identified in other faces. The

stability of the benches are determined by considering the orientation of bench slope with respect to the joint sets.

Stereographic analysis was performed for each face by changing dip and dip direction of bench slope with respect to the major joint structural geological features. Some of the analysis results are shown as below.

Table 5-6: Possible failure modes with respect to slope faces

Face	Dip of slope (^{0})	Dip Direction of slope (^{0})	Joint number	Type of failure (See abbreviation)
1	70	70	J2	T
1	75	70	J2	T
1	80	30	J1	P
1	80	70	J2	T
1	85	30	J1	P
1	85	70	J2	T
1	90	30	J1	P
1	90	70	J2	T
2	70	190	J1	T
2	70	210	J1	T
2	75	190	J1	T
2	75	210	J1	T
2	80	190	J1	T
2	80	210	J1	T
2	85	190	J1	T
2	85	210	J1	T
2	90	190	J1	T
2	90	210	J1	T
3	70	220	J1	T
3	75	220	J1	T
3	80	220	J1	T

Face	Dip of slope (^{0})	Dip Direction of slope (^{0})	Joint number	Type of failure (See abbrevation)
3	80	300	J1,J2	W
3	85	220	J4,J2	W
3	85	240	J4,J2	W
3	85	260	J2	P
3	85	280	J1,J2	W
3	85	300	J1,J2	W
3	90	260	J2	P
3	90	280	J1,J2	W
3	90	300	J1,J2	W

Table 5-6 shows probable failure types, joint number, dip and dip direction of bench faces with respect to the face number. These results were observed from the stereographic analysis. Geometrical properties of existing benches such as dip direction of Face 1, Face 2 and Face 3 are 70^0,170^0 and 260^0 respectively and dip of slopes were uneven. Above table provides evidence that the existing benches are not 100% safe kinamatically. For Face 1, existing slope dip direction exhibited toppling failure for all analyzed dip angles. For Face 2, existing slope dip direction did not exhibit any type of probable failure modes. Furthermore, Face 3 indicated mode of planer failure and wedge failure for many instants of analyzed dip angles. Finally, with the aid of stereographic analysis, safest orientation of the benches can be summarized as follows for different faces.

- For Face 1, dip direction of slope of around 50^0 and 90^0 are safe for all analyzed dip angles of slope.
- For Face 2, dip direction of slope from 130^0 to 170^0 are safe for all analyzed dip angles of slope.
- For Face 3 dip direction of slope from 280^0 to 310^0 are safe with dip angle of slope lower than 80^0.

5.7 Slope Mass Rating analysis

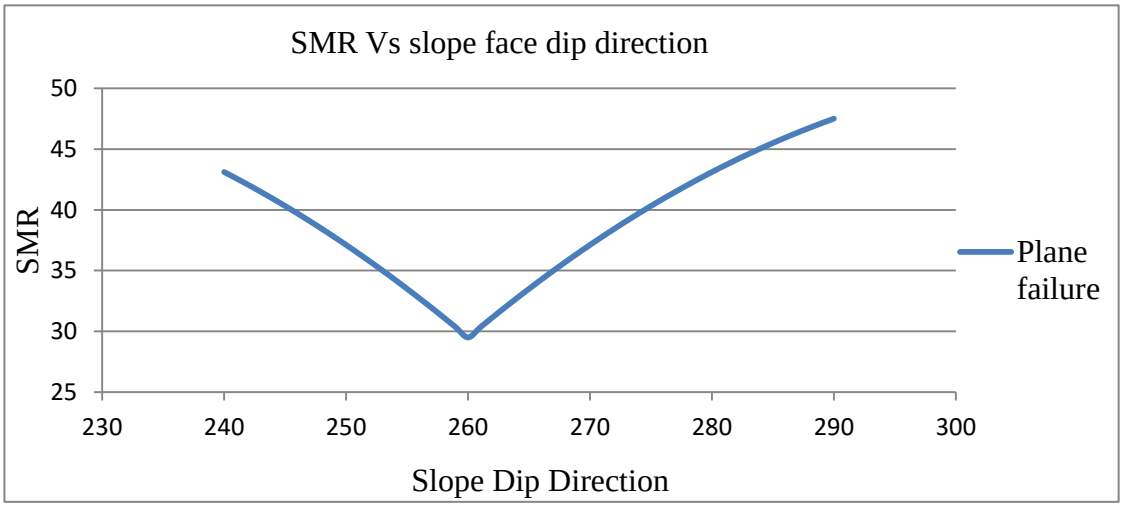

Figure 5-4: Variation of SMR with slope dip direction for plane failure mode

The above Figure 5-4 shows the variation of Slope Mass Rating with respect to slope dip direction for plane failure mode. It shows the minimum SMR value at the dip direction of 260^0. As interpreted from the graph, the slope is somewhat unstable in the face dip direction towards 260^0 and the slope stability is increased as dip direction either becomes larger than 260^0 or lesser than 260^0. For the given slope face, minimum SMR value belongs to SMR Class IV. Therefore, the slope will not be completely unstable at any dip direction. It is possible to upgrade the stability class from Class IV to partially stable stability class (stability class III) by establishing the dip direction of the slope around 280^0.

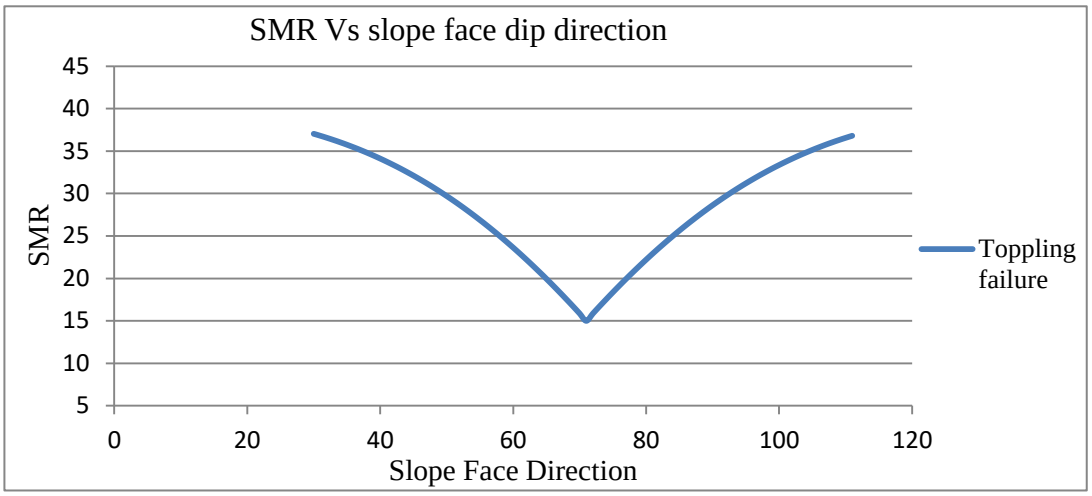

Figure 5-5: Variation of SMR with slope dip direction for toppling failure

The above Figure 5-5 shows the variation of Slope Mass Rating with slope dip direction for toppling failure. It gives a minimum Slope Mass Rating of about 15 at a slope face dip direction of 70^0. As interpreted from the Figure 5-5, the slope is unstable when the face is directing towards 70^0 and its stability is increased on either of its sides. The given slope face minimum SMR value belongs to SMR Class V or completely unstable stability class. It is able to upgrade the stability class from Class V to stability Class IV by establishing the dip direction of the slope to more than 80^0.

5.7.1 Slope stability classes variation over the site

Table 5-7 shows the stability class of slope according to the Slope Mass Rating values. Slope Mass Rating values have been calculated only for the planer and toppling failure conditions. Table 5-7 illustrates all the possible toppling and plane failure modes when varying dip and dip direction of bench slope.

Table 5-7: Slope stability classes

Face	Slope Dip (^{0})	Slope Dip Direction (^{0})	Plane dip (^{0})	Plane Dip Direction (^{0})	Joint number	Average SMR	Slope stability class	Description
1	70	70	86	251	J2	15	V	Completely unstable
1	75	70	86	251	J2	15	V	Completely unstable
1	80	30	78	23	J1	-2.5	V	Completely unstable
1	80	70	86	251	J2	15	V	Completely unstable
1	85	30	78	23	J1	-2.5	V	Completely unstable
1	85	70	86	251	J2	15	V	Completely unstable
1	90	30	78	23	J1	-11	V	Completely unstable
1	90	70	86	251	J2	15	V	Completely unstable
2	70	190	77	21	J1	45.75	III	Partially stable
2	70	210	77	21	J1	45.75	III	Partially stable
2	75	190	77	21	J1	45.75	III	Partially stable
2	75	210	77	21	J1	45.75	III	Partially stable

Face	Slope Dip (^{0})	Slope Dip Direction (^{0})	Plane dip (^{0})	Plane Dip Direction (^{0})	Joint number	Average SMR	Slope stability class	Description
2	80	190	77	21	J1	45.75	III	Partially stable
2	80	210	77	21	J1	45.75	III	Partially stable
2	85	190	77	21	J1	45.75	III	Partially stable
2	85	210	77	21	J1	45.75	III	Partially stable
2	90	190	77	21	J1	45.75	III	Partially stable
2	90	210	77	21	J1	45.75	III	Partially stable
3	70	220	80	22	J1	49.75	III	Partially stable
3	75	220	80	22	J1	49.75	III	Partially stable
3	80	220	80	22	J1	49.75	III	Partially stable
3	85	260	84	262	J2	3.5	V	Completely unstable
3	90	260	84	262	J2	3.5	V	Completely unstable

As interpreted from Table 5-7, maximum average SMR value of Face 1 is 15, all the cases in Face 1 are classified into the stability class number **V** and the existing dip direction of Face 1 slope also can be classified as stability class number **V**.

Therefore, in point of view of slope stability, Face 1 can be categorized as a completely unstable slope.

The maximum average SMR value from the Face 2 is 45.75. According to all of the possible failure cases, slope 2 is classified into stability class **III.** Hence, slope of Face 2 can be categorized as a partially stable slope.

Face 3 differs from the others. Maximum average SMR value of Face 3 is 49. Mostly, Face 3 shows two stability classes such as class **III** and class **V**. Thus, some of areas in Face 3 are partially unstable while other areas are completely unstable. Finally, considering all the results in Face 3, it can be categorized under the unstable slope category.

During the site inspection, Face 1 indicated higher joint frequency than other faces. According to the Slope Mass Rating analysis, rock in slope 1 seems to be comparatively weaker than the rocks of the other faces. Therefore, the factor of safety of Face 1 bench slope can be improved by reducing the bench height and the dip angle of the slope since it is kinamatically unstable.

If a slope has been designed with unfavorable geometry; following supporting system may be adopted to improve the stability of rock slope according to the SMR guideline.

Rock face 1 - Re-excavation

Rock face 2 - Systematic (Bolts, Anchors, Slope fences)

Rock face 3 – Corrective (Surface and deep drainage)

Table 5-8: Stability of slope based on the dip angle of discontinuities and the friction angle

Face	RMR Class No	Description	SMR stability class	Dip angle	Friction angle	Stability of Slope
1	**IV**	Poor rock	**V**	86	43	Very high failure potential
1	**IV**	Poor rock	**V**	78	43	Very high failure potential
2	**III**	Fair rock	**III**	77	41	Low failure potential
3	**III**	Fair rock	**III**	80	46	Low failure potential
3	**III**	Fair rock	**V**	84	46	Very high failure potential

Table 5-8 illustrates the RMR class and detailed stability description of slope with the dip of discontinuity and the friction angle of the rock mass. Rock classes according to the RMR and SMR analysis, some cases are overlaped with each other. Discontinuities in Face 1 are classified as Class No **IV** and **V** according to the RMR and the SMR respectively. According to the RMR, it is classified as poor rock category, while in SMR it can be included under the completely unstable category with failure probability about 0.9. Predicted failure type for slope 1 is big plainer (Romana at.al 2003).

Discontinuity in Face 2 includes Class No **III** according to the RMR as well as the SMR analysis. According to the RMR classification, it is classified as fair rock category, while it is included in partially stable stability class according to the SMR analysis having 0.4 failure probability. Hence, predicted failure type is some joints or many wedges (Romana at.al 2003).

Discontinuities in the Face 3 differ from other faces. Joint sets in Face 3 can be classified as fair rock category according to the RMR Classification while it belongs

to partially unstable and completely unstable stability class in SMR analysis having failure probability range from 0.4 to 0.9. Possible failure types of Face 3 are plainer or big wedges (Romana at.al 2003).

5.8 Validation of GEO5 Software

Thalathu Oya failed rock quarry was used for validation of GEO5 software. Stereographic analysis primarily shows that the failure type is plane failure. However, wedge type failure could also be expected. Initially, micro level failure may have developed on these rock joints, which may have later acted as drains that brought surface runoff into the underling weak and well developed foliation plane. It is manifest that failure has occurred along the currently visible slip surface eventually resulting in a plane failure.

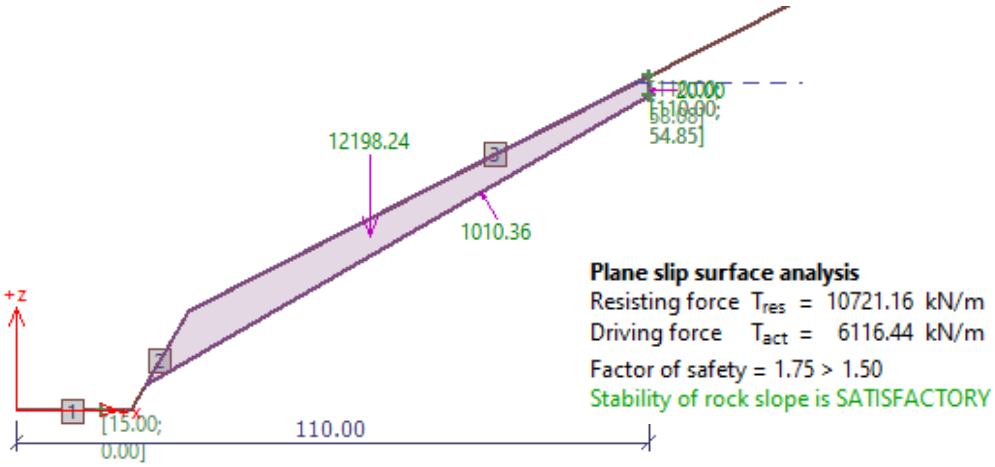

Figure 5-6: Case A, without considering ground acceleration

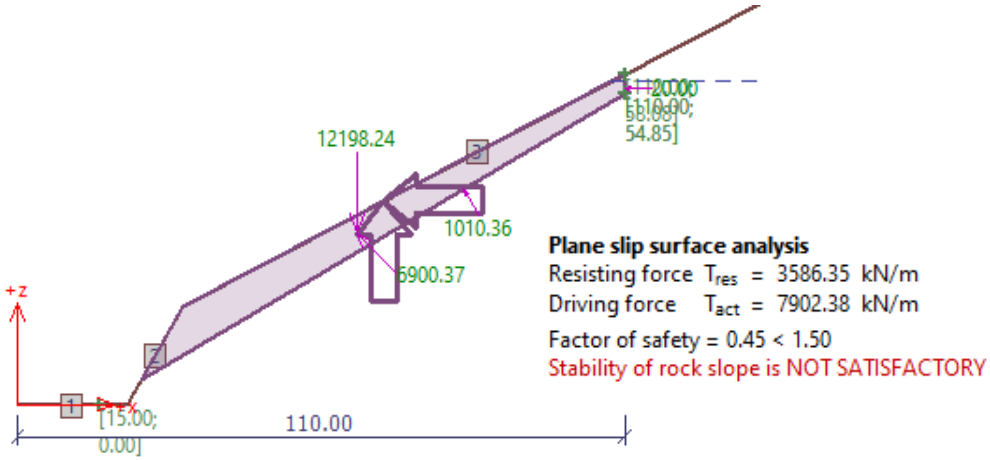

Figure 5-7: Case B, considering ground acceleration

Figure 5-6 and Figure 5-7 show the stability analysis results for Thalathu Oya slip surface after modeling the case. The validation process was carried on considering two scenarios. The case A was carried out without considering surcharge load and ground vibration due to blasting operations, while case B model was done by considering a minimum ground accelerations (0.1g) due to lack of vibration details regarding rock blasting. It is evident in Figure 5-6 that, Case A is slightly safer as the factor of safety is 1.75. But, the factor of safety has been drastically reduced up to 0.45 once the ground vibration due to rock blasting was considered. Blasting is a habitual action for almost any kind of quarry site. The factor of safety in the natural slope of Thalathu Oya quarry site had been slightly greater than required factor of safety for the stabilization without considering ground vibration due to blasting operations.

The waves induced by blasting origin might have widened the rock joint separation and therefore reduced the shear strength on the discontinuity plane. As a result, driving forces will exceed the resisting forces and ultimately failure will occur along the weak discontinuity plane. This might be the most possible process of actual failure happened in the study site which tally with the results obtained from the case B scenario in GEO5 software stability analysis.

5.9 Wedge failure analysis

Table 5-9: Structural geological parameters for wedge failure analysis

Case	Slope Dip (^{0})	Slope Dip Direction (^{0})	Plane dip (^{0})	Plane Dip Direction (^{0})	Joint number (^{0})	Trend of line of intersect	Plunge of line of intersect	Friction angle (^{0})
1	80	300	80	22	J1	330	72	44
			84	262	J2			
2	85	220	84	262	J2	225	82	44
			87	156	J4			
3	85	240	84	262	J2	225	82	44
			87	156	J4			
4	85	280	80	22	J1	329	72	44
			84	262	J2			
5	85	300	80	22	J1	330	72	44
			84	262	J2			
6	90	280	80	22	J1	329	73	44
			84	262	J2			
7	90	300	80	22	J1	330	71	44
			84	262	J2			

Table 5-9 shows the result of the stereographic analysis of line of intersection with respect to wedge failure. In all probable wedge failure observed in Face 3, plunges of intersection line are steep. In the all seven cases, the dip of slope is greater than the plunge of the intersection of two planes while friction angle is also less than plunge of the intersection line of the two planes. Therefore, results in Table 5-9 satisfy the main criteria for wedge failure to occur. The wedge failure occurs either along the line of intersection or along one of the planes forming the base of the wedge. The Markland's test has been discussed by Hocking (1976) to differentiate weather

sliding takes place along the line of intersection or along one of the planes. If the dip directions of two planes fall between the dip direction of the slope face and the trend of the line of intersection, failure will occur on that plane rather than along the line of intersection. According to Table 5-9, all the cases above do not satisfy Markland test criteria. Therefore, wedge failure is possible along the line of the intersection of the two planes.

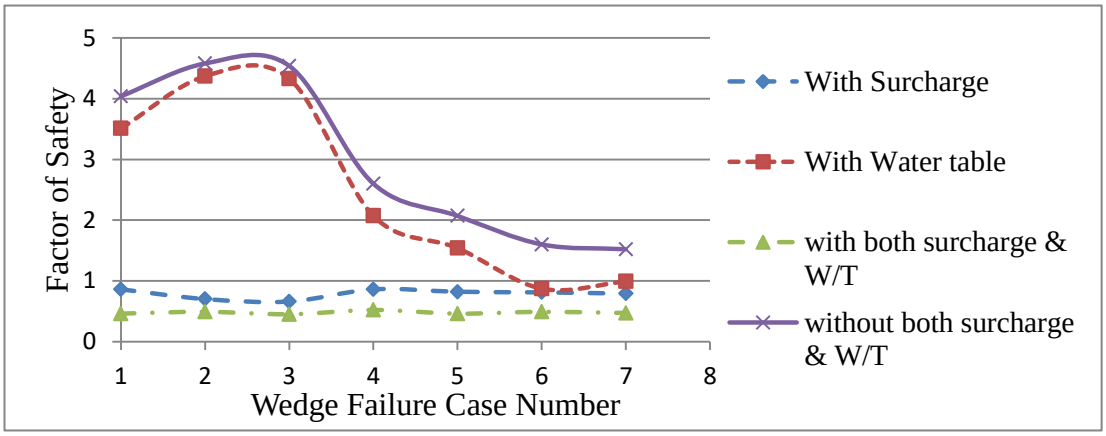

Figure 5-8: Variation of factor of safety for wedge failure cases with different conditions

Figure 5-8 shows the variation of factor of safety with wedge failure cases (Table 5-8) with different site conditions. Analysis was carried out with different conditions such as with a water table, with surcharge load, with both surcharge and water table and without both water table and surcharge. It is observed that, a higher factor of safety is achieved when the absence of both surcharge load and pore water. Lowest factor of safety is achieved in the presence both surcharge load and pore water. The analysis done with surcharge and with both surcharge and pore water showed the lowest variation of factor of safety. But, analysis without both surcharge and pore water and with pore water exhibited higher variation of factor of safety. Furthermore, most of the cases with surcharge and with only water table showed a significant difference in factor of safety. Therefore, it illustrates surcharge load plays a major role than the water table in a point of view of rock slope wedge stability.

5.10 Determination of the best slope stability improvement techniques for wedge failure

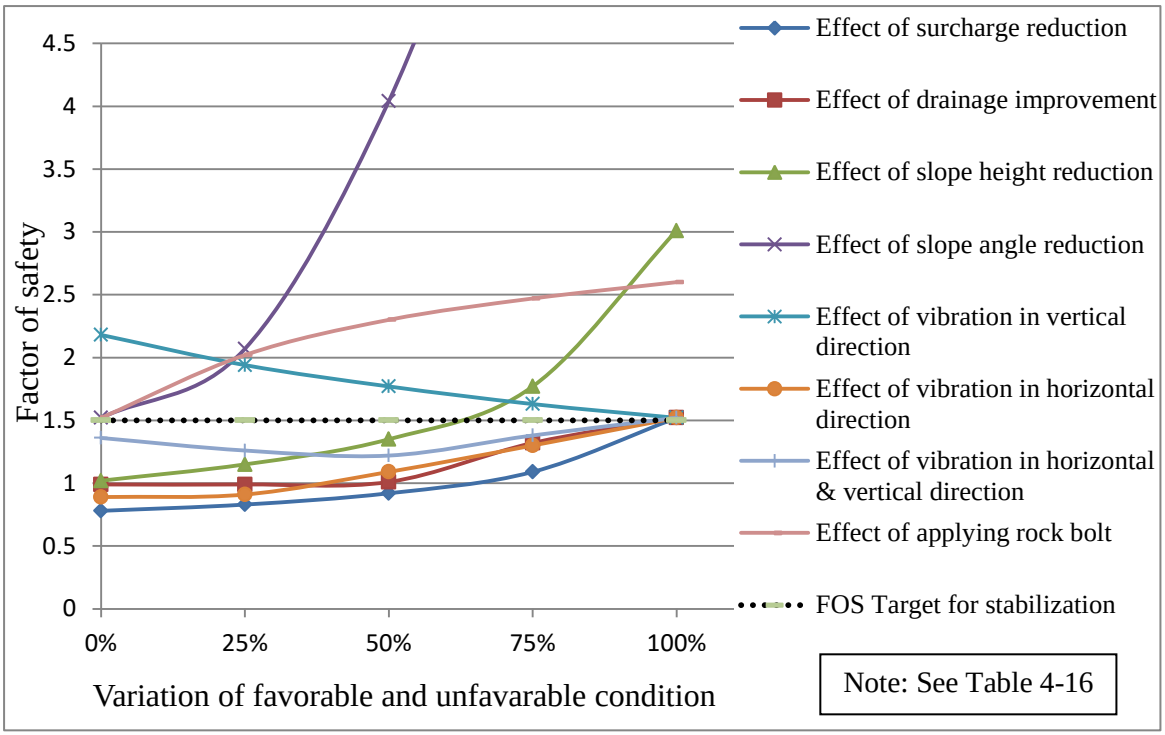

Figure 5-9: Variation of factor of safety with percentage improvement of favorable and unfavorable conditions for wedge failure

To mitigate slope failures in the form of wedge failures in the study site, efforts were made to achieve a minimum factor of safety of 1.5 by commissioning different types of improvement techniques and varying unfavorable conditions including,

(a) Reduction of slope angle
(b) Reduction of slope height
(c) Drainage improvement
(d) Increasing of shearing resistant (applying rock bolt)
(e) Changing of surcharge load
(f) Changing of ground vibration

The factor of safety was calculated by assuming the worst possible conditions with the aid of GEO5 software. Figure 5-9 shows the variation of factor of safety against

percentage variation of favorable stabilizing techniques and unfavorable conditions (Table 4-16). It is evident that the required factor of safety 1.5 can only be achieved through reduction of slope angle, reduction of slope height and introduction of rock bolts. Out of these three techniques, the most economical and practical methods could be the reduction of slope height and bench angle instead of introducing of rock bolts since it is costly process. According to the Figure 5-9, in the case of effect of slope height reduction, targeted FOS may be achieved between 50% and 75%. Therefore, maximum safe bench height for the rock slope can be selected as 5m. Further, width of the benches will be determined by the haulage facilities during the mining operations.

The ground vibration plays a significant role in Mining Industry due to regular blasting operations. Figure 5-9 manifests that vibration acceleration in horizontal direction reduces the stability of slope but, vibrator acceleration in vertical direction somewhat differs from others as increased vertical acceleration will increase the factor of safety. But, as the resultant effect of vertical and horizontal vibration is taken, slope will anyway fail. The reason behind the lack of effectiveness in reduction of surcharge can be explained through Figure 5-9 where overburden stress is comparatively low in open pit quarries compared to natural grounds.

6 CONCLUSION

6.1 Conclusion for the main objective

The current study focused on optimizing the bench geometry of mine slopes necessarily consisting soil, highly weathered rock and fractured rock in order to explore ways for safe and economical bench designing. This was achieved by integrating kinematic, empirical and limit equilibrium approaches for slope stabilization and guidelines were finally developed so that the same methodology can be universally applied for assessing the soil and rock slope stability.

The stability of any slope composed of a single bench or stacks of benches is controlled by the overburden soil stability and the quality and structural complexity of the rock mass in which the slope is situated. Various combinations of bench height and bench face angle in the overburden can be adopted in the slope designs as long as they satisfy the stability criteria. Appropriate bench height and face angle satisfying required FOS can be obtained by determining the shear strength properties of the soil and groundwater conditions followed by a stability analysis. As per the results of this work, obtaining undisturbed samples as well as disturbed samples and conducting laboratory tests on remoulded and undisturbed samples play a crucial role in determining the strength parameters of the overburden soil. In-situ observations of groundwater conditions by techniques such as installation of piezometers is also important as stability analysis requires factors relevant to the field ground water conditions. Combinations of laboratory and in-situ data then can be input into slope stability analysis software, and vary combinations of slope geometries in order to achieve the optimum bench height and the angle for the overburden profile.

When this approach was applied for slope stability analysis in the selected study area (Halbarawa overburden), it was concluded that the stability is more sensitive to variation in cohesion than variation in friction angle. As far as the bench geometry is considered, multiple benches are the most reliable mining method for steeply dipping benches.

The stability appraisal of a rock slope is much more sophisticated and if used independently, the existing approaches may have several limitations such as: (i).

stereonet process only considers the geometry, orientation of slope and the discontinuities and (ii). SMR technique does not take account of forces applied on the rock mass for the analysis. Therefore, the suitability of using a combination of kinematic, empirical and limit equilibrium techniques in assessing rock slope stability was examined. In the proposed process for rock slope optimization, probable modes of failure can be identified through Kinematic analysis. Further, the empirical method (SMR) which is based on rock mass classification system is applied to determine the probability of the failure occurrence in the cases of rock failure identified through the kinematic process. Ultimately, limit equilibrium method is adopted to determine the factor of safety with the aid of strength parameters of the rock. The recommended approach is summarized by Figure 6.1. It was concluded that this approach increases the number of rating factors and hence enhances the reliability of each system.

The rock slope stability analysis of **Halbarawa mine** site was conducted following this procedure and the process was verified with the existing condition of the site.

6.2 Conclusion for the specific objectives

The Kinematic analysis disclosed that most of joint planes intersect with each other and produce various potential failures. The dip and the dip direction of the slope faces determine the possibility of failure and the mode of failure with respect to the discontinuity plane. Further, tectonic movements in the fault zone have an unfavorable affect on the instability of the slope.

According to RQD Classification, the rocks in the particular area vary from moderately hard rocks (fair) to hard rocks (good). The RMR value obtained from the study area ranging from 35 to 58 representing poor to fair rock strength classes. Hence, the rock mass is not uniform across the study area.

According to the SMR analysis of the study area, Faces 1, 2 and 3 are considered as completely unstable (V), partially stable (III) and unstable (IV) rock stability classes, respectively. Predicted failure types according to SMR analysis are almost identical with failure types obtained through the stereographic analysis. Therefore,

stereographic analysis can be used as a convenient and economical method to analyze rock slope stability for low to medium risk level projects.

GEO5 software was also validated via Thalathu-Oya failed rock quarry. The slope of Thalathu-Oya was shown as failed according to GEO5 once the vibration effects were included in the analysis. Therefore, observed results from the Thalathu-Oya rock quarry tallied with the GEO5 software output. The accuracy of the input parameters have an obvious positive impact on the software output. Further, it is recommended to check the suitability of the software by analyzing several other actual rock failure cases.

It was also inferred that the surcharge load is a more critical factor than the static water pressure when wedge failure is considered. The analysis has shown that the most successful, economical and rapid remedial measures to improve the stability of rock slope are reduction of bench height and bench angle with control blasting operations.

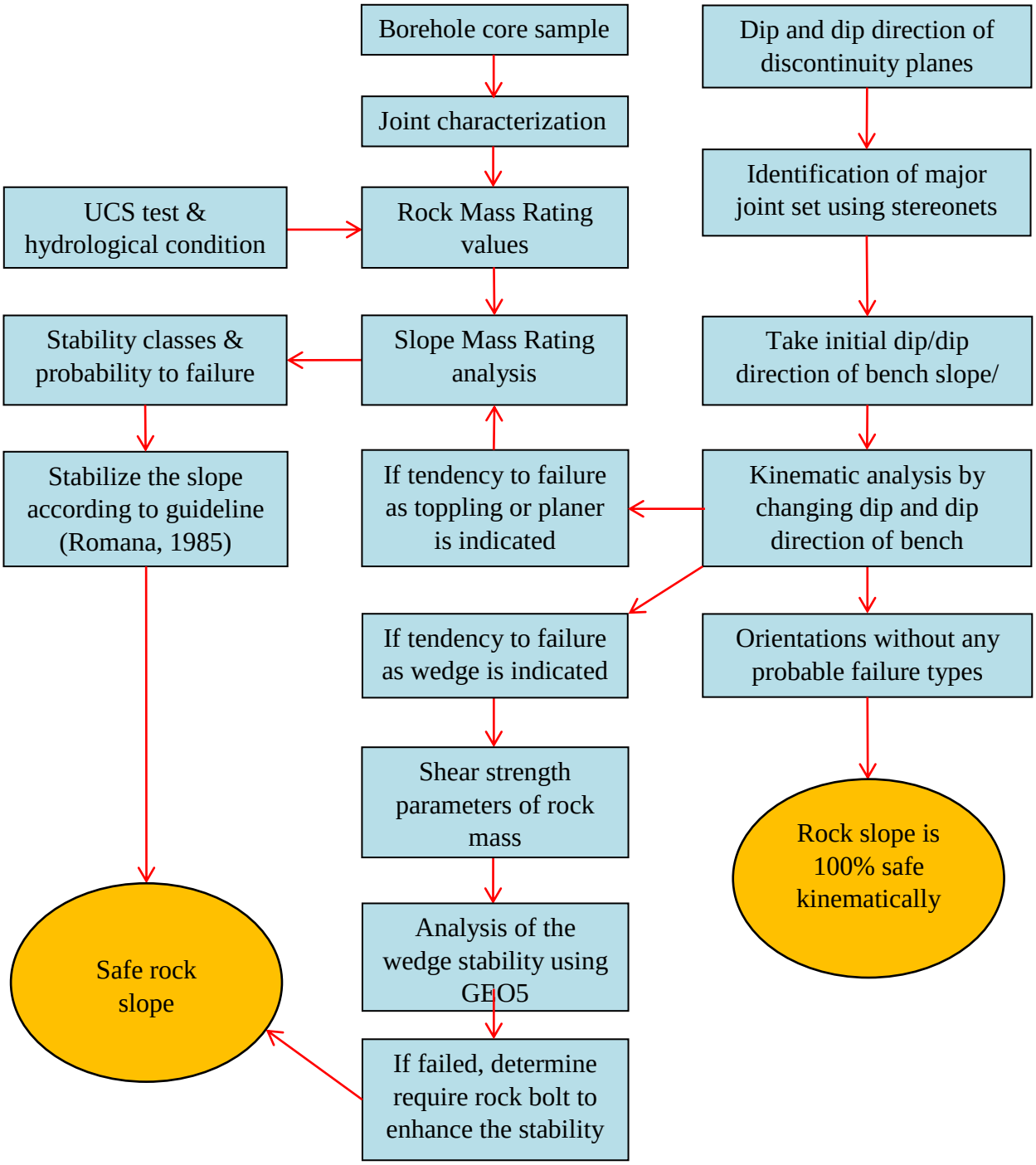

Figure 6-1: A wide-ranging procedure to optimize rock slope.

7 RECOMMENDATION

(a) The research methodology consists with kinematic method, empirical method and limit equilibrium method to assess the stability of slope. As further study, it is recommended to review on empirical stability analysis technics such as Slope Mass Rating (SMR), Modified Slope Mass Rating (MSMR), Slope Stability Probability Classification (SSPC), Chinese Slope Mass Rating (CSMR) etc.

(b) Rock Quality Designation is determined by the natural fracture intensity in the rock mass. Borehole core logging method is the most acceptable method to obtain RQD of rock mass among the others which is also a costly process. If this methodology is to be adopted in future to optimize rock slope, it is highly recommended to carry out at least one borehole to obtain the RQD accurately.

(c) Triaxial test of the rocks is the most acceptable and accurate method to obtain cohesion and friction of intact rock instead of empirical correlations. Therefore, researchers who are following this methodology to stabilize the slope, able to get more precise ultimate results by adopting Triaxial test of rocks to determine shear strength parameters.

(d) Blasting operations are done in open pit mines regularly. Therefore, it is also recommended to measure the actual ground vibration effect due to blasting operations. Then, this study can be successfully extended to stability analysis under the dynamic loading action as well.

8 REFERENCES

Aydan, Ö. and Kawamoto, T., 2001, June. The stability assessment of a large underground opening at great depth. In Proceedings of the 17th international mining congress and exhibition of Turkey (IMCET 2001), Ankara, Turkey (Vol. 1, pp. 277-288).

Basahel, H. and Mitri, H. (2017) 'Application of rock mass classification systems to rock slope stability assessment: A case study', Journal of Rock Mechanics and Geotechnical Engineering. Elsevier Ltd, 9(6), pp. 993–1009. doi: 10.1016/j.jrmge.2017.07.007.

Bieniawski, Z.T., 1973. Engineering classification of jointed rock masses. *Civil Engineer in South Africa*, *15*(12).

Bieniawski, Z.T., 1979, January. The geomechanics classification in rock engineering applications. In *4th ISRM Congress*. International Society for Rock Mechanics and Rock Engineering.

Brown, E.T., 1981. ISRM suggested methods. Rock characterization testing and monitoring. *London: Royal School of Mines*.

Deere, D., 1988. The rock quality designation (RQD) index in practice. In Rock classification systems for engineering purposes. ASTM International.

Hocking, G., 1976. A method for distinguishing between single and double plane sliding of tetrahedral wedges. *International Journal of Rock Mechanics and Mining Science*, *13*(Analytic).

Hoek E., 1994. Strength of rock and rock masses. ISRM News Journal;2(2):4e16.

Hoek, E. and Bray, J.D., 1981. *Rock slope engineering*. CRC Press.

Hoek, E., Kaiser, P.K. and Bawden, W.F., 1995. Support of Underground Excavations in Hard Rock AA BALKEMA. ROTTERDAM/BROOKFIELD.

Karam, K., He, M. and Sousa, L. (2015) 'Slope stability risk management in open pit mines', in 7th International Conference on Geo-information Technologies for

Natural Distaster Management & 5th International Conference on Earth Observation for Global Changes, pp. 1–20.

Maerz, N.H., 2000, August. Highway rock cut stability assessment in rock masses not conducive to stability calculations. In *Proceedings of the 51st Annual Highway Geology Symposium, Aug* (pp. 249-259).

Palmstrom, A., 1974. Characterization of jointing density and the quality of rock masses. *Norway: AB Berdal*.

Palmstrom, A., 1982. The volumetric joint count—a useful and simple measure of the degree of rock mass jointing. In *International Association of Engineering Geology. International congress. 4* (pp. 221-228).

Palmström, A., 1995, February. Characterizing the strength of rock masses for use in design of underground structures. In *International conference in design and construction of underground structures* (Vol. 10).

Palmstrom, A., 2005. Measurements of and correlations between block size and rock quality designation (RQD). *Tunnelling and Underground Space Technology*, *20*(4), pp.362-377.

Pantelidis, L. (2009) 'Rock slope stability assessment through rock mass classification systems', International Journal of Rock Mechanics and Mining Sciences, 46(2), pp. 315–325. doi: 10.1016/j.ijrmms.2008.06.003.

Rafek, A.G., Jamin, N.H.M., Lai, G.T., Simon, N. and Hussin, A., 2016. Systematic approach to sustainable rock slope stability evaluation. Procedia Chemistry, 19, pp.981-985.

Romana, M.R, 1985, September. New adjustment ratings for application of Bieniawski classification to slopes. In *Proceedings of the international symposium on role of rock mechanics, Zacatecas, Mexico* (pp. 49-53).

ROMANA, M.R., 1993. A geomechanical classification for slopes: slope mass rating. In Rock testing and site characterization (pp. 575-600). Pergamon.

Romana, M.R, Serón, J.B. and Montalar, E., 2003, January. SMR geomechanics classification: application, experience and validation. In *10th ISRM Congress*. International Society for Rock Mechanics and Rock Engineering.

Samarawickrama, M.N.C., Amarasinghe, U.B. and Bandaraa, K.N., 2014. Criteria to Assess Rock Quarry Slope Stability and Design in Landslide Vulnerable Areas of Sri Lanka: A Case Study at Thalathu Oya Rock Quarry. Engineer: Journal of the Institution of Engineers, Sri Lanka, 47(3).

Siddique, T., Alam, M.M., Mondal, M.E.A. and Vishal, V., 2015. Slope mass rating and kinematic analysis of slopes along the national highway-58 near Jonk, Rishikesh, India. *Journal of Rock Mechanics and Geotechnical Engineering*, *7*(5), pp.600-606.

Singh, P. and Narendrula, R., 2007. The influence of rock mass quality in controlled blasting. In *26th international conference on ground control in Mining, Morgantown* (pp. 314-319).

Sonmez, H. and Ulusay, R., 1999. Modifications to the geological strength index (GSI) and their applicability to stability of slopes. *International Journal of Rock Mechanics and Mining Sciences*, *36*(6), pp.743-760.

Standard Test Method for Determining The Shear Strength Of Soil-Geosynthetic And Geosynthetic-Geosynthetic Interfaces By Direct Shear – Designation: D 5321-17.

Standard Test Methods for Laboratory Compaction Characteristics of Soil Using Standard Effort. - Designation: D 698.

Standard Testing Methods for Unconfined Compressive Strength of Intact Rock Core Specimens, American Society for Testing and Materials – Designation: D 2938 – 79.

Stead, D. and Wolter, A. (2015) 'A critical review of rock slope failure mechanisms: The importance of structural geology', Journal of Structural Geology. Elsevier Ltd, 74, pp. 1–23. doi: 10.1016/j.jsg.2015.02.002.

Vásárhelyi, B. and Kovács, D., 2017. Empirical methods of calculating the mechanical parameters of the rock mass. Periodica Polytechnica Civil Engineering, 61(1), pp.39-50.

ANNEX A - Properties of rock joints

Location	Joint number	Longitude	Latitude	Joint Spacing(cm)	Separation(mm)	Roughness	Infilling	Weathering	Ground Water
	1	121444	177888	15,10,9,10,10	1.25, 1, 0.75, 1.42				
1	2			40,40,41,35	0.75, 1.25, 0.5	Slightly rough	No filling	weathered rock face	Present
	3			not visible joint set					
	1	121424	177923	15,17,14,14	5, 6, 2.5, 7				
2	2			14,14,14,13,19	2, 3, 1.5, 4	Slightly rough	No filling	weathered rock face	water flow through joint
	3			26,28,25,27	4, 2, 6, 5				
	1	121450	177818	38,23,50,15,25	5, 10, 7, 4				
3	2			25,36,25	2, 4, 1.5	Rough	Cracks filling	weathered rock	Not Present
	3			60,45,54,57,40	12, 10,9,11				

Location	Joint Number	Longitude	Latitude	Joint Spacing (cm)	Separation (mm)	Roughness	Infilling	Weathering	Ground Water
	1	121432	177992	28,31,29,27,28	2, 7, 4, 5				
4	2			12,18,16,18,17	1,1.25, 0.75	Smooth	Some cracks fill with clay	Highly weathered rock	Present
	3			29,27,31,33,40	2, 1.25, 4, 5				
	1	121454	177847	37,35,37,33,35	1, 0.75,1.25				
5	2			30,24,26,23	2, 1.5, 1.75, 0.5	Smooth	No filling	Weathered rock face	Present
	3			23,30,40,20,25	3, 3.5, 1.75, 1.25				
	1	121409	177952	36,39,38,37,36	1.5, 1.25, 1.75				
6	2			17,16,18,20,14	2, 4, 5	Rough	Cracks are filled	Weathered rock	Not present
	3			41,40,43,41,42	3, 2,2.3,2.5				
	4			31,29,33,30,29	0.25,0.2,0.3,0.5				

ANNEX B - The data of Unconfined Compressive Strength test

Summary of Unconfined Compressive Strength test

Sample ID	UCS value (MPa)
S1,1	25.87
S1,2	21.57
S1,3	26.40
S2,1	23.39
S2,2	20.95
S2,3	21.71
S3,1	72.46
S3,2	74.40
S3,3	71.85
S4,1	35.56
S4,2	36.91
S4,3	23.60
S5,1	36.26
S5,2	32.74
S5,3	35.52
S6,1	42.43
S6,2	46.22
S6,3	30.30

Unconfined Compressive Strength Test of rock						
Sample Description						
Lab Ref. No	S1,1					
Date	1/9/2019					
Rock type						
Sample Data						
Sample diameter (mm)			Length of sample (mm)			Failure load (KN)
55	55	55	75.5	76.05	75	65
Calculation						
Average test sample diameter (mm)	Area (mm^2)		Average test sample length (mm)			Corrected UCS (MPa)
55.00	2375.83		75.52			25.87

Unconfined Compressive Strength Test of rock						
Sample Description						
Lab Ref.No		S1,3				
Date		1/9/2019				
Rock type						
Sample Data						
Sample Diameter (mm)			Length of sample (mm)			Failure load (KN)
55	55	55	106.05	106.3	107.05	63
Calculation						
Average test sample diameter (mm)		Area (mm^2)		Average test sample length (mm)		Corrected UCS (Mpa)
55.00		2375.83		106.47		26.40

Unconfined Compressive Strength Test of rock						
Sample Description						
Lab Ref.No		S2,1				
Date		1/9/2019				
Rock type						
Sample Data						
Sample Diameter (mm)			Length of sample (mm)			Failure load (KN)
55	55	55	103.45	104.05	104.1	56
Calculation						
Average Test Sample Diameter (mm)		Area (mm^2)	Average Test Sample Length (mm)			Corrected UCS (Mpa)
55.00		2375.83	103.87			23.39

Unconfined Compressive Strength Test of rock						
Sample Description						
Lab Ref.No		S2,2				
Date		1/9/2019				
Rock type						
Sample Data						
Sample Diameter (mm)			Length of sample (mm)			Failure load (KN)
55.00	55.00	55.00	103.05	103.23	103.13	50.20
Calculation						
Average Test Sample Diameter (mm)		Area (mm^2)	Average Test Sample Length (mm)			Corrected UCS (MPa)
55.00		2375.83	103.13			20.95

Unconfined Compressive Strength Test of rock						
Sample Description						
Lab Ref.No		S2,3				
Date		1/9/2019				
Rock type						
Sample Data						
Sample Diameter (mm)			Length of sample (mm)			Failure load (KN)
55.00	55.00	55.00	104.10	103.30	103.03	52.00
Calculation						
Average Test Sample Diameter (mm)		Area (mm^2)	Average Test Sample Length (mm)			Corrected UCS (Mpa)
55.00		2375.83	103.48			21.71

ANNEX C - Structural geological parameters on discontinuities

Location	Slope					Joint		Dip Direction
	Dip				Dip Direction	Dip	Strike	
	Case1	Case2	Case3	Case4				
	90	85	80	75	70	89 SW	335	245
	90	85	80	75	70	86 SW	334	244
	90	85	80	75	70	87 SW	339	249
	90	85	80	75	70	86 SW	168	261
	90	85	80	75	70	86 SW	175	265
	90	85	80	75	70	85SW	169	259
	90	85	80	75	70	87 SW	334	244
	90	85	80	75	70	88 SW	163	253
	90	85	80	75	70	85 SW	332	242
	90	85	80	75	70	26 SW	162	252
	90	85	80	75	70	77 EN	113	23
	90	85	80	75	70	21 SW	159	249
	90	85	80	75	70	87 SW	343	253
	90	85	80	75	70	81 SW	341	251
	90	85	80	75	70	81 SW	339	249
	90	85	80	75	70	85SW	337	247
Face 1	90	85	80	75	70	25 SW	163	253
	90	85	80	75	70	24 SW	165	255
	90	85	80	75	70	31 SW	167	257
	90	85	80	75	70	83 SW	343	253
	90	85	80	75	70	84 SW	340	250
	90	85	80	75	70	73 EN	112	22
	90	85	80	75	70	79 EN	113	23
	90	85	80	75	70	75 EN	110	20
	90	85	80	75	70	74 EN	111	21
	90	85	80	75	70	71 EN	112	22
	90	85	80	75	70	79EN	114	24
	90	85	80	75	70	75 EN	110	20
	90	85	80	75	70	77 EN	109	19
	90	85	80	75	70	17 SW	164	254
	90	85	80	75	70	21 SW	163	253
	90	85	80	75	70	23 SW	170	260
	90	85	80	75	70	27 SW	169	259
	90	85	80	75	70	20 SW	164	254
	90	85	80	75	70	79 NE	113	23
	90	85	80	75	70	77 NE	292	22

Location	Slope					Joint		
	Dip				Dip Direction	Dip	Strike	Dip Direction
	Case1	Case2	Case3	Case4				
	90	85	80	75	170	66 EN	337	67
	90	85	80	75	170	86 SW	342	252
	90	85	80	75	170	82 SW	340	250
	90	85	80	75	170	81 SW	338	248
	90	85	80	75	170	84SW	337	247
	90	85	80	75	170	87 SW	340	250
	90	85	80	75	170	85 SW	171	261
	90	85	80	75	170	86 SW	175	265
	90	85	80	75	170	83SW	170	260
	90	85	80	75	170	86 SW	331	241
	90	85	80	75	170	88 SW	177	267
	90	85	80	75	170	85 SW	334	244
	90	85	80	75	170	33 SW	160	250
Face 2	90	85	80	75	170	79EN	114	24
	90	85	80	75	170	75 EN	108	18
	90	85	80	75	170	79 EN	106	16
	90	85	80	75	170	22 SW	161	251
	90	85	80	75	170	77 EN	108	18
	90	85	80	75	170	18 SW	169	259
	90	85	80	75	170	18 SW	163	253
	90	85	80	75	170	72 EN	112	22
	90	85	80	75	170	79 EN	114	24
	90	85	80	75	170	76 EN	113	23
	90	85	80	75	170	85 SW	333	243
	90	85	80	75	170	63 EN	144	54
	90	85	80	75	170	88 SW	344	254
	90	85	80	75	170	17 SW	169	259
	90	85	80	75	170	89 SW	337	247
	90	85	80	75	170	74 EN	111	21
	90	85	80	75	170	70 EN	110	20
	90	85	80	75	170	23 SW	171	261
	90	85	80	75	170	27 SW	170	260
	90	85	80	75	170	20 SW	162	252
	90	85	80	75	170	27 SW	170	260
	90	85	80	75	170	20 SW	162	252
	90	85	80	75	170	26 SW	162	252
	90	85	80	75	170	20 SW	160	250

Location	Slope					Joint		
	Dip				Dip Direction	Dip	Strike	Dip Direction
	Case1	Case2	Case3	Case4				
	90	85	80	75	260	79 NE	113	23
	90	85	80	75	260	81 NE	292	22
	90	85	80	75	260	82 SE	243	153
	90	85	80	75	260	23 SW	171	261
	90	85	80	75	260	85 SW	168	258
	90	85	80	75	260	27 SW	170	260
	90	85	80	75	260	88 SE	255	165
	90	85	80	75	260	76 EN	343	73
Face 3	90	85	80	75	260	20 SW	162	252
	90	85	80	75	260	84 SW	177	267
	90	85	80	75	260	89 SE	248	158
	90	85	80	75	260	86 SW	174	264
	90	85	80	75	260	83 SW	171	261
	90	85	80	75	260	87 SW	173	263
	90	85	80	75	260	81 SW	169	259
	90	85	80	75	260	82 SW	171	261
	90	85	80	75	260	72 SE	233	143
	90	85	80	75	260	87 SE	237	147
	90	85	80	75	260	82 SE	247	157
	90	85	80	75	260	83SW	337	247
	90	85	80	75	260	86 SW	340	250
	90	85	80	75	260	85 SW	171	261
	90	85	80	75	260	86 SW	175	265
	90	85	80	75	260	84SW	170	260
	90	85	80	75	260	78EN	113	23
	90	85	80	75	260	76 EN	108	18
	90	85	80	75	260	77 EN	108	18
	90	85	80	75	260	75 EN	112	22
	90	85	80	75	260	78 EN	112	22
	90	85	80	75	260	76 EN	113	23
	90	85	80	75	260	19 SW	167	257
	90	85	80	75	260	20 SW	164	254
	90	85	80	75	260	25 SW	162	252
	90	85	80	75	260	24 SW	165	255
	90	85	80	75	260	31 SW	166	256

ANNEX D - Data of rock specific gravity test

Specific Gravity Test of rock						
Sample Description						
Lab Ref.No						
Date	08/09/2019					
Rock type						
Sample Data						
Sample No	1	2	3	4	5	6
Dry weight of rock sample (g)	8.7	4.5	4.6	3	2.3	4.6
Wt of sample in water (g)	4.8	2.6	2.8	1.8	1.3	2.5
S.G of sample	2.23	2.37	2.56	2.50	2.30	2.19

ANNEX E – Observation data of Proctor compaction test

PROCTOR COMPACTION TEST																
Client :									Test Date : 2018/12/18							
Location : Halbarawa Top soil L-1									Sample Type : Earth							
Weight of Rammer :									Blows per Layer : 25Nos.							
Drop of Rammer :									Volume of Mold : 965cm^3							
No. of Layers : 03																
Dry Density	Trial Number		**1**		**2**		**3**		**4**		**5**		**6**			
	Wt. of Sample + Mold	g	5780.0		5907.1		6020.3		6066.7		6025.1		6018.1			
	Wt. of Mold	g	3995.3		3995.3		3995.3		3995.3		3995.3		3995.3			
	Wt. Sample	g	1784.7		1911.8		2025.0		2071.4		2029.8		2022.8			
	Bulk Density	g/cm^3	1.849		1.981		2.098		2.147		2.103		2.096			
	Dry Density	g/cm^3	1.734		1.832		1.904		1.899		1.796		1.762			
Moisture Content	Container No		**1**		**2**		**3**			**4**			**5**		**6**	
	Weight of Container	g	14.80	12.20	16.80	18.60	16.10	10.40	9.70	9.90	14.60	10.50	6.60	6.70		
	Wt.of wet Sample + Container	g	39.70	46.20	68.80	62.30	62.70	65.70	89.00	70.10	97.10	119.40	75.90	64.30		
	Wt.of dry Sample + Container	g	38.07	44.17	64.90	58.98	58.30	60.68	79.84	63.16	84.82	103.78	64.99	55.00		
	Weight of water	g	1.63	2.03	3.90	3.32	4.40	5.02	9.16	6.94	12.28	15.62	10.91	9.30		
	Weight of dry sample	g	23.27	31.97	48.10	40.38	42.20	50.28	70.14	53.26	70.22	93.28	58.39	48.30		
	Moisture Contents	%	6.68%		8.17%		10.21%		13.05%		17.12%		18.97%			

PROCTOR COMPACTION TEST												
Client :							Test Date : 2018/12/18					
Location : Halbarawa Top soil L-2							Sample Type : Earth					
Weight of Rammer :							Blows per Layer : 25Nos.					
Drop of Rammer :							Volume of Mold : 965cm^3					
No. of Layers : 03												
Dry Density	Trial Number		1	2	3	4	5					
	Wt. of Sample + Mold	g	5643.9	5854.3	5928.9	5891.5	5883.0					
	Wt. of Mold	g	3995	3995	3995	3995	3995					
	Wt. Sample	g	1649	1859	1934	1897	1888					
	Bulk Density	g/cm^3	1.709	1.927	2.004	1.965	1.956					
	Dry Density	g/cm^3	1.606	1.745	1.732	1.636	1.627					
Moisture Content	Container No		1		2		3		4		5	
	Weight of Container	g	18.60	12.30	14.90	19.50	14.90	10.60	6.90	7.00	10.00	9.50
	Wt.of wet Sample + Container	g	27.70	22.10	30.70	37.20	31.60	27.90	29.00	33.40	29.10	37.40
	Wt.of dry Sample + Container	g	27.12	21.55	29.14	35.72	29.38	25.50	25.31	28.96	26.08	32.42
	Weight of water	g	0.58	0.55	1.56	1.48	2.22	2.40	3.69	4.44	3.02	4.98
	Weight of dry sample	g	8.52	9.25	14.24	16.22	14.48	14.90	18.41	21.96	16.08	22.92
	Moisture Contents	%	6.38%		10.40%		15.72%		20.13%		20.26%	

ANNEX F - Observation data of direct shear test

Top soil L1 (Normal stress 50KN)

Shear Displacement	Proving Ring reading	Vertical Gauge Reading	Vertical Displacement	Shear Force	Shear Displacement (mm)	Shear area (mm^2)	Shear stress
0	0	50	0	0	0.00	3600	0.00
10	12	51	0.0254	20.484	0.10	3594	5.70
20	15	51.1	0.02794	25.605	0.20	3588	7.14
30	20	51.1	0.02794	34.14	0.30	3582	9.53
40	23.2	51.1	0.02794	39.602	0.40	3576	11.07
50	25.1	51.5	0.0381	42.846	0.50	3570	12.00
60	30	51.7	0.04318	51.21	0.60	3564	14.37
70	32.8	51.7	0.04318	55.99	0.70	3558	15.74
80	34.8	51.7	0.04318	59.404	0.80	3552	16.72
90	38.5	51.2	0.03048	65.72	0.90	3546	18.53
100	41.3	51.3	0.03302	70.499	1.00	3540	19.92
125	49.2	50.5	0.0127	83.984	1.25	3525	23.83
150	54.9	49.5	-0.0127	93.714	1.50	3510	26.70
175	62	48.3	-0.04318	105.83	1.75	3495	30.28
200	67	46.7	-0.08382	114.37	2.00	3480	32.86
225	69.2	45	-0.127	118.12	2.25	3465	34.09
250	72.2	43.5	-0.1651	123.25	2.50	3450	35.72
275	75.9	41.9	-0.20574	129.56	2.75	3435	37.72
300	78.1	40	-0.254	133.32	3.00	3420	38.98
325	79	37.7	-0.31242	134.85	3.25	3405	39.60
350	73	36	-0.3556	124.61	3.50	3390	36.76
375	70.2	34.2	-0.40132	119.83	3.75	3375	35.51
400	61.3	33	-0.4318	104.64	4.00	3360	31.14
425	58	31.8	-0.46228	99.006	4.25	3345	29.60
450	54.8	30.6	-0.49276	93.544	4.50	3330	28.09

(Normal stress 100KN)

Shear Displacement	Proving Ring reading	Vertical Gauge Reading	Vertical Displacement	Shear Force	Shear Displacement (mm)	Shear area (mm^2)	Shear stress
0	0	9	0	0	0.00	3600	0.00
10	25	9.5	0.0127	42.675	0.10	3594	11.87
20	37	9.7	0.0178	63.159	0.20	3588	17.60
30	46.5	10.1	0.0279	79.376	0.30	3582	22.16
40	53.5	11	0.0508	91.325	0.40	3576	25.54
50	61	11.5	0.0635	104.13	0.50	3570	29.17
60	67	11.5	0.0635	114.37	0.60	3564	32.09
70	74	11.9	0.0737	126.32	0.70	3558	35.50
80	80.4	12.1	0.0787	137.24	0.80	3552	38.64
90	84.5	12.2	0.0813	144.24	0.90	3546	40.68
100	91	12.2	0.0813	155.34	1.00	3540	43.88
125	102.2	12.2	0.0813	174.46	1.25	3525	49.49
150	112.3	12.2	0.0813	191.7	1.50	3510	54.61
175	121.5	12.5	0.0889	207.4	1.75	3495	59.34
200	129	12.5	0.0889	220.2	2.00	3480	63.28
225	133.4	11.6	0.066	227.71	2.25	3465	65.72
250	138.5	10.5	0.0381	236.42	2.50	3450	68.53
275	141.8	9.2	0.0051	242.05	2.75	3435	70.47
300	145.4	7.9	-0.028	248.2	3.00	3420	72.57
325	148	6.9	-0.053	252.64	3.25	3405	74.20
350	151.8	5.9	-0.079	259.12	3.50	3390	76.44
375	152.3	4.8	-0.107	259.98	3.75	3375	77.03
400	153.1	3.5	-0.14	261.34	4.00	3360	77.78
425	154	2.5	-0.165	262.88	4.25	3345	78.59
450	154	1.5	-0.191	262.88	4.50	3330	78.94
475	147.2	0.4	-0.218	251.27	4.75	3315	75.80
500	139.3	-1.1	-0.257	237.79	5.00	3300	72.06
525	131.8	-1.9	-0.277	224.98	5.25	3285	68.49
550	127.7	-2.5	-0.292	217.98	5.50	3270	66.66

(Normal stress 150KN)

Shear Displacement	Proving Ring reading	Vertical Gauge Reading	Vertical Displacement	Shear Force	Shear Displacement (mm)	Shear area (mm^2)	Shear stress
0	0	40.7	0	0.00	0.00	3600	0.00
10	20	41	0.00762	34.14	0.10	3594	9.50
20	33	41.2	0.0127	56.33	0.20	3588	15.70
30	44.5	41.5	0.02032	75.96	0.30	3582	21.21
40	53	41.6	0.02286	90.47	0.40	3576	25.30
50	61.5	41.6	0.02286	104.98	0.50	3570	29.41
60	66	41.6	0.02286	112.66	0.60	3564	31.61
70	72.5	41.6	0.02286	123.76	0.70	3558	34.78
80	81.4	41.6	0.02286	138.95	0.80	3552	39.12
90	90	41.6	0.02286	153.63	0.90	3546	43.32
100	95	41.6	0.02286	162.17	1.00	3540	45.81
125	98.1	41.6	0.02286	167.46	1.25	3525	47.51
150	100.2	42.1	0.03556	171.04	1.50	3510	48.73
175	101.3	41.9	0.03048	172.92	1.75	3495	49.48
200	101.5	42.9	0.05588	173.26	2.00	3480	49.79
225	101.8	43.2	0.0635	173.77	2.25	3465	50.15
250	102.3	43.7	0.0762	174.63	2.50	3450	50.62
275	110.1	43.8	0.07874	187.94	2.75	3435	54.71
300	130	43.8	0.07874	221.91	3.00	3420	64.89
325	146	43.8	0.07874	249.22	3.25	3405	73.19
350	158.8	43.8	0.07874	271.07	3.50	3390	79.96
375	170.9	43.8	0.07874	291.73	3.75	3375	86.44
400	180	43.8	0.07874	307.26	4.00	3360	91.45
425	185	43	0.05842	315.80	4.25	3345	94.41
450	187	41.7	0.0254	319.21	4.50	3330	95.86
475	190	38.3	-0.06096	324.33	4.75	3315	97.84
500	191	36.8	-0.09906	326.04	5.00	3300	98.80
525	191.5	35	-0.14478	326.89	5.25	3285	99.51
550	191.5	32.9	-0.19812	326.89	5.50	3270	99.97
575	187	31	-0.24638	319.21	5.75	3255	98.07
600	180	29	-0.29718	307.26	6.00	3240	94.83
625	168	27.7	-0.3302	286.78	6.25	3225	88.92
650	154.7	26.3	-0.36576	264.07	6.50	3210	82.27

ANNEX G - Analytical outputs of Slope W analysis

Bench angle (^{0})	Factor of safety			
	S-T	S-B	M-T	M-B
45	2.003	2.573	2.07	3.403
55	1.818	2.247	1.854	2.976
65	1.623	1.97	1.7	2.655
75	1.433	1.728	1.459	2.474

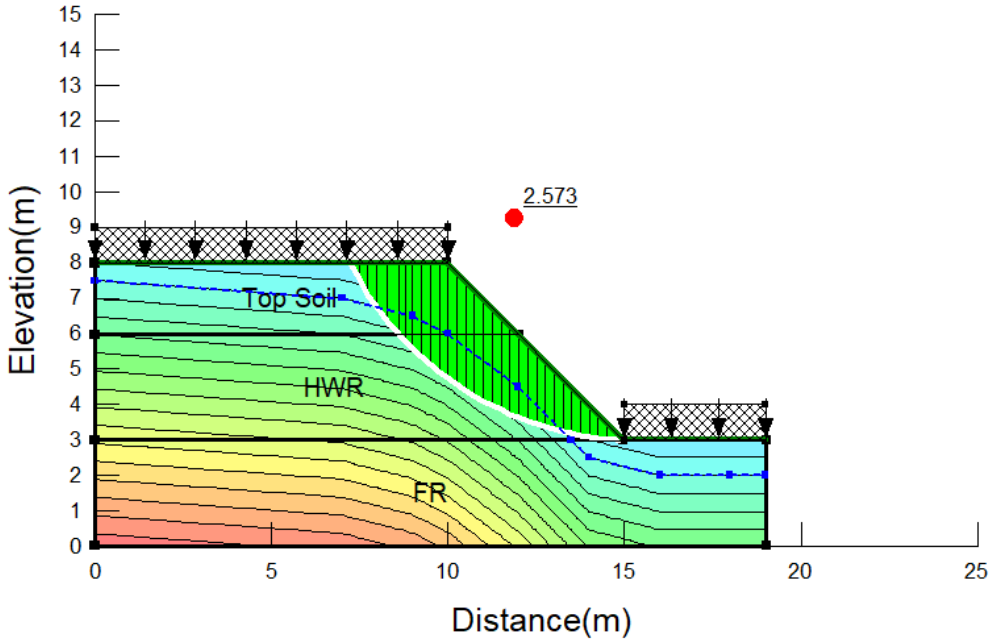

Failure exit occurs in HWR when slope maintains a single bench (Dip of slope 45^0)

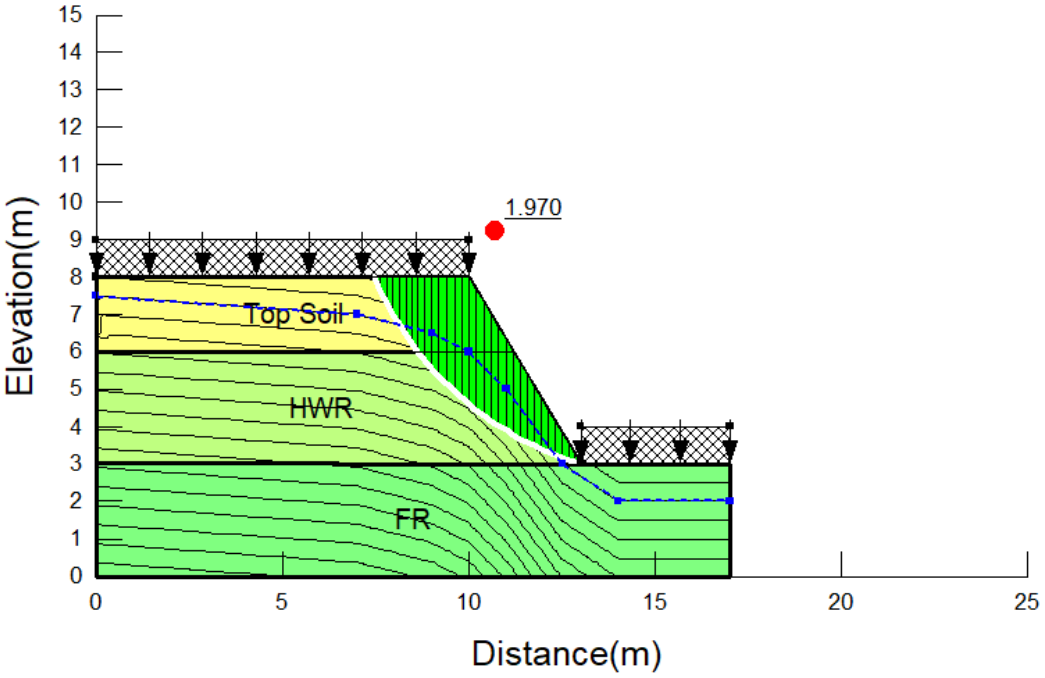

Failure exit occurs in HWR when slope maintains a single bench (Dip of slope 65^0)

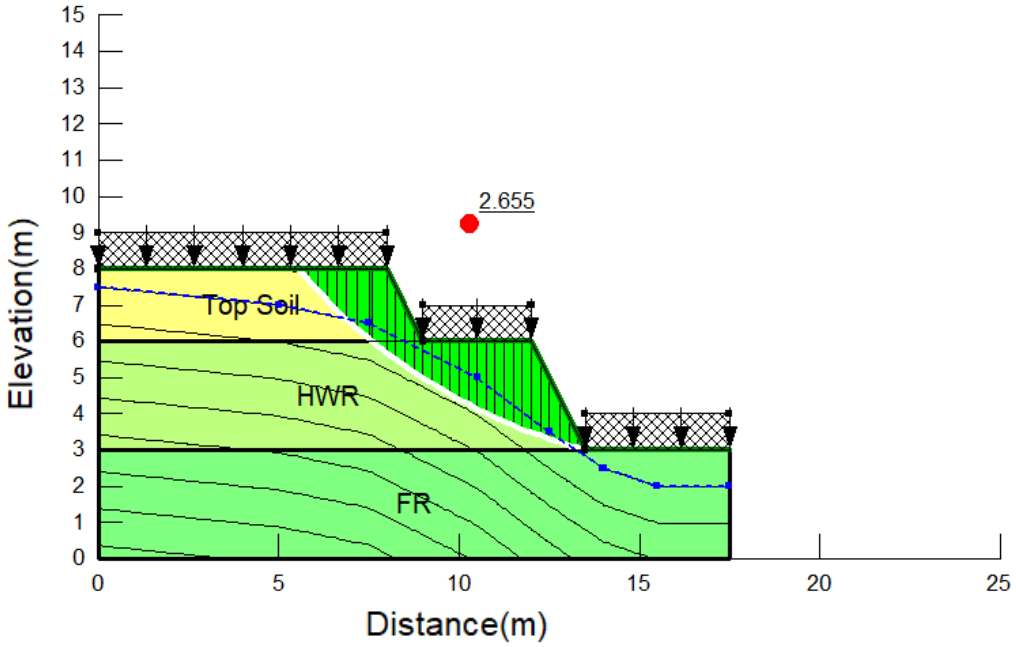

Failure exit occurs in HWR when slope maintains a multiple bench(Dip of slope 65^0)

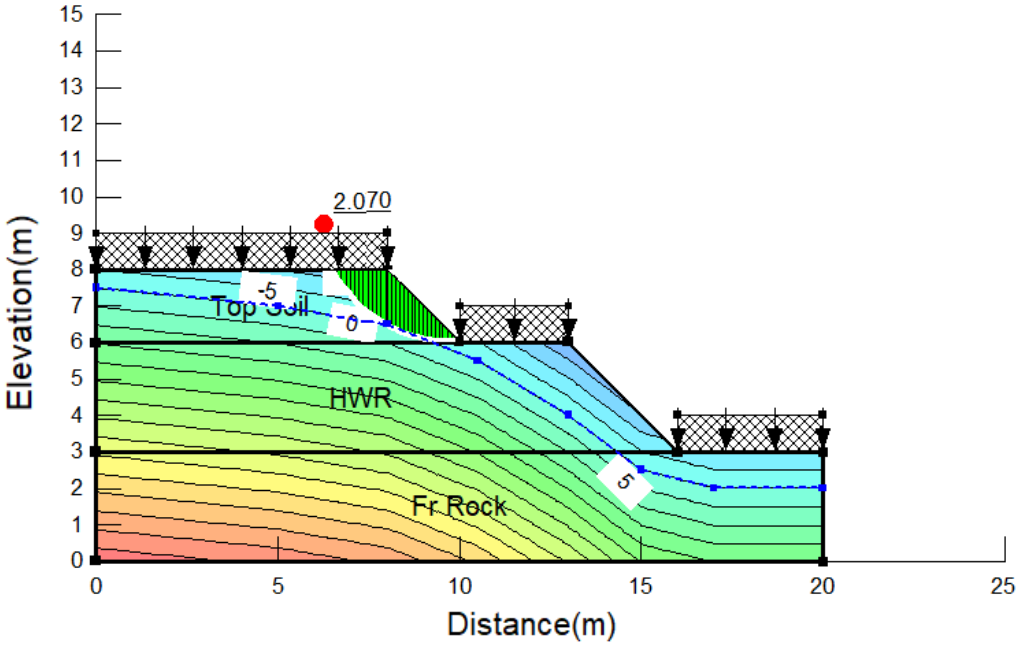

Failure exit occurs in top soil when slope maintains a multiple bench(Dip of slope 45^0)

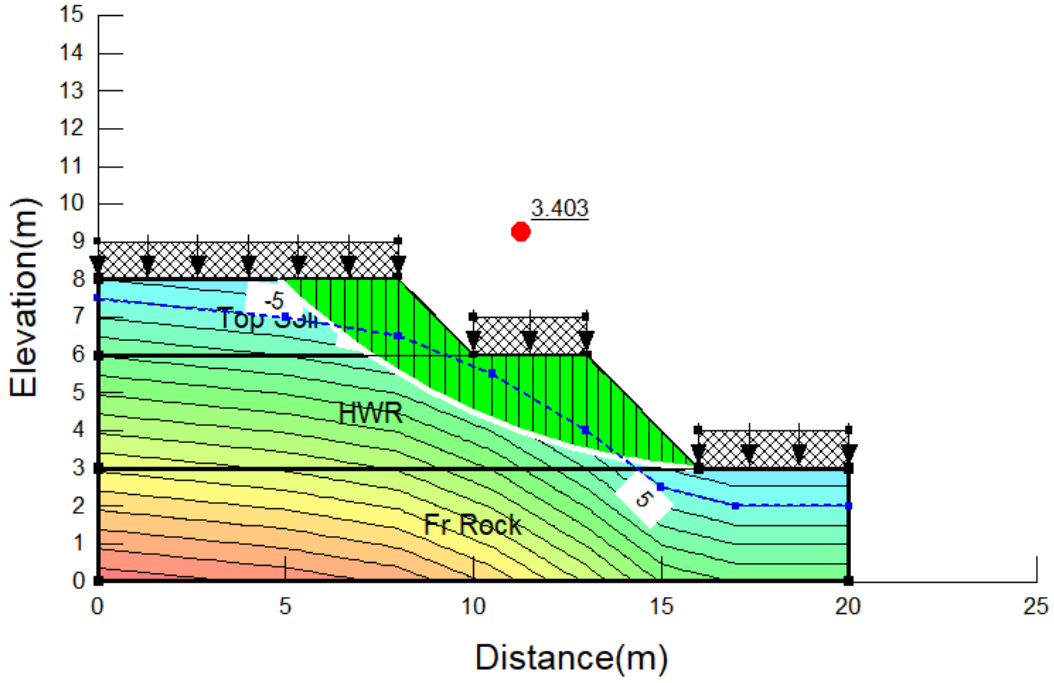

Failure exit occurs in HWR when slope maintains a multiple bench(Dip of slope 45^0)

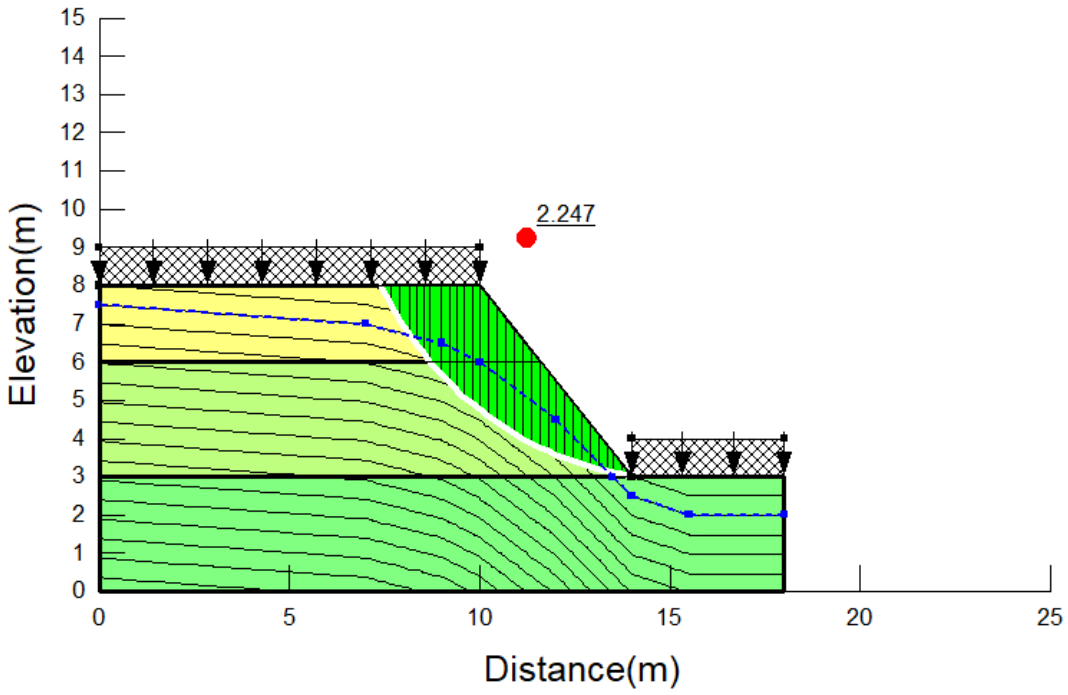

Failure exit occurs in HWR when slope maintains a single bench(Dip of slope 55^0)

ANNEX H - Analytical outputs of kinematic analysis

Face 1

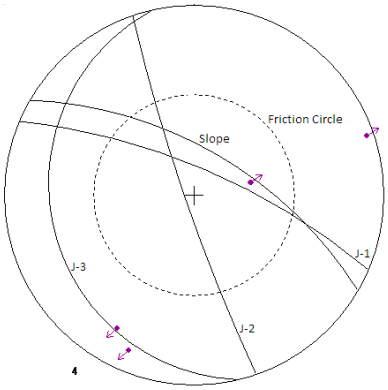

Slope Dip - 70, Slope D/D - 30

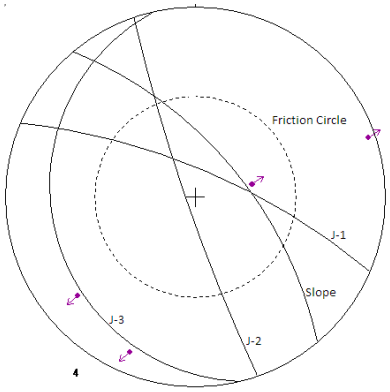

Slope Dip - 70, Slope D/D - 50

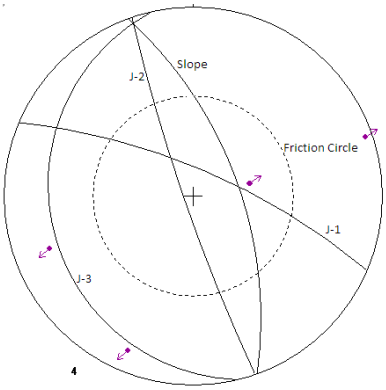

Slope Dip - 70, Slope D/D - 70

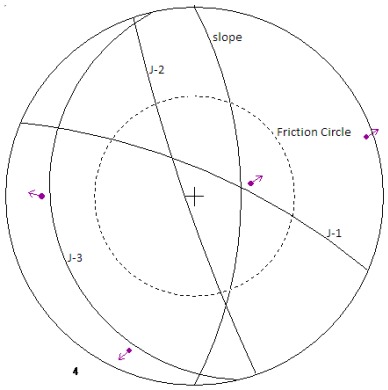

Slope Dip - 70, Slope D/D – 90

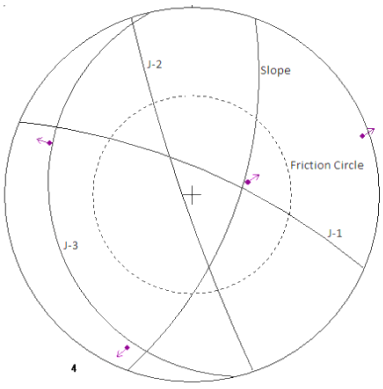

Slope Dip - 70, Slope D/D - 110

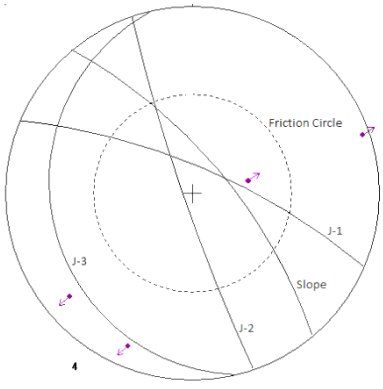

Slope Dip - 75, Slope D/D – 50

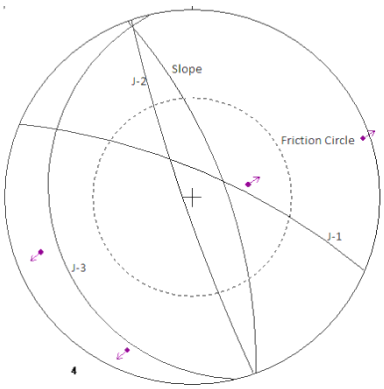

Slope Dip - 75, Slope D/D – 70

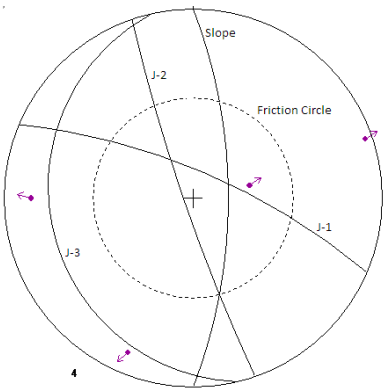

Slope Dip - 75, Slope D/D - 90

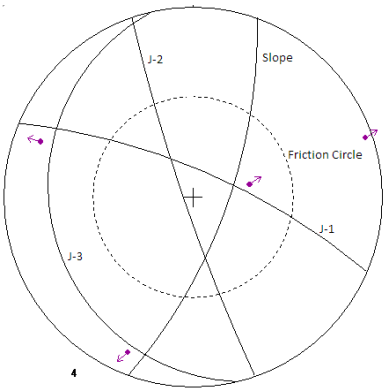

Slope Dip - 75, Slope D/D - 110

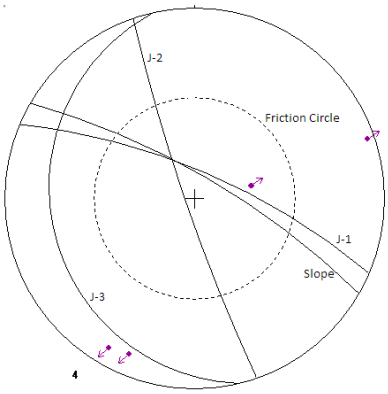

Slope Dip - 80, Slope D/D - 30

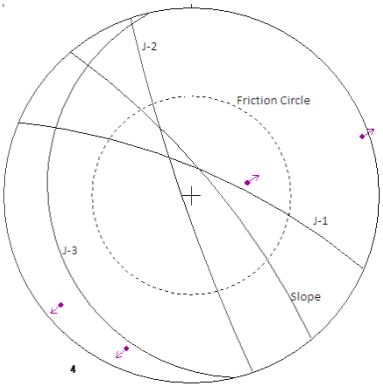

Slope Dip - 80, Slope D/D - 50

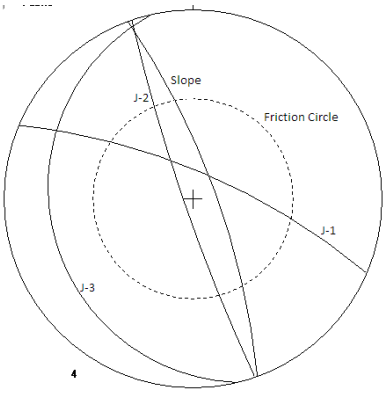

Slope Dip - 80, Slope D/D – 70

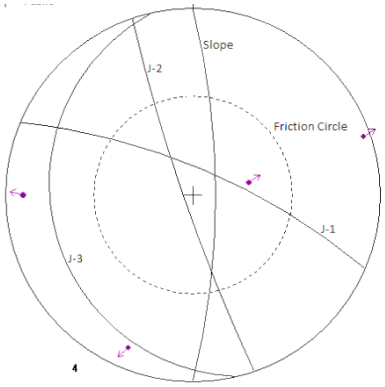

Slope Dip - 80, Slope D/D - 90

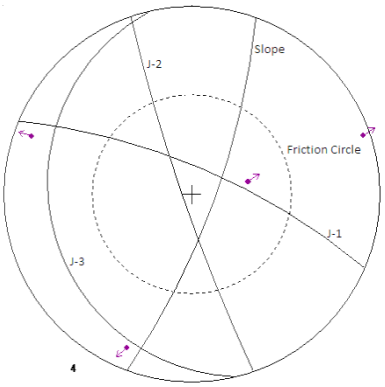

Slope Dip - 80, Slope D/D – 110

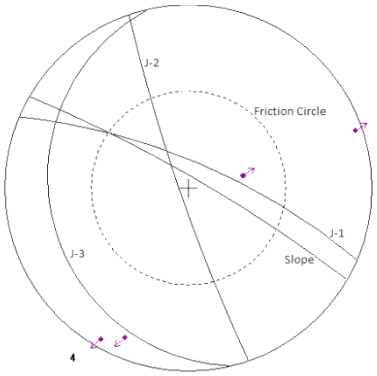

Slope Dip - 85, Slope D/D – 30

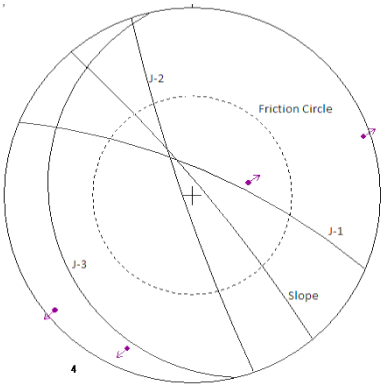

Slope Dip - 85, Slope D/D – 50

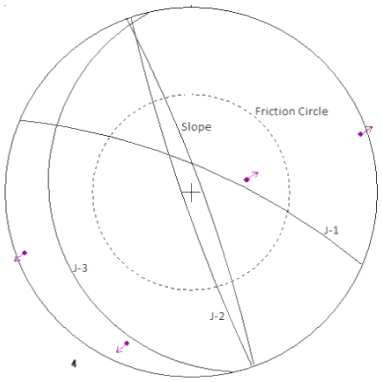

Slope Dip - 85, Slope D/D – 70

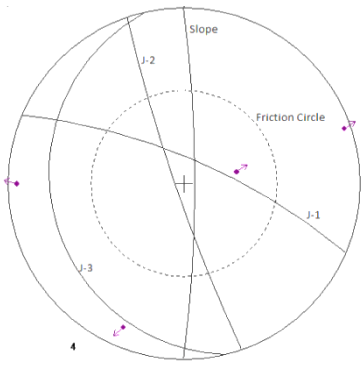

Slope Dip - 85, Slope D/D – 90

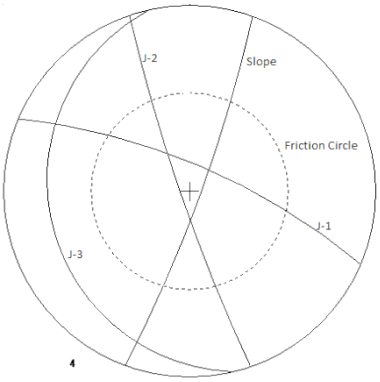

Slope Dip - 85, Slope D/D – 110

Slope Dip - 90, Slope D/D – 30

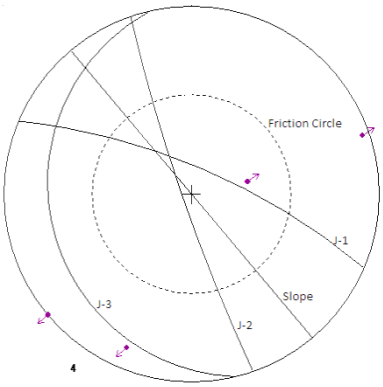

Slope Dip - 90, Slope D/D – 50

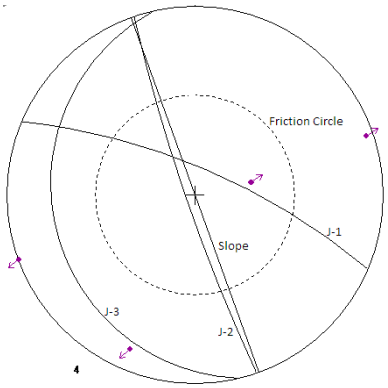

Slope Dip - 90, Slope D/D – 70

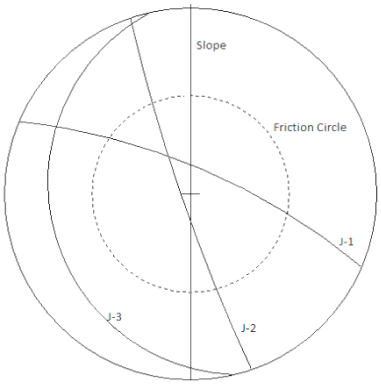

Slope Dip - 90, Slope D/D – 90

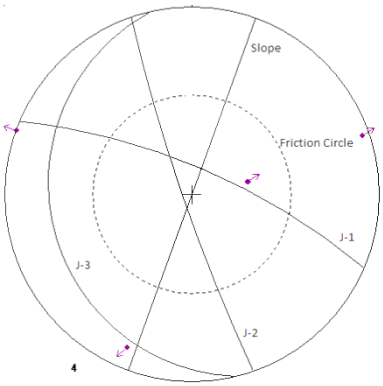

Slope Dip - 90, Slope D/D – 110

Face 2

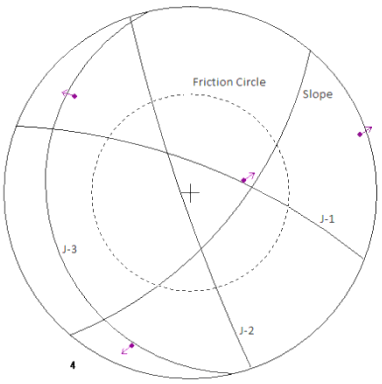

Slope Dip - 70, Slope D/D – 130

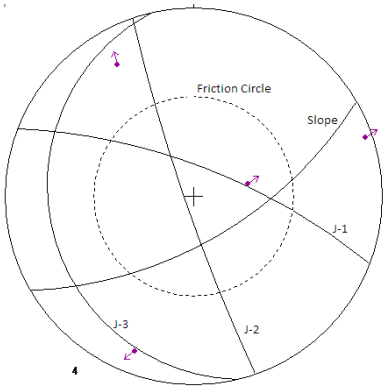

Slope Dip - 70, Slope D/D - 150

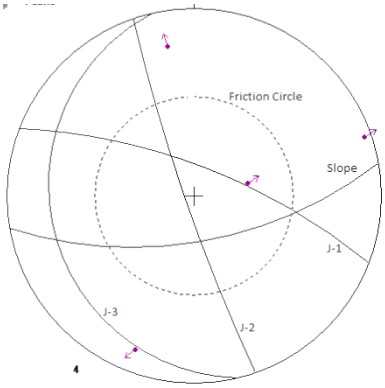

Slope Dip - 70, Slope D/D – 170

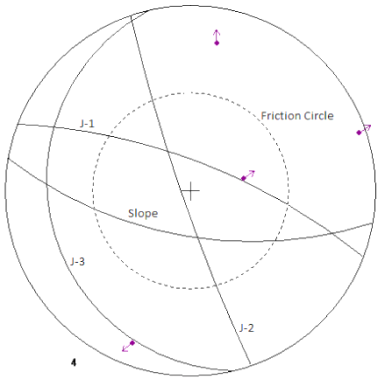

Slope Dip - 70, Slope D/D - 190

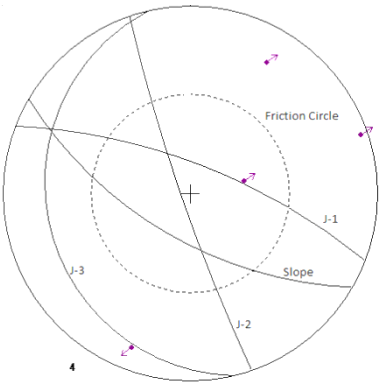

Slope Dip - 70, Slope D/D - 210

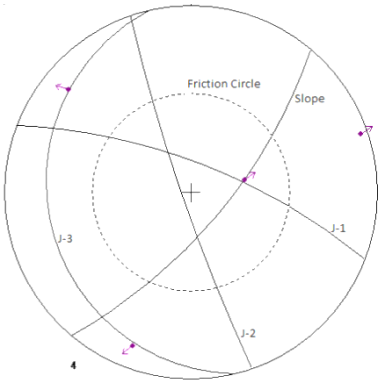

Slope Dip – 75, Slope D/D - 130

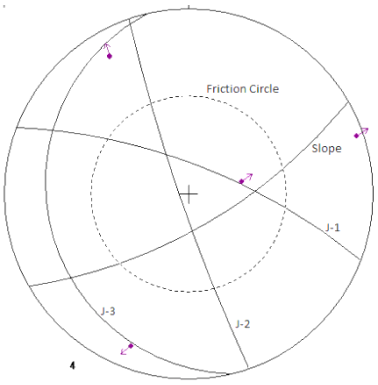

Slope Dip – 75, Slope D/D – 150

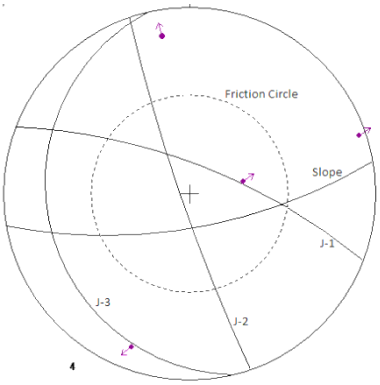

Slope Dip– 75, Slope D/D - 170

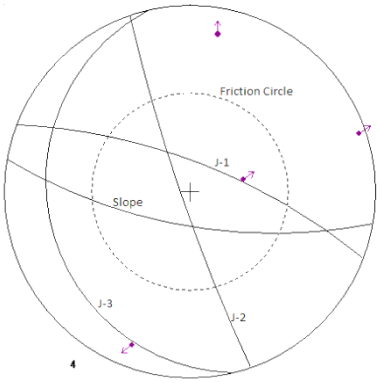

Slope Dip – 75, Slope D/D – 190

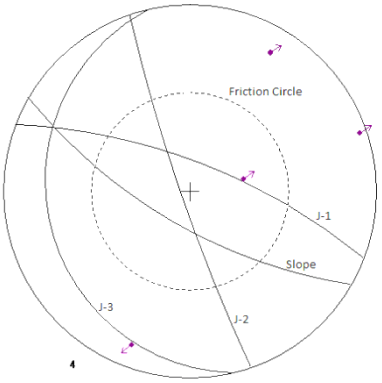

Slope Dip– 75, Slope D/D - 210

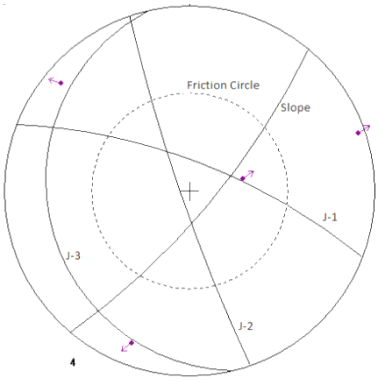

Slope Dip – 80, Slope D/D - 130

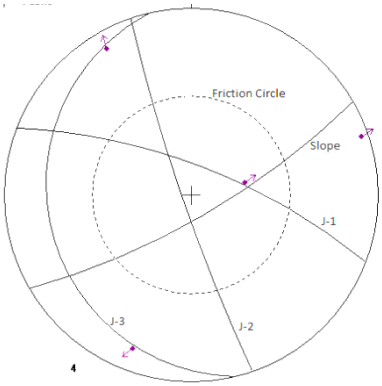

Slope Dip– 80, Slope D/D - 150

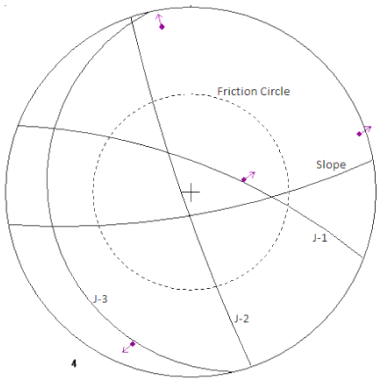

Slope Dip – 80, Slope D/D - 170

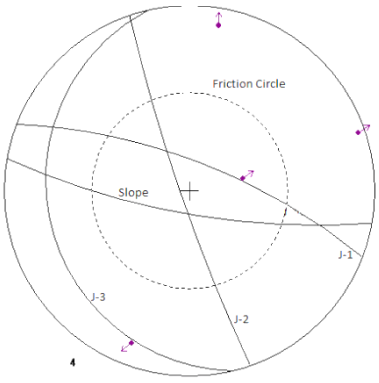

Slope Dip– 80, Slope D/D - 190

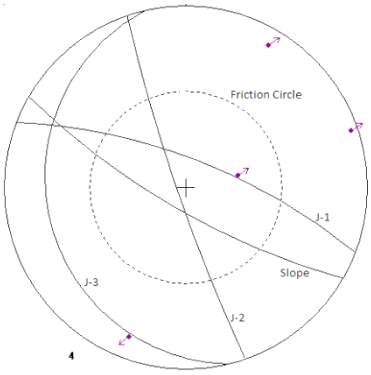

Slope Dip – 80, Slope D/D - 210

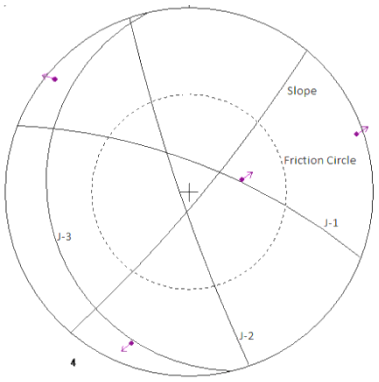

Slope Dip– 85, Slope D/D - 130

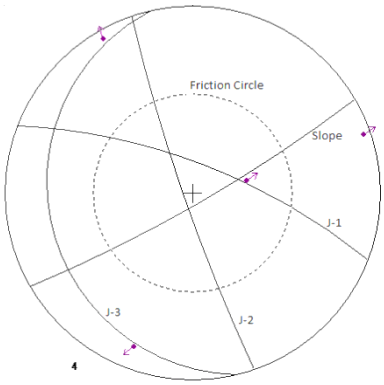

Slope Dip– 85, Slope D/D - 150

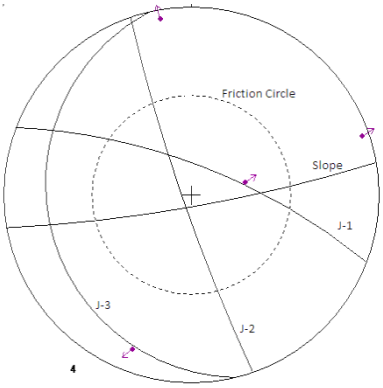

Slope Dip– 85, Slope D/D - 170

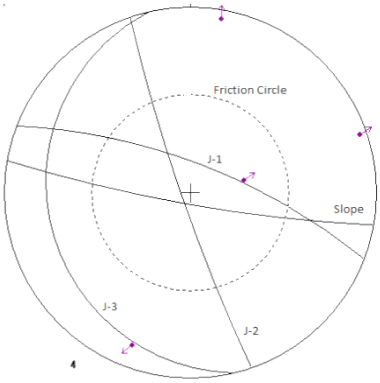

Slope Dip – 85, Slope D/D - 190

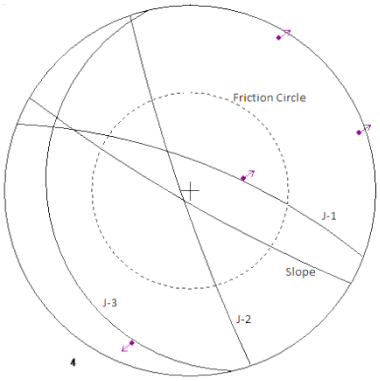

Slope Dip– 85, Slope D/D – 210

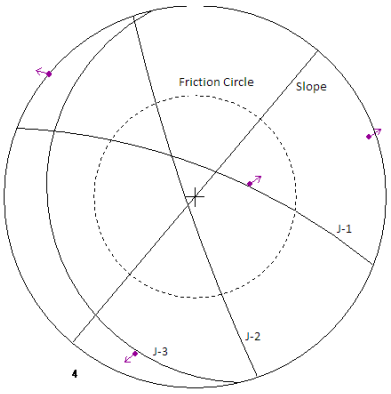

Slope Dip – 90, Slope D/D – 130

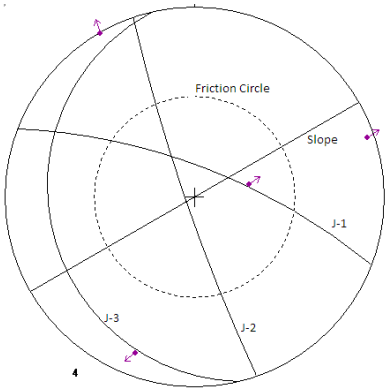

Slope Dip– 90, Slope D/D – 150

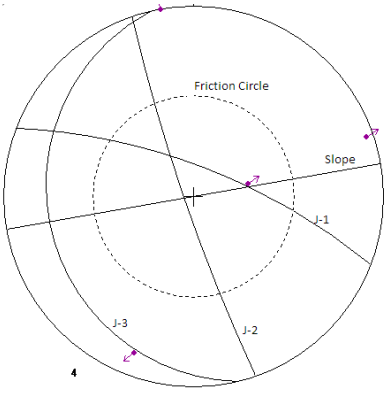

Slope Dip – 90, Slope D/D – 170

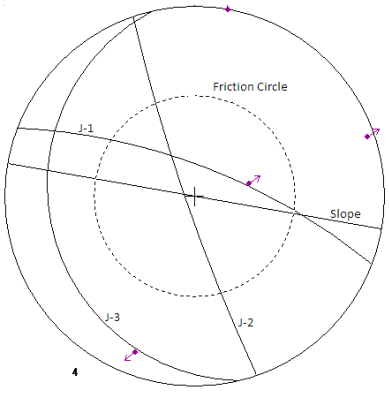

Slope Dip– 90, Slope D/D – 190

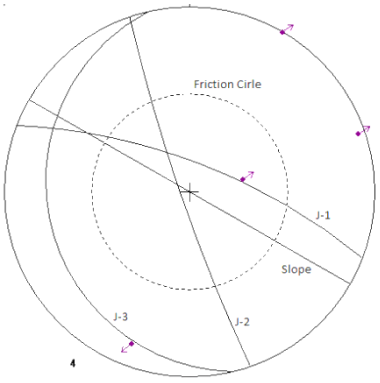

Slope Dip– 90, Slope D/D – 210

Face 3

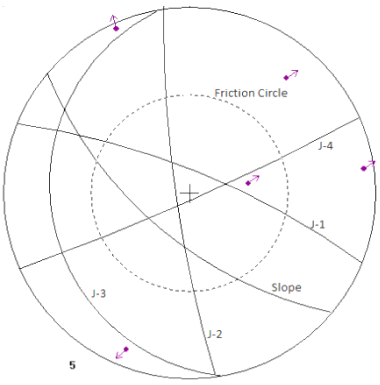

Slope Dip 70, slope D/D 220

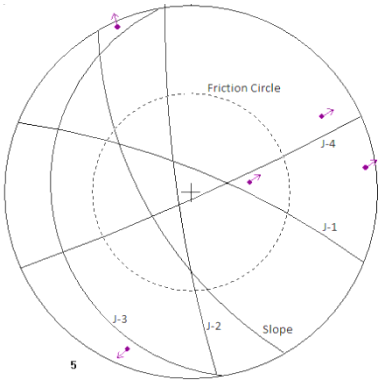

Slope Dip 70, slope D/D 240

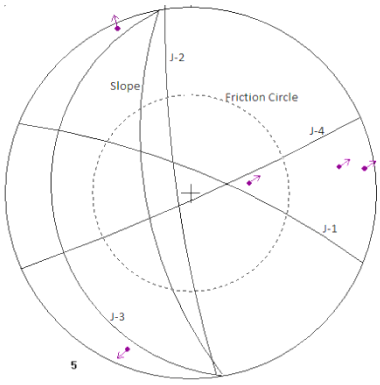

Slope Dip 70, slope D/D 260

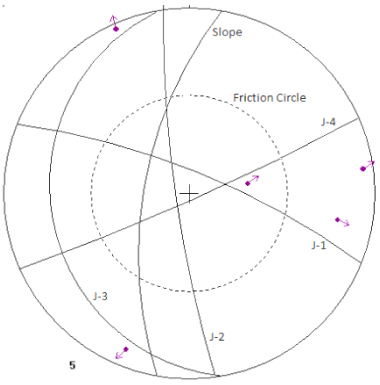

Slope Dip 70, slope D/D 280

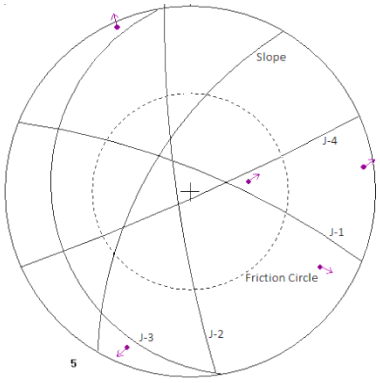

Slope Dip 70, slope D/D 300

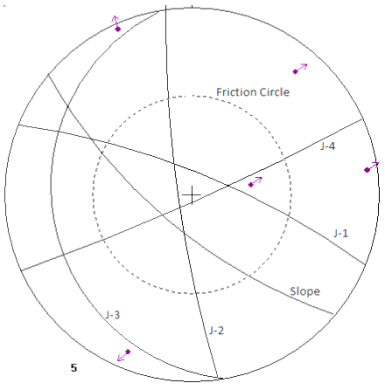

Slope Dip 75, slope D/D 220

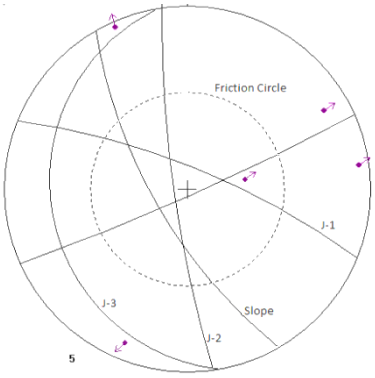

Slope Dip 75, slope D/D 240

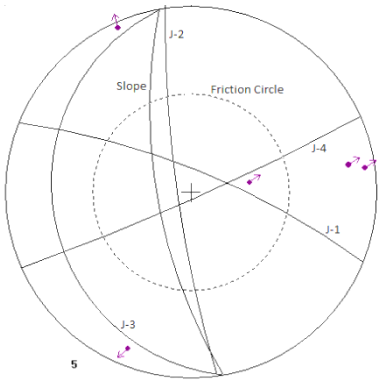

Slope Dip 75, slope D/D 260

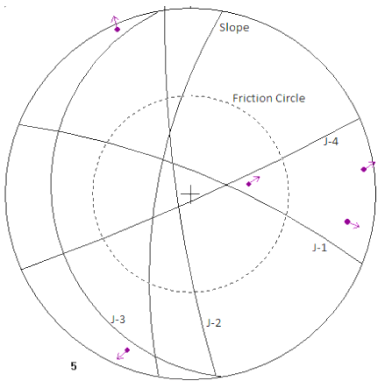

Slope Dip 75, slope D/D 280

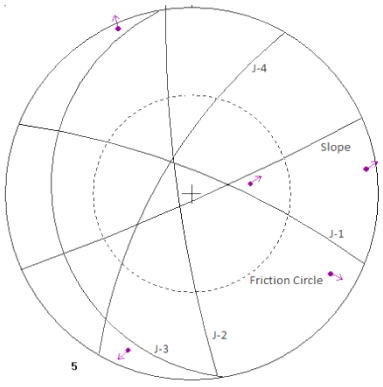

Slope Dip 75, slope D/D 300

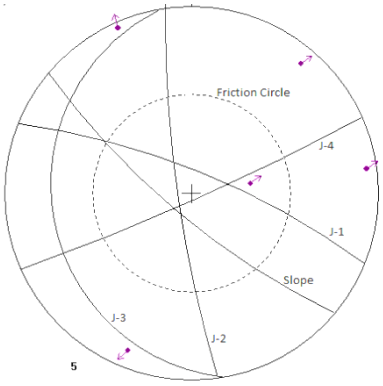

Slope Dip 80, slope D/D 220

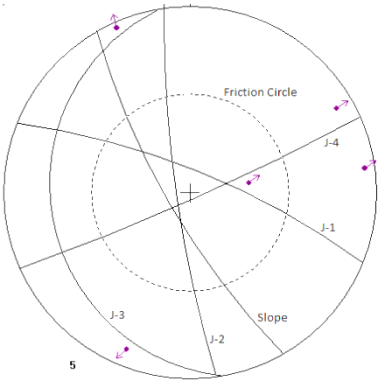

Slope Dip 80, slope D/D 240

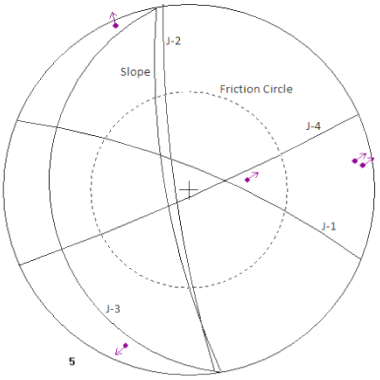

Slope Dip 80, slope D/D 260

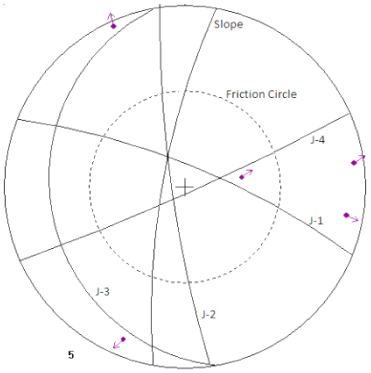

Slope Dip 80, slope D/D 280

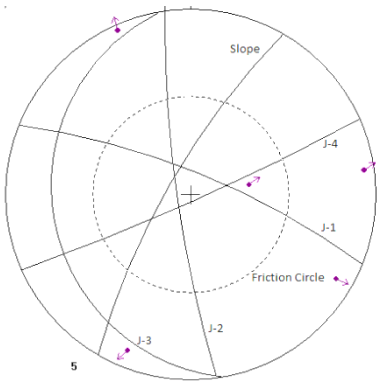

Slope Dip 80, slope D/D 300

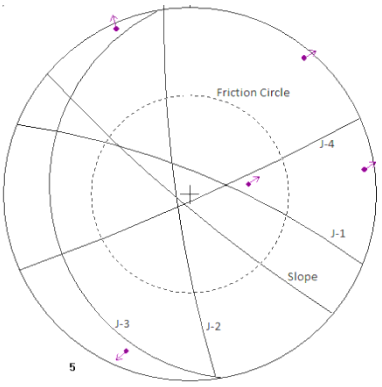

Slope Dip 85, slope D/D 220

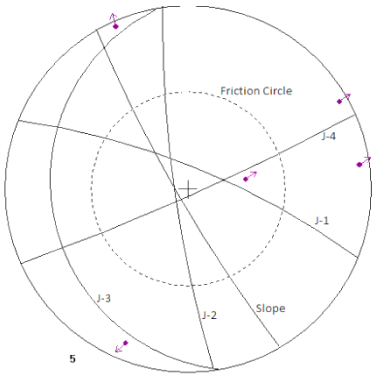

Slope Dip 85, slope D/D 240

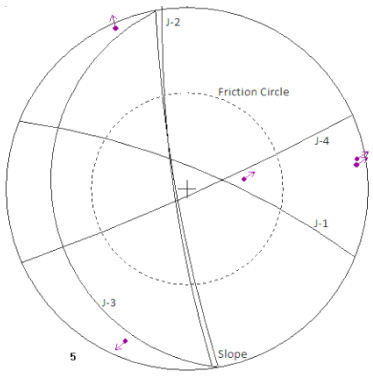

Slope Dip 85, slope D/D 260

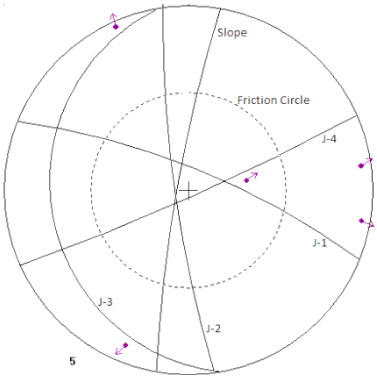

Slope Dip 85, slope D/D 280

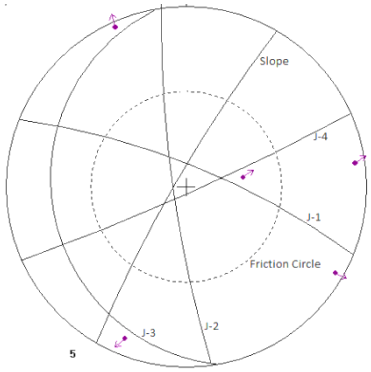

Slope Dip 85, slope D/D 300

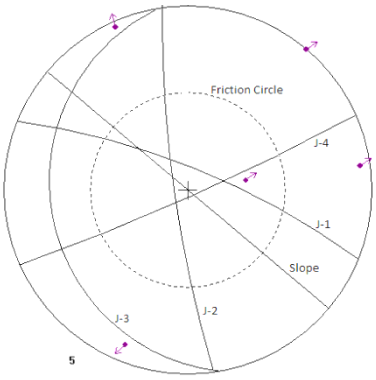

Slope Dip 90, slope D/D 220

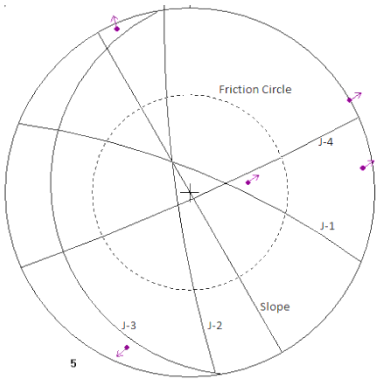

Slope Dip 90, slope D/D 240

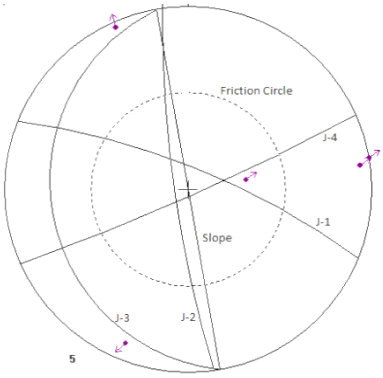

Slope Dip 90, slope D/D 260

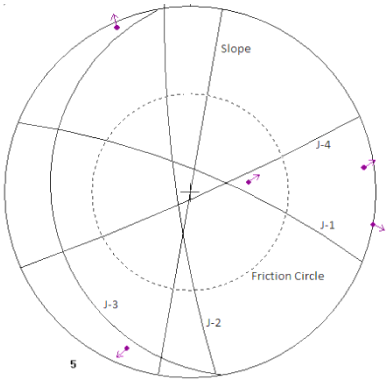

Slope Dip 90, slope D/D 280

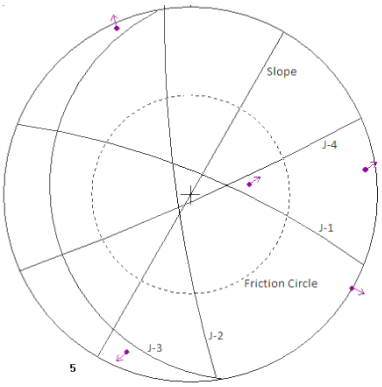

Slope Dip 90, slope D/D 300

ANNEX I - Analytical outputs of wedge stability analysis

Summary of wedge stability analysis

Wedge failure case No	Factor of Safety			
	With only surcharge	With only W/T	With surcharge and W/T	Without surcharge and W/T
1	0.86	3.51	0.46	4.04
2	0.7	4.37	0.49	4.58
3	0.66	4.33	0.45	4.54
4	0.86	2.07	0.52	2.6
5	0.82	1.54	0.46	2.07
6	0.81	0.87	0.49	1.6
7	0.79	0.99	0.47	1.52

Stability analysis with ground water table

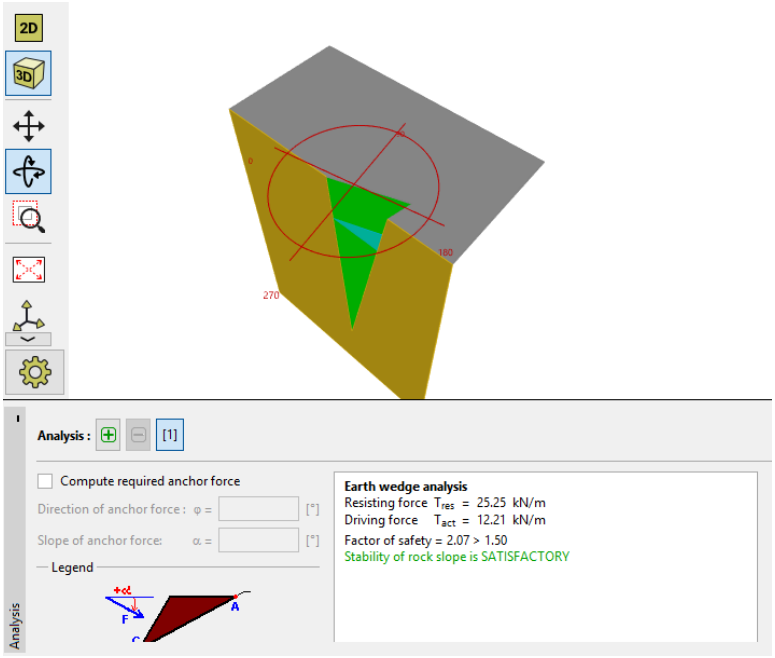

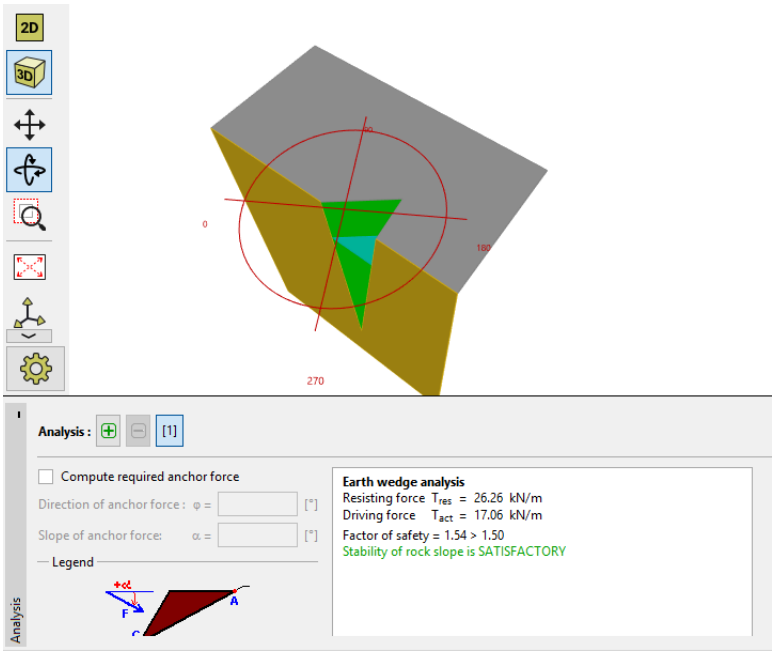

Stability analysis with surcharge

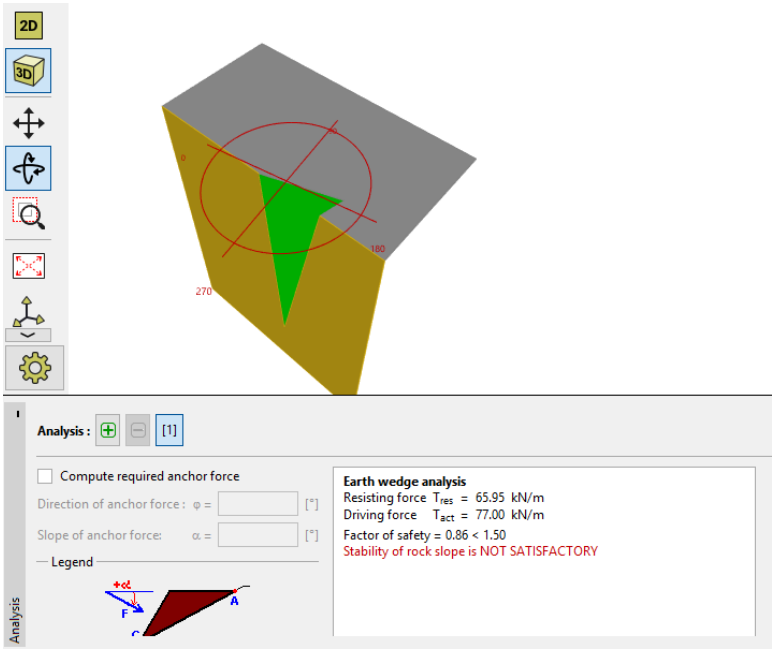

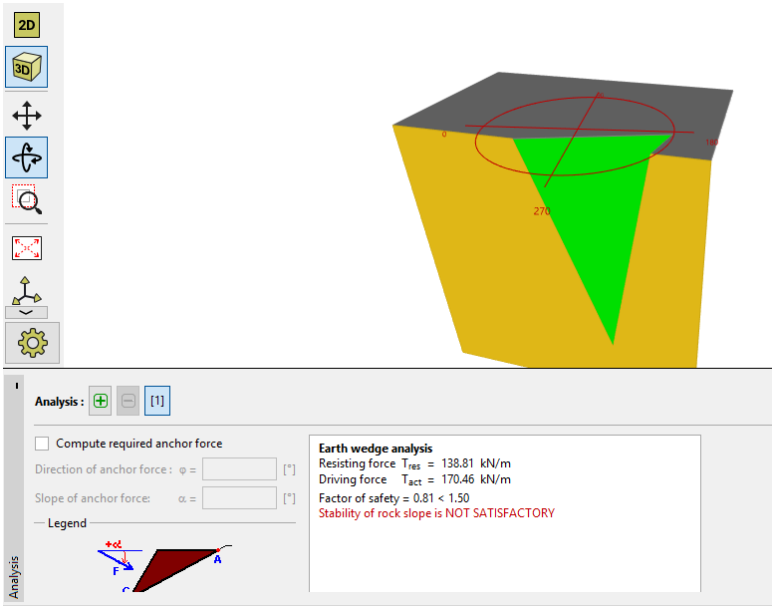

Stability analysis with both surcharge and ground water table

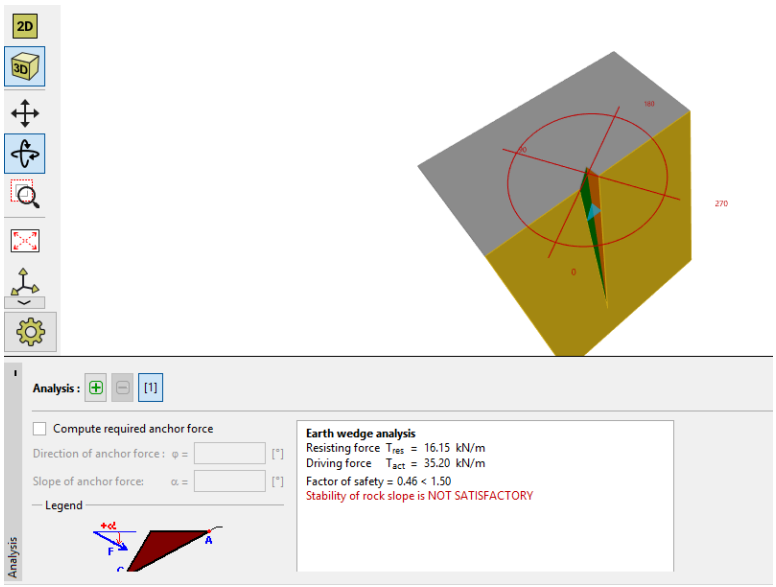

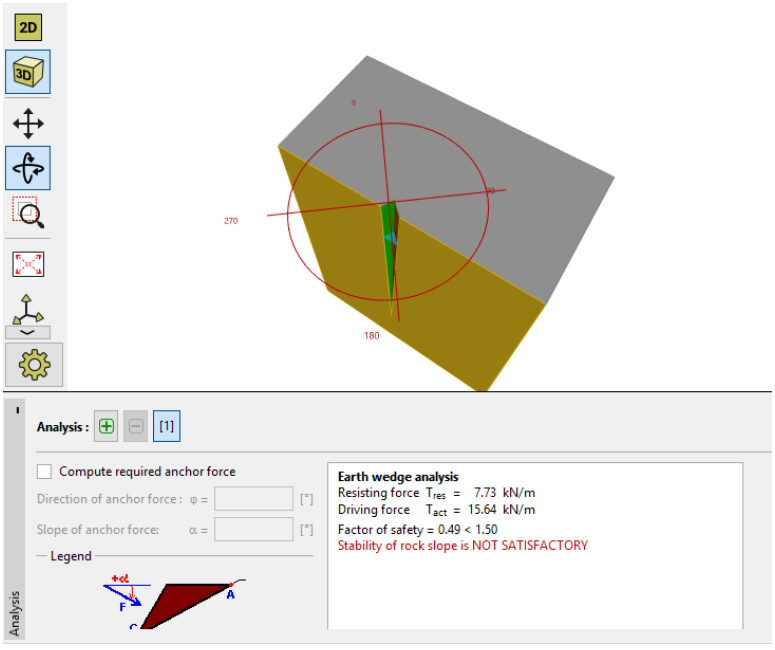

Stability analysis without both surcharge and ground water table